Synthesis, optimization, characterization, and interaction studies of plant-oil based epoxidized monoesters for polar polymeric materials

Dissertation

zur Erlangung des Doktorgrades der Naturwissenschaften

(Dr. rer. nat.)

der

Naturwissenschaftlichen Fakultät II

Chemie, Physik und Mathematik

der Martin-Luther-Universität

Halle-Wittenberg

vorgelegt von

Herrn Irfan Shahzad

First Reviewer

Prof. Dr. Dariush Hinderberger

Second Reviewer

Prof. Dr. Valentin Cepus

Third Reviewer

Prof. Dr. Ulrich Geise

Date of defence: 04.12.2023

Ich erkläre an Eides statt, dass ich die hier vorliegende Arbeit selbstständig und ausschließlich unter Nutzung der angegebenen Hilfsmittel und Quellen angefertigt habe.

Alle Textstellen, die wörtlich oder sinngemäß aus Veröffentlichungen entnommen sind, habe ich als solche kenntlich gemacht.

Ich versichere weiterhin, dass ich diese Arbeit an keiner anderen Institution eingereicht habe habe.

Mir ist bekannt, dass bei Angabe falscher Aussagen sterben Prüfung als nicht bestanden gilt, und versichere mit meiner Unterschrift die genauen dieser Angaben. Ich erkenne alle rechtlichen Grundlagen an.

_____   _____

Irfan Shahzad   Datum

Abstract

The increasing environmental and toxic health concerns due to phthalate and petroleum-based plasticizers are pushing researchers to eliminate these market leader plasticizers and to find nature-friendly bio-based plasticizers with reduced migration. Which have aroused comprehensive research studies on chemicals obtained from renewable resources, such as plant oils. The present study is also an effort in this regard. Herein, the epoxidized monoester of glycerol formal from soybean oil (Bio oil 1) was investigated as plasticizer in acrylonitrile–butadiene rubber (NBR). Since the migration of plasticizers not only have environmental impact but also effects the durable performance of the product. A robust method for the investigation of these migrating penetrants (plasticizers) was developed where the migration of the plasticizer from plasticized NBR sample to unplasticized NBR sample during short-term thermal ageing was investigated using infrared spectroscopy (IR). Which can serve as a swift handy tool to predict the life span of the product under different environmental conditions. P[1] To further reduce the migration, Bio oil 1 was synthetically modified to carbonated monoester of glycerol formal (Bio oil 2) in the presence of tetrabutylammonium bromide catalyst (TBAB) and constant supply of CO_2 gas, so that the polarity of the plasticizer is enhanced, and its migration is curtailed. Corresponding migration analysis demonstrated reduction in migration with this modification step. While the mechanical analysis presented comparable results to Bio-oil 1. Moreover, this green modification step not only adds value to the product by reducing migration but also contributes to mitigate the global issue of CO_2 by utilizing it in a chemical reaction. P[2] Although this cycloaddition reaction needed optimization, as tedious reaction time of 70 hours under atmospheric pressure conditions was required due to the steric hindrance offered by the internal epoxy groups and mass transfer limitations due to the two-phases (gas-liquid) involved. Different approaches were evaluated to optimize reaction output and the time required to complete the cycloaddition of CO_2 in Bio oil 1. Deep eutectic solvents (DES) along with the conventionally used TBAB catalyst demonstrated best results under high pressure conditions of 40 bars while the catalyst system comprising Potassium iodide (KI) and 18-crown-6 ether as phase transfer catalysts provided satisfactory conversion results. P[3]

Contents

Publication List

1) I. Shahzad, S. Wittchen, V. Cepus,

   "***In situ* migration analysis and diffusion coefficient determination of bio-based plasticizer from NBR using FTIR-ATR and estimation of migrated plasticizer contents by TGA analysis**"

   Macromolecular symposia **2019,** DOI: 10.1002/masy.201800158

2) I. Shahzad, M. Rahman, S. Wittchen, K. Reincke, B. Langer, V. Cepus,

   "**Synthetical modification of plant oil-based plasticizer with CO_2 leads to reduced migration from NBR rubber**"

   Journal of Applied polymer science **2021,** DOI: 10.1002/app.51854

3) I. Shahzad, V. Cepus,

   "**CO2 cycloaddition to plant oil based epoxidized monoester: Optimization and catalyst screening**"

   Macromolecular symposia **2022,** https://doi.org/10.1002/masy.202100508

4) *S. Wittchen, H. Kahl, D. Waltschew, I. Shahzad, M. Beiner, V. Cepus,

   "**Diffusion coefficients of polyurethane coatings by swelling experiments using dielectric spectroscopy**"

   Journal of Applied polymer science, **2020,** DOI: 10.1002/app.49174

*4th publication will not be the part of this thesis work, as the work was not related to this project work.

List of abbreviations and symbols

ACN	Acrylonitrile content
ASTM	American society for testing and materials
ATR	Attenuated total reflection
BBP	Butylbenzyl phthalate
Bio-oil 1	Epoxidized monoester of glycerol formal from soybean oil
Bio-oil 2	Carbonated monoester of glycerol formal from soybean oil
$CaCl_2$	Calcium chloride
CBS–N	Cyclohexylbenzothiazole-2-sulfenamide
$CDCl_3$	Chloroform
DBP	Di-n-butyl phthalate
DEHP	Bis(2-ethylhexyl) phthalate
DEHT	Di-(2-ethylhexyl) terephthalate
DESs	Deep eutectic solvent
DIDP	Di-isodecyl phthalate
DINP	Di-isononyl phthalate
DNOP	Di-n-octyl phthalate
ECGE	Epoxidized cardanol glycidyl ether
EDS	Energy dispersive X-ray spectroscopy
EFAME	Epoxidized fatty acid methyl ester
ESBO	Epoxidized soybean oil
EVO	Epoxidized vegetable oils
FAME	Fatty acid methyl ester
FTIR	Fourier transform infrared spectroscopy
GC/MS	Gas chromatography/Mass spectroscopy
HBD	Hydrogen bond donor
IL	Ionic Liquids
IR	Infrared radiation

IRHD–m	international rubber hardness degree–microtest
IUPAC	International Union of Pure and Applied Chemistry
KI	Potassium Iodide
NBR	Acrylonitrile–butadiene rubber
ODR	Oscillating disc rheometer
PEG-400	Polyethylene glycol with a molecular weight of 400
Phr	Parts per hundred rubber/resin
P-NBR	Plasticized NBR
Ppm	Parts per million
PTC	Phase transfer catalyst
PVC	Polyvinyl chloride
S	Sulfur
SEM	Scanning electron microscopy
TBAB	Tetrabutylammonium bromide
TEBACl	Triethylbenzylammonium chloride
TGA	Thermogravimetric analysis
UP-NBR	Unplasticized NBR
UV	Ultraviolet radiation
Zn	Zinc
ZnO	Zinc Oxide
^{13}C-NMR	Carbon 13 nuclear magnetic resonance spectroscopy
^{1}H-NMR	Proton nuclear magnetic resonance spectroscopy
6PPD –N	(1,3-dimethylbutyl)-N'-phenyl-p-phenylenediamine

Symbols

A_t Carbonyl-peak area at time t

A_∞ Carbonyl-peak area at equilibrium

L Pathlength of the evanescent infrared beam into the sample

D Diffusion coefficient

t_2 Scorch time during vulcanization

t_{90} Cure time during vulcanization

F_m Maximum torque

F_a Minimum torque

F_t Torque at 90% of the maximum torque

σ_{max} Tensile strength

ε_R Tensile strain at break

T_s Tearing strength

δ Chemical shift

T_g Glass transition temperature

1. Introduction

1.1 Motivation

To comply with the very large scope of applications, polymeric materials are modified by various additives. Few properties which are incorporated using these additives include flame retardancy, UV protection, and electrical conductivity. Concerning versatility and flexibility, it will not be wrong to say that polymers owe to plasticizers. Plasticizers are primarily added to improve the flexibility and processability of polymers by lowering the second order transition temperature (Tg). These are low molecular weight (generally low volatility) liquids which by forming secondary bonds to the polymer chains keep the chains apart, thereby partly reducing polymer-polymer chain interactions due to secondary bonding and provide more ease of mobility to macromolecules which results in a flexible and soft final product [1][2][3].

The most significant commercial application of plasticizer in polymers is in polyvinyl chloride (PVC) production, as non-plasticized PVC is hard and rigid. Among the commercially used plasticizers in vinyl industry, Diesters of Phthalic acids leads the way. A prominent example of these plasticizers includes Di-2-ethylhexyl phthalate (DEHP) which served as a benchmark for industrial standards. However, a drawback associated with the usage of these plasticizers is their migration and leaching to the surface since they are not chemically bound to the polymer matrix. This loss of plasticizer is one of the major factors contributing to the ageing of flexible PVC, making it useless for many applications [4][5]. The "new car smell" is also often related to plasticizers or their degradation products [6]. Moreover, since the phthalate-based plasticizers are notorious to be toxic and deemed to cause disorder in human reproduction system and endogenous hormones. Their usage as plasticizers in polymers and elastomers received tremendous amount of criticism from researchers. Consequently, studying the human exposure to these compounds has become an essential topic to prevent associated adverse effects to human health.

Besides these plasticizers also play a significant role in rubber formulation, as they assist to improve processing, reduces tackiness to machine parts, improves filler dispersion, and flow of the unvulcanized compound. Moreover, enhances the low temperature performance of the vulcanized compound, last but not the least reduces production cost [7]. Among the different

plasticizers used in elastomers, the petroleum-based oils find their usage quite extensively in rubber compounding [8]. But they are nonrenewable in nature and in some cases the aromatic contents of certain mineral oils are known to be carcinogenic [7]. A competent replacement to theses mineral oils should not only overcome the beforementioned problems but also have good compatibility with elastomers, as otherwise it may bleed out which can affect physical properties and gives a sticky surface.

NBR, the unsaturated copolymer of acrylonitrile and butadiene is an important polar elastomer and mostly finds its applications where oil resistance and low gas permeability is of paramount importance, particularly for oil resistant rubber sealing applications in automotive, aviation and petroleum industries [7][9][10][11]. Filler is usually incorporated into NBR matrix to enhance its mechanical properties, although its viscosity is increased making it difficult to process. So, plasticizer is added as an extender which not only reduces the mixing time but also imparts the required flexibility to the final product.

Sustainable and harmless bio-based plasticizers have been the focus of research lately to replace these market leader phthalate-based plasticizers. In this regard, considerable efforts have been devoted to the replacement of phthalates. Besides synthetic plasticizers, bio-oil derived plasticizers are also recommended. Many vegetable oils e.g., coming from soybean, linseed, palm, castor bean can serve as adequate plasticizers after suitable chemical modification. One of the most significant methods being employed recently to produce bio-compatible plasticizer is the epoxidation of vegetable oils and their fatty acids methyl esters. Epoxidized Soyabean oil (ESBO) is known for a long time as an important secondary plasticizer in many PVC formulations due to its dual role as plasticizer and stabilizer [12]. ESBO usage as primary plasticizer in PVC demonstrated acceptable plasticizing properties but their prolonged UV-exposure resulted in sticky surface indicating exudation phenomena [13]. Plasticizers obtained by the epoxidation of olive, corn, cottonseed are also reported in literature [14].

Epoxy biodiesels (Epoxidized fatty acid methyl esters (EFAME)) were developed recently as bio-based plasticizers, as they have better lubricity, compatibility and dispersibility in polymer matrix than epoxidized vegetable oils (EVO) and gives better flexibility to the plastic even at low temperature and, therefore, can be used as primary plasticizers [15] [16]. Epoxidized methyl ester of soybean oil, which is a monoglyceride (three time less molecular weight as compared to triglyceride), is more compatible with PVC as it can penetrate easily through the

polymer chains. However, an adverse effect of migration is associated with this plasticizer due to lower molar mass [17]. Chiaradia et al. [18] tried to overcome this problem in their patent work by esterifying fatty acid (vegetable oil) with cyclic hydroxy acetal or hydroxy ketal and then epoxidizing the double bonds in hydrocarbon chain. The obtained epoxidized monoester of glycerol formal plasticizer (Bio oil 1) from soybean oil was claimed to have less migration and can be utilized up to 50 phr. All these intriguing properties made the EFAME a competitive candidate for the plasticization of polymers/elastomers.

The aim of this work was to synthetically modify the epoxidized fatty acid methyl ester (EFAME) based on vegetable oil to enhance its polarity so that its migration from the matrix is reduced. Moreover, it imparts good mechanical properties to the material. Meanwhile, a laboratory grade epoxidized fatty acid methyl ester with glycerol formal based on Soybean oil (Bio-oil 1) was modified by following a conventional carbonation reaction using TBAB catalyst for 70 hours and characterized using different analytical techniques including FTIR, ^{1}H-NMR, ^{13}C-NMR, GPC, and GC-MS. Afterward, this modified oil (Bio-oil 2) and pristine oil (Bio-oil 1) along with other additives were incorporated in Nitrile butadiene rubber (NBR) during compounding. After the vulcanization step samples were evaluated for different properties for example, in situ migration analysis, tensile testing, tearing testing, and hardness test. Moreover, light microscopic and Scanning electron microscopic (SEM) analysis along with energy dispersive x-ray spectroscopic (EDS) analysis was also performed to check the dispersion of the oil in the matrix. Since the tedious reaction time of 70 hours was required for the carbonation reaction, optimization of the reaction was carried out following three different strategies. Where the deep eutectic solvents (DESs), simple catalysts based on potassium Iodide (KI) and different phase transfer catalysts (PEG 400/600, crown ether) and lastly a co-catalyst system was evaluated. The corresponding experimental procedures, important parameters and results are discussed herein this thesis work.

1.2 Outline of the thesis

In the present work [19], epoxidized monoester of glycerol formal from soybean oil (Bio oil 1) was investigated as plasticizer in NBR. Here, the migration of the plasticizer from the plasticized NBR sample to unplasticized NBR sample during short-term thermal ageing was investigated using infrared spectroscopy (IR).

To further reduce the migration, the epoxidized monoester of glycerol formal based on soybean oil was synthetically modified to carbonated monoester of glycerol formal in the presence of tetrabutylammonium bromide catalyst and constant supply of CO_2 gas, so that the polarity of the plasticizer is enhanced, and its migration is curtailed. Corresponding mechanical and migration analysis were performed on NBR samples prepared using modified (Bio-oil 2) and pristine oil (Bio-oil 1).

Although this simple chemical carbonation reaction needed optimization, as tedious reaction time of 70 hours under atmospheric pressure conditions was required due to the steric hindrance offered by the internal epoxy groups and mass transfer limitations due to the two-phases (gas-liquid) involved. Three different approaches were evaluated to optimize reaction output and the time required to complete the cycloaddition of CO_2 in epoxidized monoester of soybean oil with glycerol formal. In first approach deep eutectic solvent (DESs) was utilized along with conventionally used TBAB (tetrabutylammonium bromide) catalyst to analyze the effect of DESs on reaction, while in second approach simple catalyst system comprising KI (potassium iodide) and PEG 400 (Polyethylene glycol with a molecular weight of 400) or 18-crown ether as phase transfer catalysts was investigated. In the third strategy, a co-catalyst system along with onium halide was employed.

2. Theory

2.1 Methods

2.1.1 Infrared Spectroscopy (IR)

IR spectroscopy is one of the mostly widely used spectroscopic technique employed by chemists to identify the structures of compounds under investigation. This spectroscopic technique deals with the infrared region of the electromagnetic spectrum, that is light with a longer wavelength and lower frequency than visible light. The infrared portion of the electromagnetic spectrum is mostly divided into three regions, the near IR region, mid IR region, and the far IR region. The near IR region, which is higher in energy, approximately 14000-4000 cm^{-1} can excite overtone or harmonic vibrations. The mid IR region which expands from 4000-400 cm^{-1} is mostly used to study the fundamental vibrations and helps to identify the associated structure of the functional group. While the far IR region which ranges from 400-10 cm^{-1} has low energy and can be used for rotational spectroscopy. [20]

Theory of IR Spectroscopy

To obtain an IR spectrum, IR radiations is passed through the sample and the fraction of incident radiation which is absorbed at a particular energy is determined. The specific energy at which any peak in an absorption spectrum appears correlates to the frequency of a vibration of a part of a sample molecule. [21]

IR absorptions only occurs in those molecules which show change in their electric dipole moment during the movement. The atoms in a molecule can move relative to one another, that is, bond length can vary, or one atom can move out of its present plane. This description corresponds to stretching and bending movements which are collectively termed as vibrations. These vibrations can involve either change in bond length due to stretching or bond angle e.g., due to bending. The stretching in bonds can be in-phase which is called symmetrical stretching or out-of-phase which is asymmetric stretching. In case of different terminal atoms, then the stretching modes are neither symmetric nor asymmetric, but will have varying proportions of stretching motion of each group. In simple words, the amount of coupling will vary.

Even for a simple molecule there will be many different vibrations. The complexity of an IR spectrum arises from the coupling of vibrations over a large part of or over the complete molecule and are termed as skeletal vibrations. Bands related to skeletal vibrations are likely to conform to a pattern or fingerprint of the molecule as a whole, rather than a specific group within the molecule.

2.1.1.1 Attenuated total Reflection (ATR) Technique

The solid or liquid sample is brought near the optical element where a light is totally internally reflected and where the sample interacts with the evanescent wave. The effective path length for this interaction depends on several parameters and it is typically a fraction of the wavelength. Since the light penetration depth is small, this ATR technique is appropriate for highly absorbing samples and for surfaces and thin film measurements. Generally, the ATR spectra are like regular transmission, However, for thick samples when spectra are recorded at angles greater than the critical one, the wavelength dependance is observed. In this case penetration depth can be defined by the following equation

$$L = \frac{\lambda}{2\pi\sqrt{n_1^2 - sin^2(\theta) - n_2^2}} \tag{1}$$

Where L is the penetration depth of evanescent wave, λ is the wavelength of IR radiation, n_1 and n_2 are the refractive indices of flat diamond crystal and sample respectively and Ɵ is the angle of incidence. [22]

2.1.1.2 Background and derivation of the main equation used to determine diffusion coefficient

To elaborate the derivation of the main equation (19) used in the first publication, the literature work of Barbari et al. [23] must be explained in detail from where the main idea was inspired. Conventionally the method of sorption kinetics is applied to study the diffusion of small molecules in polymers. In this method a polymer film of thickness 2*L* is immersed in an infinite bath of penetrant, and the concentrations at the two surfaces of the film (*z = L* and *z = -L*) are instantaneously established at a concentration, C_s. If the initial concentration of penetrant is zero, then the concentration C, at any spot within the film at time *t* is given by the following equation [6]

$$\frac{C}{C_s} = 1 - \frac{4}{\pi} \sum_{n=0}^{\infty} \frac{(-1)^n}{2n+1} \exp\left[\frac{-D(2n+1)^2\pi^2 t}{4L^2}\right] * \cos\left[\frac{(2n+1)}{2L}\pi x\right] \qquad (2)$$

To obtain the sorbed mass of penetrant by the film as a function of time, the above equation is integrated over the thickness of the film as follow

$$\frac{M_t}{M_\infty} = 1 - \sum_{n=0}^{\infty} \frac{8}{(2n+1)^2\pi^2} \exp\left[\frac{-D(2n+1)^2\pi^2 t}{4l^2}\right] \qquad (3)$$

Where M_t represents the mass sorbed at time t while the M_∞ is the mass sorbed at equilibrium.

For the process which takes place at short times, the above equation (3) can be written, for a thickness of 2l, as:

$$\frac{M_t}{M\infty} = \frac{2}{l}\left[\frac{D}{\pi}\right]^{1/2} t^{1/2} \qquad (4)$$

Plotting $\frac{M_t}{M\infty}$ as a function of $t^{\frac{1}{2}}$, diffusion coefficient can be calculated from the linear portion of the curve, as shown in the figure (1) a. Using equation 4 instead of equation 3, the error is in the range of 0.1 % when the ratio of $\frac{M_t}{M\infty}$ is ≤ 0.5. [25] In the case of long-time diffusion by which there may be limited data at $\frac{M_t}{M\infty}$ ≤ 0.5, Equation 3 can be written as follow:

$$\frac{M_t}{M\infty} = 1 - \frac{8}{\pi^2} \exp\left[\frac{-D\pi^2 t}{4L^2}\right] \qquad (5)$$

The Equation 5 is mostly used in the following form:

$$ln\left[1 - \frac{M_t}{M\infty}\right] = ln\left(\frac{8}{\pi^2}\right) - \frac{D\pi^2 t}{4l^2} \qquad (6)$$

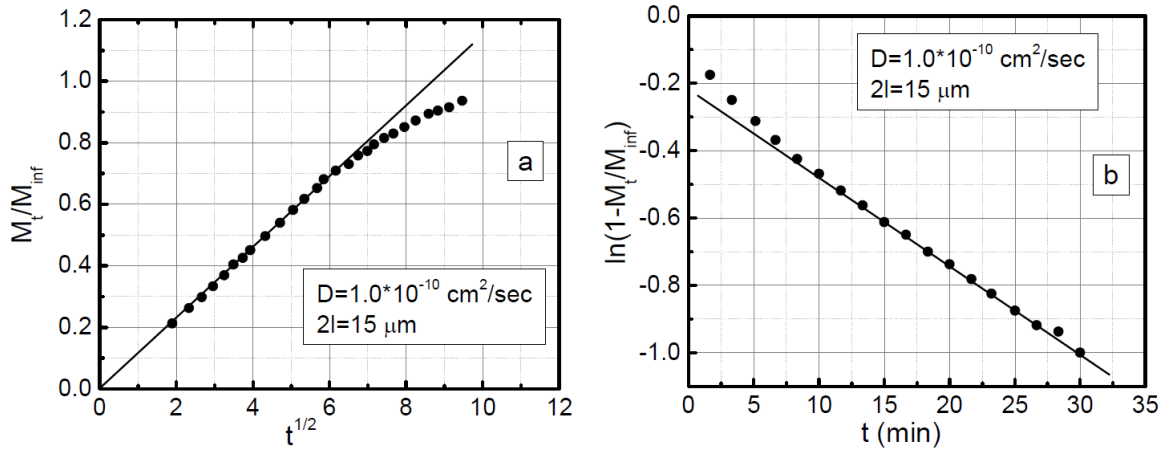*Figure 1. (a) Mt/M∞ versus t^ (1/2) for one-dimensional Fickian diffusion (b) ln (1- Mt/M∞) as a function of t. Data were extracted from literature (Fieldson and Barbari, 1993)*

2.1.1.3 Use of FTIR-ATR spectroscopy to study diffusion in polymers

The root of this technique lies in the relationship between the absorption of electromagnetic waves and the quantity of the absorbing material. This relationship is described by Lambert-Beer law as follow:

$$dI = \alpha I \, dz = -\varepsilon C I \, dz \tag{7}$$

Where I indicate the light intensity at position z, α is the absorbance coefficient, ε is the molar extinction coefficient and C is the concentration of the absorbing group.

Integrating Equation (7) for FTIR transmission spectroscopy, following equation is obtained:

$$A = -\ln\left(\frac{I}{I_0}\right) = \int_{-L}^{L} \varepsilon C dz \tag{8}$$

Where A is the measured absorption, I is intensity of transmitted beam, I_0 is the intensity of incident beam, ε is the molar extinction coefficient, C is the concentration of the absorbing group and $2L$ is the thickness over which the absorbing group is present.

The absorbance explained in equation 8 is comparable to mass uptake in equation 3 as it implies the integration of the concentration profile over the film thickness. However, using transmission acquisition technique, many limitations are imposed like the pat and weigh technique. For example, the polymer must be removed from the penetrant bath and blotted before the spectroscopic analysis. To overcome these limitations, FTIR-ATR spectroscopy was utilized in this work, which can be used to study sorption kinetics while in direct contact with the penetrant. As ATR technique differs from the normal transmission technique in the nature

of the incident light path and an evanescent wave is formed, which is due to the superposition of incident and reflected waves at the surface. Since the requirement that the electric field be continuous through the interface. The electric field strength, E, of the evanescent wave decays exponentially, as represented in the Figure (2).
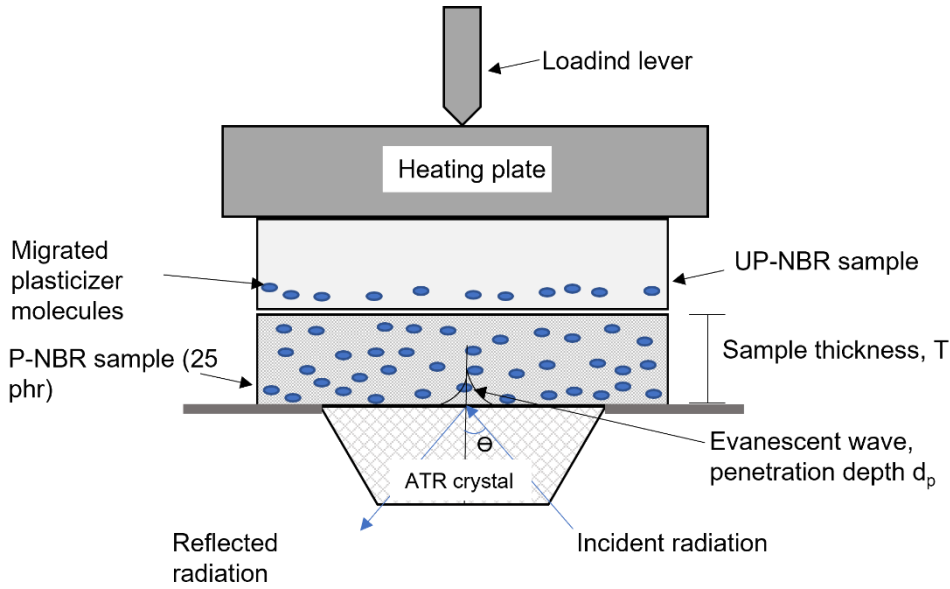

Figure 2. Evanescent wave representation at a totally reflecting interface

The decay of the evanescent field is described by the following equation [7][8]

$$E = E_0 \, exp(-\gamma z) \tag{9}$$

Where E_0 is the electric field strength at the interface and γ is defined as the reciprocal of the penetration depth, which is described as follow

$$\gamma = \frac{2n_2\pi \left(sin^2\theta - \left(\frac{n_1}{n_2}\right)^2 \right)^{1/2}}{\lambda} \tag{10}$$

Where n_1 is the refractive index of the rare medium while n_2 is the refractive index of the propagating medium. When the rare medium absorbs specific frequencies of evanescent wave, the reflection is frustrated and the reflected wave has a reduced intensity at these wavelengths, resulting in an absorption spectrum. It is assumed that only weak absorptions occur due to the small penetration depth of the evanescent wave. Considering this assumption, the following equation is developed

$$\frac{I}{I_0} = e^{-A} \approx (1 - A) \tag{11}$$

Or $\quad\quad\quad dI = -I_0\,dA \tag{12}$

Substituting equation 12 in equation 8 and integrating to obtain:

$$A = \int_0^L \frac{\varepsilon CI}{I_0}\,dz \tag{13}$$

Since in the ATR technique, penetration takes place from one side so the integration is taken from 0 to L. As $I = E^2$, we can substitute the field strength of the evanescent wave in equation 9 and rewrite the above expression for multiple reflections, N, as follow:

$$A = \int_0^L N\varepsilon^* C E_0^2 \exp(-2\gamma z)\,dz \tag{14}$$

Where $\varepsilon^* = \dfrac{\varepsilon}{I_0}$

Substituting equation 2 into equation 14 and integrating gives the following equation:

$$\frac{A_t}{A\infty} = 1 - \frac{8\gamma}{\pi[1 - \exp(-2\gamma L)]} \times \sum_{n=0}^{\infty}\left[\frac{\exp(g)[f\,\exp(-2\gamma L) + (-1^n)(2\gamma)]}{(2n+1)(4\gamma^2 + f^2)}\right] \tag{15}$$

Where,

$$g = \frac{-D(2n+1)^2\pi^2 t}{4L^2} \quad \text{and} \quad f = \frac{(2n+1)\pi}{2L}$$

Equation 15 is analogous to the mass uptake equation used in gravimetric sorption experiment (equation 3), the important difference being that the Fickian concentration profile is convoluted with the FTIR-ATR absorption equation before it is integrated.

In Equation 15, $A\infty$ represents the absorance at equilibrium which is analogous to $M\infty$ and this equation represents an exact solution for ATR technique of penetrant in a thin film. This equation can be modified according to the experimental conditions applied. For example, for the present work all terms in the series beyond the first were eliminated for simplification as follow:

$$\frac{A_t}{A\infty} = 1 - \frac{8\gamma}{\pi[1 - exp(-2\gamma L)]} \times \left[\frac{exp\left(\frac{-D\pi^2 t}{4L^2}\right)\left(\frac{\pi}{2L} exp(-2\gamma L) + (2\gamma)\right)}{\left(4\gamma^2 + \frac{\pi^2}{4L^2}\right)}\right] \quad (16)$$

The values of *L, D*, and γ which are typical for the experimental system used here, absorbances from equation 16 are compared to those from equation 15.

To develop the simplified equation, γ is assumed to be constant, which is not entirely correct since γ depends on the refractive index of the polymer n_1, which can vary as the concentration of the penetrant changes. However, the importance of γ in this equation is dependent on the experimental conditions. Especially, when

$$4\gamma^2 \gg \frac{\pi^2}{4L^2} \quad (17)$$

And

$$1 \gg exp(-2\gamma L) \quad (18)$$

γ can be eliminated from equation 16. This requirement is fulfilled by most of the experimental systems. Following these conditions, equation 16 can be reduced to the final equation 19 as:

$$\frac{A_t}{A\infty} = 1 - \frac{4}{\pi} exp\left(-\frac{Dt\pi^2}{4L^2}\right) \quad (19)$$

which was used in the first publication for diffusion coefficient calculations by plotting $\frac{A_t}{A\infty}$ as a function of time, and the slope of a linear least squares' regression yields a value for the diffusion coefficient, D. This is comparable to the use of equation 6 to determine the diffusion coefficient in gravimetric sorption experiments at long times.

2.1.2 Thermogravimetric analysis (TGA)

In TGA analysis the quantity of the mass change of the samples against temperature and time in a controlled atmosphere for example under the purging of nitrogen gas is determined. [28] This thermal analysis technique can be used to investigate the thermal and oxidative stability.

Moreover, it can be used to determine the compositional properties for example, fillers, plasticizers, polymer resin and solvents of the sample. However, the mass gain/loss of the samples depends on different factors. Mostly, mass gain is associated to the adsorption or oxidation, whereas mass loss is attributed to decomposition, desorption, dehydration, desolvation, or volatilization.[29]

This technique can also be used to determine the low level of volatile matter evolved in polymer system such as plasticizer contents. Plasticizer is often made up of small molecules compared to the base polymeric material, it will migrate to the surface and evaporate from the polymer matrix upon heating. TGA can indicate the percentage of weight loss quantitatively and accurately.

This characteristic was applied to determine the plasticizer contents in the unknown sample by plotting a mass loss percentage content of the similar polymeric systems with step wise increasing plasticizer contents at a specific temperature. The obtained calibration curve, helped to estimate the plasticizer contents in the investigated sample as described in detail in the first publication.

2.1.3 Nuclear magnetic resonance spectroscopy (NMR)

NMR spectroscopy is a powerful analytical technique which provide us information about the overall molecular structure or the framework of C-C and C-H bonds. [30]

Theory

The working principle of this spectroscopic technique is based on the phenomenon in which some atomic nuclei spin about their axes and as a result generate their own magnetic field or magnetic moment. Such nuclei are termed as NMR-active. However, not all nuclei have a magnetic moment, whereas only nuclei with an odd number of protons and/or neutrons have one. From the viewpoint of the quantum mechanical picture of the nucleus in the magnetic field, the theory of NMR spectroscopy is based on the spin quantum number (I). For example, the H atom has an odd atomic mass and atomic number, and upon calculation, it has a spin equal to 1/2, and it shows the NMR spectra.

When the magnetic field is applied to the sample, the total number of possible orientations can be calculated by the formula, $2I + 1$, where "I" is the spin quantum number. As the spin quantum number of the hydrogen is $I = 1/2$, the possible number of orientations will be 2. Hence, there are two possible orientations of the H atom, i.e., $+1/2$ and $-1/2$.
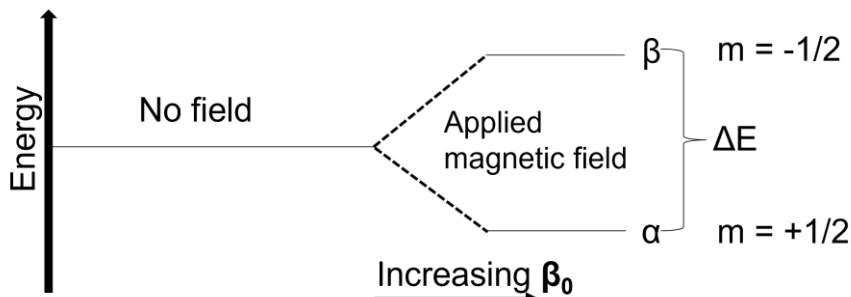
Energy levels for a nucleus with spin quantum number equals 1/2

Nevertheless, nuclei that are important for organic compounds, for example ^1H isotope of hydrogen, the ^{13}C isotope of carbon, the ^{14}N isotope of nitrogen, ^{19}F and ^{31}P are all NMR-active and hence can be observed by this spectroscopic technique. While the other nuclei, such as the common ^{12}C isotopes of carbon and ^{16}O isotope of oxygen, don't possess magnetic moments and therefore cannot be detected by NMR.

When no external magnetic field is applied, the magnetic moment of all its protons is oriented randomly. Although, when the same sample is placed within the field of a strong magnet (applied external magnetic field (B_0)), each proton will attain one of two possible orientations with respect to the external magnetic field. These two orientations correspond to the two spin states termed as α and β. In the α spin state, the proton's magnetic moment is aligned with the direction of external magnetic field B_0, while in the β spin state it is aligned opposite to the direction of applied magnetic field.

The α spin state is slightly lower in energy as compared to the β state, whereas the energy gap between them, ΔE, depends upon the strength of applied magnetic field. In an external magnetic field, slightly more than half of the protons will occupy the lower energy state α, while slightly less than half will occupy the higher spin state β. NMR, exploits this population difference, whereas this difference increases with the strength of applied B_0.

The required energy to excite the protons from α spin state to β spin state is supplied by electromagnetic radiation in the form of radio frequency (RF) region. When a proton in an external magnetic field is exposed to RF radiation with the energy that matches the energy

gap ΔE, the energy of the RF is absorbed and the proton will flip its magnetic moment from the α spin state to β spin state, and the nuclei are said to be in resonance with the electromagnetic radiation.

The radiation frequency absorbed by a proton during a spin transition is termed as its resonance frequency (v). This resonance frequency is directly related to the strength of applied B_0, which can be explained by the following equation

$$\nu = \frac{\gamma B_0}{2\pi}$$

Whereas γ is the magnetogyric ratio, and different nuclei have different values of γ.

Working Principle

When a sample is placed in the strong external magnetic field (B_0) of the device, the protons begin to spin with one of the two spin states. As described earlier, slightly more than half of the protons have the magnetic moment in α spin state, while slightly less than half have β spin state. Afterwards, the sample is exposed to a range of radio frequencies. Only the frequencies that matches the resonance frequencies of the protons are absorbed, causing those protons to spin flip so that they align themselves against applied B_0. When these flipped protons flip back down to their ground state, they emit energy, again in the form of radio frequency radiation. The NMR device detects and records the frequency and intensity of this radiation by using Fourier transform (FT) technique. We observe the NMR spectrum where the FT converts the signal from time versus amplitude to frequency versus amplitude.

Shielding and deshielding effect

If all the hydrogen atoms (protons) in an organic sample had the same resonance frequency, then they would have all presented the same signal, and this spectroscopic technique would not have been of much use for chemists. Fortunately, resonance frequencies are different for different protons in a molecule, which varies depending upon the electronic environment a given proton inhabits.

For hydrogen atoms in any bonds, for example C-H, O-H, etc., the applied external magnetic field causes the s electrons to circulate in a way that generates an induced local magnetic field (B_{local}) at the proton and the direction of this local field is opposite to the applied external field.

The proton therefore experiences a magnetic field, which is smaller in magnitude than the applied magnetic field

$B_{eff} = B_o - B_{local}$

This B_{local}, to a small but significant degree, shields the proton from experiencing the full force of B_o, this effect is called shielding effect. Different hydrogen atoms in an organic molecule have the different electronic environments and possesses different electron densities, therefore have different B_{local} and B_{eff}. That is why different hydrogens are in a different resonance frequency and show different signals in the spectrum.

The hydrogen atoms which are close to electronegative groups, their electron density is withdrawn by the electronegative group and hence shielding of the protons by circulating electrons is diminished. Such hydrogen atoms are said to be deshielded from the external magnetic field and have a higher resonance frequency than shielded protons. As the electronegativity of the substituent group increases, the deshielding effect also increases and so the chemical shift.

2.1.3 Tensile testing

Tensile tests are performed to measure the force required to break a plastic sample specimen and the extent to which the specimen stretches or elongates to that breaking point.

Applying this test, the stress-strain diagram is obtained, which can be a helpful tool to investigate tensile behavior of the material and its properties.

Plastic tensile test device, provide a constant rate of extension because plastic tensile test behavior is dependent on the speed of the test machine. The specimens loaded on the machine are designed as per ASTM, DIN, ISO tensile test specimen dimensions and the machine should always rely on standard terms and conditions.

Importance of tensile properties:

- o Tensile properties provide useful data for plastic engineering design purposes
- o This data helps to ensure quality
- o These tests are quite helpful during development of new materials and processes

- o Last but not the least, these properties are used to predict the behavior of a material under forms of loading other than uniaxial tension

Few of the factors affecting tensile strength:

- o Molecular weight
- o Cross-linking
- o Crystallinity

2.1.4 Scanning electron microscopy coupled with energy dispersive X-Ray (SEM/EDX) Spectroscopy

High resolution images of surface topography, with excellent depth of field, are produced using a highly focused, scanning (primary) electron beam. The main type of signals that are detected are generated from backscattered secondary electrons (BSE), which produces a grayscale image of the sample at very high magnifications.

The electron beam and matter interaction generate variety of signals that carry different information about the sample, e.g., backscattered electrons produce images with contrast that carries information on the differences in atomic number, whereas secondary electrons give information about topography. Cathodoluminescence provides information about the electronic structure and chemical composition of material, while transmitted electrons gives the information about material's inner structure and crystallography. Last but not the least, another widely used signal in SEM is X-rays. [31]

Working principle of EDX analysis:

The generation of X-rays in a SEM is a based on two steps. In the first step, the electron beam hits the sample and transfers part of its energy to the atoms of the sample. This transferred energy can be used by the electrons of the atoms to jump to the energy shell with higher energy or to be kicked off from the atom. In such case, the electron leaves behind a hole. These Holes have a positive charge and attract the negatively charged electrons from higher energy shells. In the second step such kind of transition takes place, where the energy difference of this transition is released in the form of X-rays.

This X-ray has the characteristic energy which depends upon the atomic number and that is unique for every element. In this way, X-rays are a fingerprint of each element and can be used to identify the type of element that exists in a sample.

2.2 An overview of Plasticizers

2.2.1 Definitions

As reported by the International Union of Pure and Applied Chemistry (IUPAC) in 1951, A plasticizer can be defined as a substance or material incorporated in a material (usually a plastic or an elastomer) to increase its flexibility, workability, or distensibility. Which may also play a pivotal role to reduce the melt viscosity, lower the second-order transition temperature (T_g), or lower the elastic modulus of the product without altering the fundamental chemical character of the plasticized material [32].

Amorphous polymers comprise tangled masses of polymer chains. The efficacy to deform this mass depends upon the ability of the polymer chains to untangle and slip past one another. One way of enhancing this ability is by raising temperature, thereby increasing segmental mobility of the polymer chains. While in other way this task can be achieved by adding a low molecular weight (generally low volatility) liquid as an external plasticizer to the polymer. These low molecular weight liquids by forming secondary bonds to the polymer chains keep the chains apart, therefore partly reducing polymer-polymer chain interactions due to pre-existing secondary bonds and provide more ease of mobility to macromolecules which results in a flexible, easily deformable, and soft final product. Which also justifies the major function of plasticizer that is lowering glass transition temperature (T_g) [1].

Plasticizers play significant roles during polymer processing since they reduce tackiness to machine parts, improves filler dispersion, and flow of the unvulcanized compound. Moreover, by optimizing experimental parameters, shortens the mixing time, and the pressure of extrusion, consequently, reduces the production cost. Few of the other properties which also got indirectly effected due to the addition of plasticizers are viscosity, density, and dielectric constant [3].

2.2.2 Classification of Plasticizers

As illustrated in the flow chart Figure 3, plasticizers can be broadly classified into two categories: internal and external plasticizers. Internal plasticizers become the part of the polymer molecule which are either co-polymerized into polymer structure or reacted (grafted) with the original polymer thereby making the polymer chain bulkier and makes it more difficult for polymer chains to fit with each other more compactly. Consequently, the free volume in polymer matrix increases rendering the polymer soft by lowering the glass transition temperature and reducing the elastic modulus [33]. The most widely used internal plasticizers monomers include vinyl acetate and vinylidene chloride to name a few. But this plasticization technique is implemented rarely because the complexity of reaction can lead to longer reaction times and increased costs. Moreover, such plasticized materials show dimensional instability at higher temperatures. Last but not the least every co-polymer is suited to certain flexibility needs which also hinders the extensive usage of this plasticization
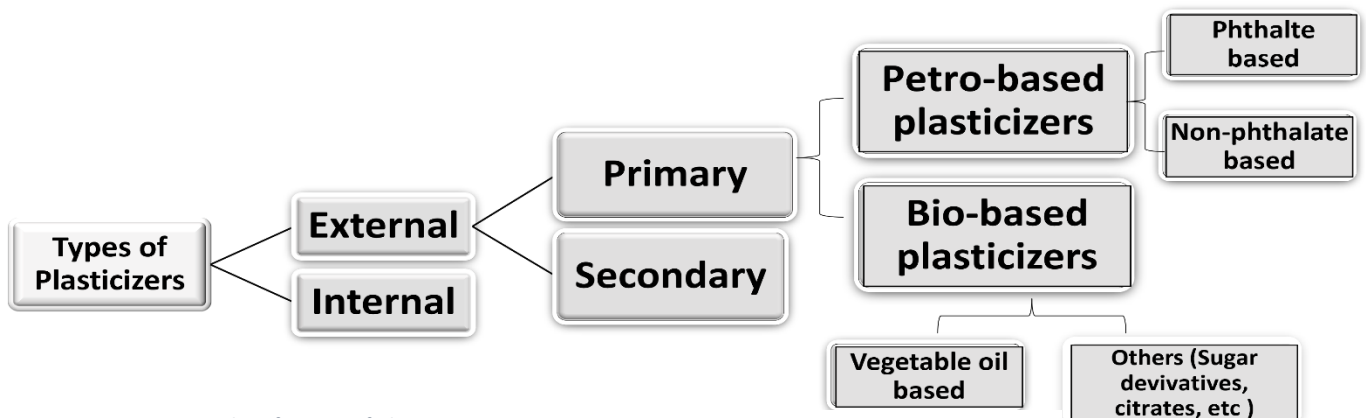

Figure 3. Classification of plasticizers

technique. External plasticizers, on the other hand, are low volatility molecules which are added to interact with polymers without chemical reactions. These molecules are held with polymer chains via weak secondary forces such as dispersion forces, dipole-dipole interactions, and hydrogen bonding. Since these plasticizers are not chemically bonded to the polymer chains they can be lost by migration, evaporation, or extraction phenomena. Despite these drawbacks this plasticization technique is most widespread [3]. The added benefit of using external plasticization technique is the possibility to select the right substance based on the desired product properties (from semi-rigid to highly flexible) [34].

External plasticizers can be further sub-divided to primary and secondary plasticizers. To be called as primary plasticizer, the plasticizer should possess the following features:

a. It should be completely soluble in polymer even at high concentration.

b. It should not exudate from the final material.

c. It should be used as a sole plasticizer.

Secondary plasticizers, on the other hand, have slower gelation ability and have slight compatibility with the polymer which can lead to surface tackiness if used in excess. They are typically blended with primary plasticizers, to improve product properties or to reduce the cost of production.

Last but not the least, they can also be classified as *petro-based* and *bio-based* plasticizers [35]. The petro-based class of plasticizers is dominated by phthalate ester which accounts for almost 80 % of the total consumption of the plasticizers. Due to this domination, the petro-based plasticizer market can be further sub-divided into phthalate-based and non-phthalate-based plasticizers. The general chemical structure of phthalate ester is represented below:
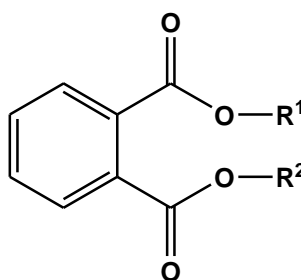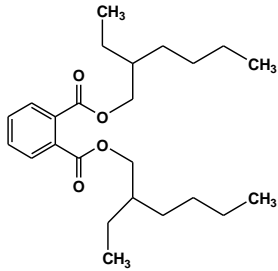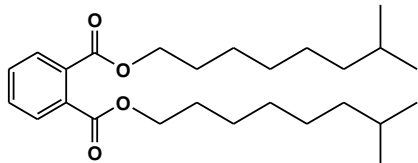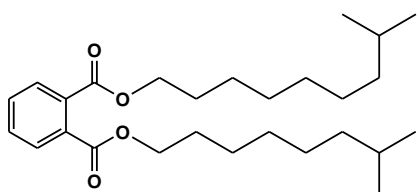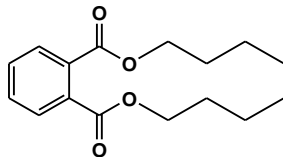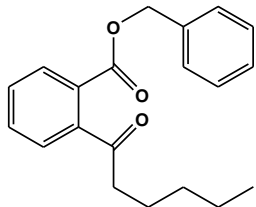

Figure 4. General chemical structure of phthalate ester plasticizer

2.2.2.1 Phthalate-based Plasticizers

Previously Di-(2-ethylhexyl) phthalate (DEHP) was the leading phthalate based plasticizer which accounted for above 50% of the worldwide phthalates production [36]. But as described earlier due to its toxicity and potential endocrine disruption activity other high molecular weight phthalates e.g., Di-(2-ethylhexyl) terephthalate (DEHT), Di-isononyl phthalate (DINP), Di-isodecyl phthalate (DIDP), Di-n-octyl phthalate (DNOP) and few low molecular weights such as Di-n-butyl phthalate (DBP) and butylbenzyl phthalate (BBP) have been produced to replace this market leader phthalate. Among these plasticizers DINP has significantly replaced DEHP in the applications like child toys and health care. Since it possesses longer hydrocarbon chains

and higher molecular weight it presents slower migration rates. The chemical structures and the major applications of commonly used phthalate-based plasticizers are listed in Table 1.

Table 1: Chemical structures and major applications of commonly used phthalate-based plasticizers

Phthalate name	Abbreviation	Chemical formula	Previous uses
Di-(2-ethylhexyl) phthalate	DEHP		PVC (toys, shoes, medicals devices, cable insulation, flooring, storage bags)
Di-isononyl phthalate	DINP		PVC (toys, teethers, spoons, gloves, beverage straws)
Di-isodecyl phthalate	DIDP		PVC (flooring, electrical cable insulation, seat covers for cars)
Di-n-butyl phthalate	DBP		PVC, PVA (polyvinyl alcohol) and rubber
Butyl benzyl phthalate	BBP		PVC (vinyl flooring, adhesives, sealants, conveyer belts, food wrapping material and artificial leather), PU (polyurethane)

2.2.2.2 Non-phthalate based Plasticizers

Other non-phthalate chemical families employed as plasticizers includes, Trimellitates, Phosphates, Adipates, Sebacates and, Polyesters [37]. Among these listed compounds, Adipates are widely used in PVC artefacts, while others find their usage in specific applications because of their high price therefore cannot be utilized in commodity applications. Since the plasticizer market is dominated by phthalate-based plasticizers these plasticizers could not receive much attention from researchers, therefore their potential effects on human health and environment still needs to be explored. Although many of these alternative plasticizers have presented promising application potential [38].

2.2.2.2.1 Bio-based Plasticizers

Keeping in mind the before mentioned issues (leeching and toxicity) with petro-based plasticizers, an adequate 'green' replacement should be non-toxic, miscible with polymer, comparatively efficient, highly resistant to migration phenomena and last but not the least should be relatively cheap. Bio-based plasticizers can be obtained from the by-products and wastes of agricultural resources which are sustainable, cheap, and readily available.

Vegetable oils

Vegetable oils which are extracted from oleaginous trees and plants are one the major sources for bio-based plasticizers. These oils are based on the varied compositions of fatty acids which are dependent on plant and its growing conditions [39]. Chemically, these oils are mostly composed of triglycerides which constitute glycerol and various fatty acids as shown in Figure 4. The fatty chains and ester groups present in the vegetable oil make them good candidate to be employed as plasticizer. As the fatty chains insert themselves between the polymer chains and act as a 'spacer' thereby increase intermolecular spaces and enhance chain mobility. While the ester group helps to improve compatibility by interacting with polymer chains via week secondary forces e.g., van der Waals interactions. Despite these characteristics some further chemical modifications are required to increase the compatibility of vegetable oils with polymer. The ester groups and the double bonds present in the triglyceride structure are susceptible for chemical modification. As represented in Figure 5, modified glycerol and fatty esters can be utilized as plasticizer after transesterification

reaction. The double bonds present in triglyceride or fatty esters can undergo modifications by epoxidation, acetylation or by Diel-Alder reactions.

Figure 5. Fatty acid derivatives coming from vegetable oils. The figure is redrawn from JOURNAL OF POLYMER SCIENCE, PART A: POLYMER CHEMISTRY 2016, 54, 11–33

Epoxidized Soybean oil (ESBO) is long known as secondary plasticizer utilized in PVC formulation due to its dual role as plasticizer and stabilizer. Since it scavenges HCl molecules generated during PVC thermal degradation. But as described earlier it is not used as primary plasticizer due to the exudation phenomena observed during its utilization. Epoxidation of the oils obtained from other oleaginous plant sources e.g., olive, corn, cottonseed, sunflower, and palm oil was also performed to check their suitability to be used as plasticizer [14][40][41]. However, most of these reported epoxidized oils performed well as secondary plasticizer in PVC, Although the epoxy esters based on palm oil demonstrated poor compatibility since it has very few double bonds [42].

2.2.2.2.2 Chemical modification

These epoxidized tri-esters or fatty alkyl esters can undergo further synthetical modification to achieve a performance-oriented plasticizer with specific properties for example reduced migration and/or fire retardancy. Chiaradia et al. [18] tried to reduce the migration of fatty acid alkyl ester in their patent work by esterifying fatty acid (vegetable oil) with cyclic hydroxy acetal or hydroxy ketal and then epoxidizing the double bonds in hydrocarbon chain. The obtained plasticizer as presented in Figure 6, was claimed to have less migration, and can be utilized up to 50 phr in PVC.

Methyl ester of epoxidized oleic acid

Glycerol formal ester of epoxidized Oleic acid
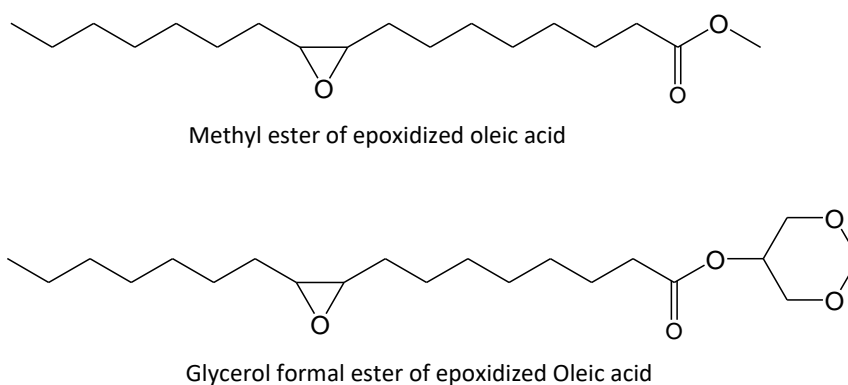
Figure 6. Epoxidized ester of glycerol formal with Oleic acid

Puyou Jia et al. [43] modified a castor oil-based plasticizer to obtain a flame-retardant plasticizer as represented in Figure 7, which also demonstrated better leaching resistance properties than DOP.
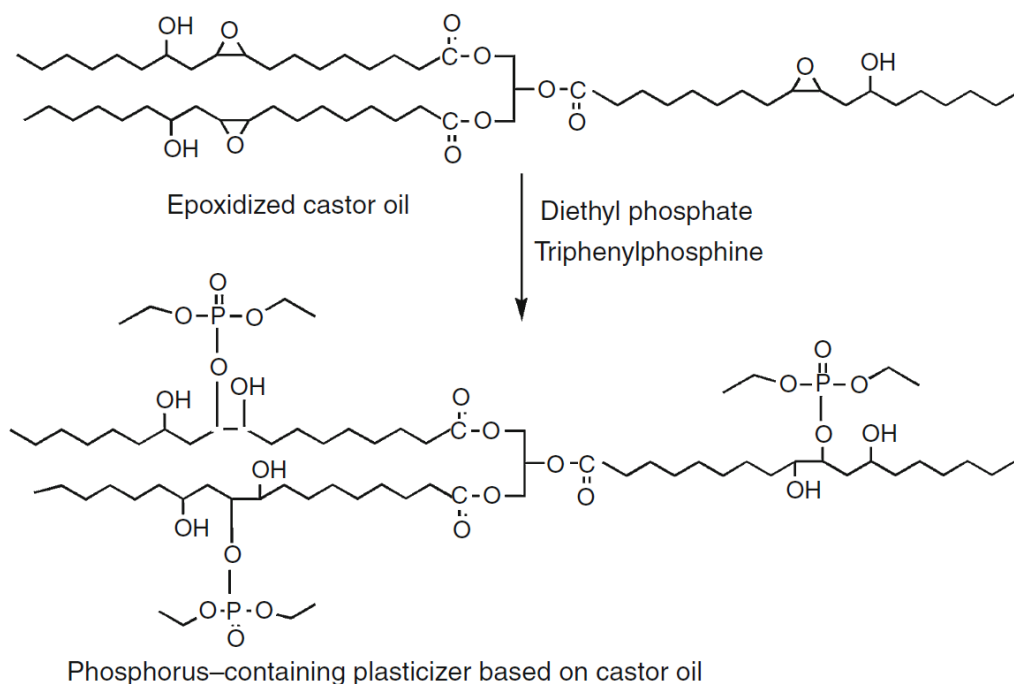
Figure 7. modification of castor oil to obtain flame retardant plasticizer. The figure is redrawn from J Therm Anal Calorim (2015) 120:1731–1740

Moreover, by ring-opening of the epoxy groups, acetylated oils can be obtained which have good plasticization properties. Various catalysts were evaluated for the ring-opening of epoxy group, among them quaternary ammonium salts demonstrated best results [44][45].

Cardanol oil has recently emerged as promising renewable source. It is obtained by the distillation of cashew nutshell liquid which is a nonedible by-product of cashew. It is of particular importance because its chemical structure is not composed of conventional triglycerides as represented in Figure 8. The oil comprises more than one compound since the side chains varies in the degree of unsaturation, on average two double bonds are present in each compound which are susceptible for chemical modification e.g., epoxidation. Chemical and physical properties of epoxidized cardanol based plasticizer have demonstrated similar properties to DOP plasticizer [46].

Epoxidized cardanol glycidyl ether (ECGE)
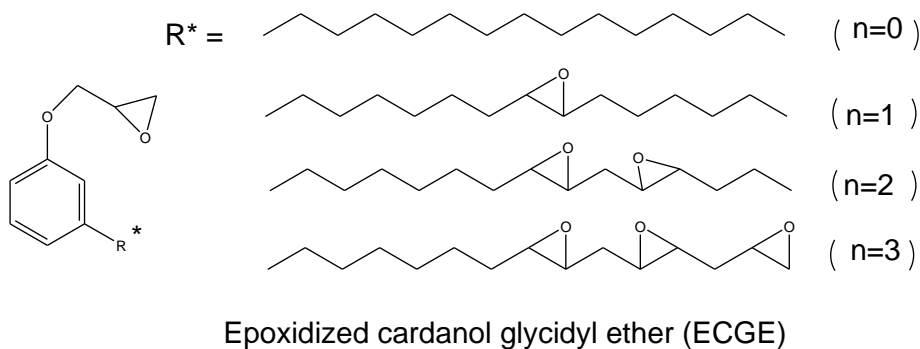
Figure 8. Epoxidized cardanol glycidyl ether

Few of the well-known bio-based plasticizers which are developed on the industrial scale to replace petro-based plasticizers are listed as follow [3]. For example, Danisco claims a fully biodegradable plasticizer (Grindsted® Soft-N-Safe®) which is produced by the acetylation of castor oil. Arkema developed few bio-based plasticizers (Virkoflex®) which are based on epoxidized soybean oil (ESBO) and epoxidized esters for PLA and PVC plasticization. Novance prepared some plasticizers (Radia®) based on soybean, rapeseed oil and epoxidized fatty esters especially for PVC. While DSC® named plasticizer was developed by Jayant-Agro-Organics which is based on castor oil and claimed to be fully bio-based plasticizer.

Other by-products and wastes of agricultural resources which can be used as plasticizer after modifications include, e.g., starch and cellulose obtained from cereals (wheat, potatoes, corn, straws), Tall-oil and Tung-oil from trees(tung tree, chestnut, pines) and citric acid coming from citrus fruits [3].

2.3 Mechanisms of Plasticization

Several theories were developed to explain the action of plasticizer in the polymer matrix. While a number of reviews were also published by distinguished researchers in this regard which highlighted three primary theories explaining the plasticization mechanism [47][3][32].

2.3.1 The Lubricity Theory

This theory can be ascribed to Kirkpatrick [48], Clark [49], and Houwink [50] among others. According to this theory plasticizer molecules in the polymer matrix act as a lubricant allowing the polymer chains to glide pass each other when an external force is applied to the plasticized polymer. Assuming that the unplasticized polymer chains do not move freely because of

surface roughness. Thus, in accordance with this theory, a plasticized polymer can be represented as parallel alternating layers of polymer and plasticizer [37][47] as represented in the Figure 9. Moreover, it is also assumed in this theory that the plasticizer molecules break the pre-existing secondary bonds among the polymer chains and make new weak secondary bonds to the polymer chains masking the inter chain bonds to reform [37][47]. In conclusion this theory assumes that the rigidity in polymers is due to the internal friction among the polymer chains and the plasticizer act as lubricant easing the chains to slide pass each other [3].

2.3.2 The Gel Theory

This theory can be attributed to Aiken [51] and others [52]. According to this theory polymer chains are held by secondary forces at varying intervals and these plasticizers enhances the random motion of polymer chains in the regions where the chains are non-associated. Thus, forming the gel structure either due to permanent intermolecular forces or by forces which exist and disappear in dynamic fashion as plasticizer solvates then desolvates theses regions [47]. This theory assumes that rigidity in the polymers is due to the secondary bonds among the polymer chains and the plasticizers reduces these sites of attraction [3] as represented graphically in the Figure 9.

2.3.3 The Free Volume Theory

This is the most widely accepted theory explaining the action of plasticizer in polymer matrix which was postulated by Fox and Flory [53]. This theory attempts to justify the reduction in polymer glass transition temperature upon the addition of plasticizer. The glass transition temperatures (T_g) of the polymers can be defined as a change from hard, non-crystalline, glass-like materials to a rubbery solid. It was established that the specific volume of the polymer diminishes linearly with the decrease in temperature until the T_g is approached, below this temperature diminution in specific volume takes place but at much slower rate. This increase in the specific volume above T_g was ascribed to free volume (internal space available among polymer chains) [37]. In rigid polymers very little free volume is available for the chains to move, although when plasticizer molecules are added in the polymer matrix, they increase the free volume allowing more mobility to polymer chains rendering the polymer soft and rubbery. This increase in free volume is preserved when the polymer-plasticizer mixture is

cooled down after melting. According to Sears and Darby [54] free volume comes from three principal sources:

1. The motion of chain ends

2. The motion of side chains

3. The motion of the main chain

This theory reflects more precisely the action of plasticization as compared to the other two theories since it is based on the relationships between variables like molecular weight and terminal group contents and their effect on the properties like specific volume and viscosity [3]. A graphical representation of the plasticization mechanism about this theory is depicted in Figure 9.
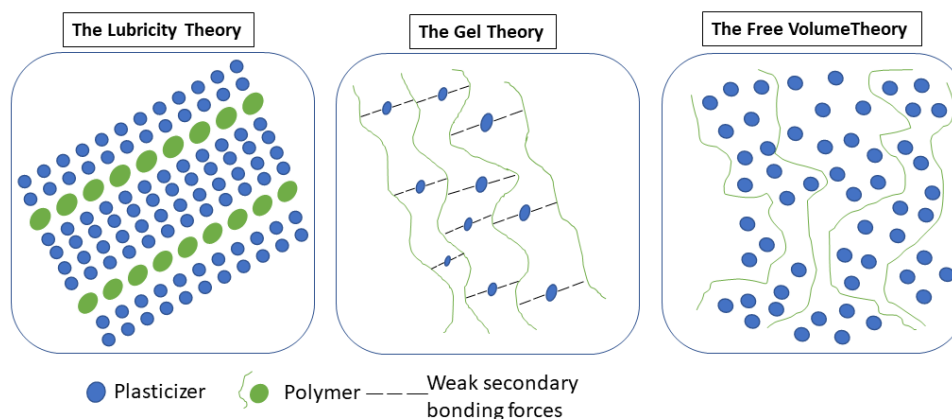
Figure 9. Graphical representation of plasticization theories. The figure is redrawn from JOURNAL OF POLYMER SCIENCE, PART A: POLYMER CHEMISTRY 2016, 54, 11–33

2.4 Migration of plasticizer and strategies to reduce migration

Under different environmental and loading conditions, the plasticizer molecules tend to migrate out of the product due to their low-molecular weight [55][56]. The loss of plasticizer is one of the major factors contributing to the ageing of flexible PVC, making it useless for many applications [4][5]. Some of the major mechanisms by which plasticizer molecules can release include, loss by volatility or evaporation, migration into liquids, migration into solids and last but not the least it can also exudate under pressure [57].

Different strategies were adopted by various research groups to diminish this migration process. Yuan et al. [58] covalently attached chlorinated paraffin (CP-52) to Di (2-ethyl hexyl) phthalate (DEHP) plasticizer to curtail plasticizer migration. The obtained plasticizer was claimed to be highly compatible and non-leaching. Jayakrishnan et al. [59] modified the surface structure of flexible PVC samples by carrying out nucleophilic substitution of chlorine by sodium azide in aqueous media with tetrabutyl ammonium bromide as phase transfer catalyst. It was found that the leaching was considerably reduced, although, color change was observed probably due to dehydrochlorination occurred during grafting process and the elongation at break was reduced considerably. Effect of plasma-induced surface crosslinking of flexible PVC packaging films on limiting leaching of plasticizer molecules was investigated by Audic et al. [60] Argon plasma was found to give best results and the reduction in leaching tendency was observed with increasing plasma treatment time. While others tried treatment or coating to reduce plasticizer migration. [61] In the present work synthetical modification route was adopted to achieve the task of reduction in migration.[62]

Several studies have been performed to observe the permeation and diffusion of plasticizer through polymers [63]. As there is an increasing interest in efficient measuring methods for characterizing the diffusion behavior of low molecular weight additives in polymer matrices. However, various problems are associated with most of the methods, for example, high expense in terms of time and preparation and the application limitation imposed by the measuring principles.

Lundsgaard et al. [64] observed the migration process of plasticizers into liquids via gas chromatography/mass spectroscopy (GC/MS) technique and studied their dynamics. Rosca et al. [65] investigated the diffusion of phthalates in nitrile rubber using FTIR spectroscopy by following the macroscopical (time-lag) method and microscopical (concentration-distance) method. Plasticizer structure, contents of nitrile group and cross-linking density of the rubber were highlighted as important factors affecting diffusion of plasticizer. In another literature work [66], the ability of plasticizer to migrate from polyvinyl chloride (PVC) to another polymer was investigated. Few of the important factors which influence plasticizer migration from the polymer matrix include [57]:

- Polymer type, its compatibility with the plasticizer and its molecular weight,

- Plasticizer type and its concentration, its molecular weight, branching and polarity greatly influence its interaction with polymer matrix,

- the plasticization process and the homogeneity of the product.

Thorough investigations are prerequisite to determine the optimal end use and life span of the product. Primarily, the investigations of plasticizers are being done in polyvinyl chloride while their behavior in elastomers still need more research. The present work is an effort in this regard, where the FTIR spectroscopic and TGA thermal investigations are performed to characterize the migration of bio-based plasticizers in acrylonitrile–butadiene rubber (NBR). Infrared spectroscopy is an efficient technology for the identification of polymer, evaluation of raw materials, polymer blend ratio calculation, microstructure determination and last but not the least for the in-situ analysis of migration processes [67] [68]. In one of the reported literature work [69], ratio of characteristic absorbance peaks obtained by FTIR were correlated with acrylonitrile contents determined by Kjeldhal method. In another literature work [4] [66], TGA analysis was performed to establish the mass-loss relation with the plasticizer contents. FTIR-based monitoring of plasticizer loss from PVC to polystyrene sheet was also reported elsewhere [67]. In the present work in-situ FTIR-ATR based studies were performed on the plasticized NBR sample to study the migration of plasticizer molecules. [19]

2.5 Synthetic modification of the Plasticizer to reduce migration

2.5.1 Cycloaddition reaction of CO_2 with epoxidized monoester of plant oil-based plasticizer

The rise in global CO_2 emissions is one of the current major global challenges. Recently, the CO_2 mitigation and fixation has received much attention. The production of useful chemicals from CO_2 not only has economic incentive, but also renders positive impact on global environment. However, the lack of chemical activity of CO_2 is a major hindrance for its utilization in chemical reactions [70][71]. Usually, hydrogen, epoxides, or electrical energy are required to transform this stable molecule into other compounds. The coupling reaction of epoxides with CO_2 is an intensively studied field of research and various homo- and heterogeneous catalysts have been reported [72][73][74][75].

In the present work, a simple synthetical modification path was adopted to reduce the migration of plasticizer by incorporating CO_2 in the epoxy groups of the molecule. Epoxidized

mono ester from soya bean oil with glycerol formal (Bio-oil 1) was effectively converted to carbonated monoester (Bio-oil 2) containing five membered cyclic carbonates by reaction with carbon dioxide in the presence of tetrabutylammonium bromide as catalyst at 110 °C for 70 hours in high yield (Scheme 1) [76][77][78].
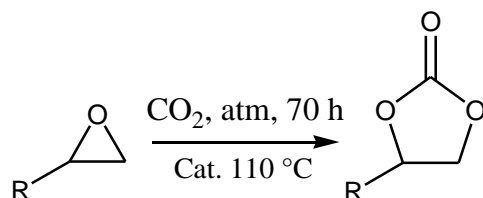
Scheme 1. Schematics of the reaction of oxirane with CO_2

Where the conventional reaction path based on tetrabutylammonium bromide (TBAB) as phase transfer catalyst was followed. As represented in the exemplary reaction scheme 2, the role of the TBAB catalyst in cyclic carbonate synthesis is to open the epoxide ring to form bromo-alkoxide, which then reacts with carbon dioxide and cyclizes to give the cyclic carbonate with regeneration of the tetrabutylammonium bromide catalyst [79].
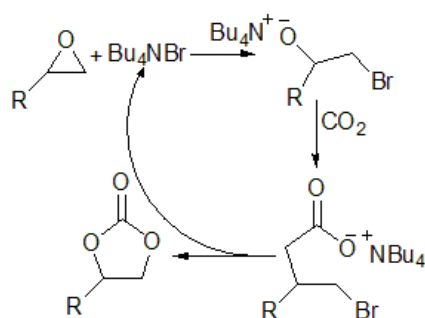
Scheme 2. role of TBAB in cyclic carbonate synthesis

2.5.2 Optimization of carbonation reaction

The cycloaddition of CO_2 to epoxides is a catalyst-based reaction, which depends on the type of the catalyst. Therefore, the biggest challenge is to develop efficient catalyst that promote the cycloaddition reaction under moderate reaction conditions. Although, utilizing TBAB catalyst alone as phase transfer catalyst high yield was observed. However cumbersome reaction time of 70 hours was required. In the next section different approaches were evaluated to reduce the reaction time without compromising the quality.

2.5.2.1 Utilizing Deep eutectic solvents (DES)

Deep eutectic solvents (DES) are classified as type of Ionic liquids (ILs) with special properties. These solvents are formed from the eutectic mixture of Lewis or Bronsted acids and bases which can contain a variety of anionic and/or cationic species. Whereas Ionic liquids (ILs) are primarily composed of one type of discrete anion and cation.[80]

These are the emerging class of solvents which are characterized by significant depression in melting points compared to those of the constituent components. Moreover, the usage of these solvents has demonstrated promising results in tuning the physiochemical properties. Last but not the least DES have also been regarded as environmentally benign alternative for synthesis.

DES consist of large, nonsymmetric ions that have low lattice energy and therefore have low melting point. They are usually obtained by the complexation of a quaternary ammonium salt with a metal salt or hydrogen bond donor (HBD). Complex hydrogen bonding is postulated as the main cause of their melting point depression, for instance delocalization of charge occurring through hydrogen bonding in a halide ion and the hydrogen-donor moiety.[81]

The term DES attribute to liquids close to the eutectic composition of the mixture, that is the molar ratio of the components which gives the lowest melting point.

The general formula for the DES can be described as

$$Cat^+X^-zY \qquad\qquad (i)$$

Where Cat^+ indicates any ammonium, phosphonium, or sulfonium cation, and X is Lewis base, generally a halide anion. The complex anionic species are formed between X^- and either a Lewis or Bronsted acid Y (z indicates the number of Y molecules that interact with the anion). [80]. DES can be classified into four different types. *Type I* is based on quaternary ammonium salt and a metal chloride. *Type II*, constitutes quaternary ammonium salt and metal chloride hydrate while *Type III*, consists of a quaternary ammonium salt and a hydrogen bond donor (HBD) which is typically based on the organic component such as carboxylic acid, amide, or polyol. Whereas *Type IV* is based on metal chloride hydrate and HBD.[82]

Although, conventional ILs and DES have different chemical properties, but they have comparable physical properties, especially the potential of tunability which can be tailored for

a particular type of chemistry. Moreover, they exhibit low vapor pressure and nonflammability. However, DES have several additional properties, which gives them edge over ILs for example ease of preparation, easy availability and relatively inexpensive components which are toxicologically well-characterized. The production of DES involves the simple mixing of the two components, while moderately heating. So comparatively less production cost is required with respect to conventional ILs.

Phase behavior

The depression in the freezing point (ΔT_f) at the eutectic composition of binary mixture of A + B is dependent on the interaction between these components. The larger the interaction; the larger will be ΔT_f. This is represented in the schematic Figure 10 below
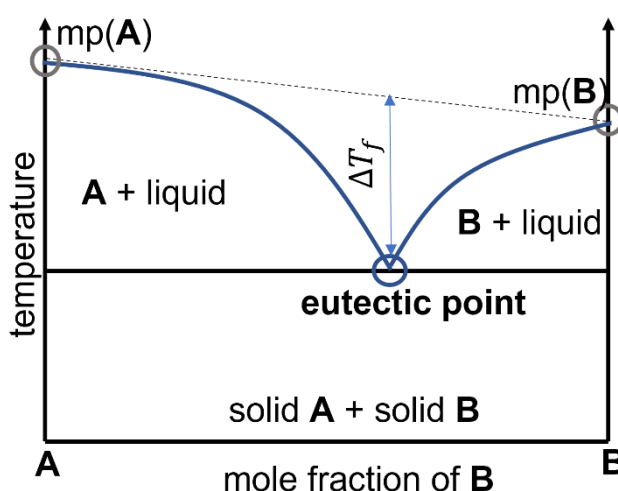
Figure 10. Graphical representation of eutectic point based on two component system

2.5.2.2 Applications of deep eutectic solvents in CO_2 gas capture

The adsorption and sequestering of CO_2 are of universal interest across many scientific disciplines, as the global warming issue is associated to the high emission of this gas in environment. Usage of DES in this regard have demonstrated promising results.

Sarmad et al. reported the better solubility of CO_2 by DES as compared to ILs in his studies.[83] Although, the exact mechanism of CO_2 solubilization is still not clear, but this process is

evidently affected by the composition of hydrogen bond acceptor (HBA) and hydrogen bond donor (HBD) in mixtures[84][85][86], in addition to the temperature and pressure.[87]

In another study performed by Wang et al. it was again highlighted that the maximum capacities and adsorption rates were affected with the choice of HBA and HBD components, indicating the optimization of these solvents for a specific separation is necessary.[88]

For the chemical fixation of CO_2 to cyclic carbonates, Han et al. reported the high catalytic efficiency of a DES catalyst system based on choline chloride: urea which was impregnated on molecular sieves.[89] Few of the important findings of this work indicated the effect of pressure on the solubility of CO_2, where the increase in the solubility of CO_2 is reported with the increase in pressure alongside other parameters such as temperature and molar ratios of the catalyst constituents.[87] The relationship between solubility of CO_2 and pressure was described by Henry's Law. The gaseous phase was assumed to be pure CO_2 due to the negligible vapor pressure of the liquid at the experimental temperature. Henry's law can be expressed by the following equation 20.[90]

$$k_H = \lim_{x_1 \to 0} \frac{f_1}{x_1} \approx \frac{P_1}{x_1} \tag{20}$$

Where k_H represents Henry's constant, x_1 is the mole fraction of gas in the liquid phase and f_1 and P_1 are the fugacity and pressure of the CO_2, respectively.

The enthalpy of dissolution Δh_1 which is described by the following equation 21, is also highlighted an important parameter of the system, since this value yields information about the strength of interaction between IL and gas.[90]

$$\Delta h_1 = \overline{h_1} - h_1^{ig} = R \left(\frac{\partial \ln P}{\partial (1/T)} \right)_{x_1} \tag{21}$$

Where $\overline{h_1}$ is the partial molar enthalpy of pure gas in solution, h_1^{ig} is the enthalpy of gas in the ideal gas phase, P is the partial pressure of gas, T is the temperature of the system, and x_1 is the mole fraction of gas dissolved in the IL. At all the conditions, the enthalpy of solution demonstrated negative value, i.e., the dissolution of the gas is exothermic.

The high solubility of CO_2 is likely due to its large quadrupole moment. In another research work based on the ATR-IR study of CO_2 in ionic liquids based on the 1-alkyl-3-methylimidazolium cation in conjunction with either $[PF_6]^-$ or $[BF_4]^-$ {[bmim][PF_6] and [bmim][BF_4]}, it was indicated that the evidence of chemical interactions between anion and CO_2 were recognized, which is one of the contributing factors alongside others to the high solubility of this gas.[91]

2.5.2.3 Tetrabutylammonium bromide (TBAB) based DES

Tetrabutylammonium bromide (TBAB) has emerged as a popular phase-transfer catalyst in various chemical reactions.[92] This quaternary ammonium salt serves as a valuable source of bromide[93] and is sometimes used as an IL.[94] Not only this salt is economically affordable but also environmentally benign. Moreover, this salt possesses greater selectivity and operational simplicity with non-corrosive nature and ease of recyclability.[92]

Rizana et al. studied the physical properties of DES based on tetrabutylammonium bromide (TBAB) paired with ethylene glycol, 1,3-propanediol, 1,5-pentanediol and glycerol as HBD.[95] The properties (density, viscosity, ionic conductivity) were found to be greatly influenced by the selection of HBD, temperature and the percentage of the constituents. The length of alkyl chain and numbers of hydroxyl groups in HBD lead to changes in physical properties, where the DES composed of longer HBD, and more hydroxyl groups demonstrated higher viscosity. The entanglement of the longer molecular chain in case of lengthy HBDs was postulated to be the reason behind increase in viscosity, while the existence of extra hydroxyl group creates more hydrogen bonds, which increase the attractive forces between the molecules and consequently viscosity increases. Nevertheless, TBAB based DES represented comparable physical properties to other DES systems for example based on choline chloride and urea although they possess bigger tetrabutylammonium cation.

Since the cycloaddition reaction of epoxides and CO_2 is a gas-liquid two-phase reaction and the solubility of carbon dioxide in epoxides is not very well, many reaction systems used organic solvents or additives to improve the mass transfer of the reaction, to enhance the efficiency of the reaction [96]. However, the use of organic solvent is not environmentally benign and increases the production costs. Reportedly, TBAB is one of the most widely used

catalyst for chemical fixation of CO_2 to epoxides to form cyclic carbonates [97]. In the present work TBAB based DES were utilized to optimize the reaction time.

Wie Liu et. al performed carbonation of epoxidized methyl soyates using TBAB based DES and reported significant reduction in the reaction time. [98] TBAB based DES served the role of both solvent and promotor, which can efficiently mediate the cycloaddition.

3. Results

3.1 Overview of the 1st publication

Since the migration of plasticizer from a product can restrict the usability of product as this process affects material properties and shorten their service life. The first publication presented in this thesis intend to describe a newly developed novel method based on in situ Fourier transform infrared spectroscopy (FTIR) to study the precise migration of plasticizer from plasticized to unplasticized polymer/elastomer matrix which is represented by the schematic Figure 11. Following the Lambert-Beer law the reduction in area of the characteristic peak from plasticizer which corresponds to its concentration was observed in comparison to the reference (butadiene characteristic) peak as depicted in Figure 12. The data obtained was further utilized to determine the diffusion coefficient following Equation (19) which is originated from Fick's second law and modified by Crank and Park [99] and the final version which is applied in the present work is inspired from the literature work of Barbari et al. [23]

$$\frac{A_t}{A_\alpha} = 1 - \frac{4}{\pi} \exp^{\left(\frac{-Dt\pi^2}{4L^2}\right)} \qquad \text{Equation (19)}$$
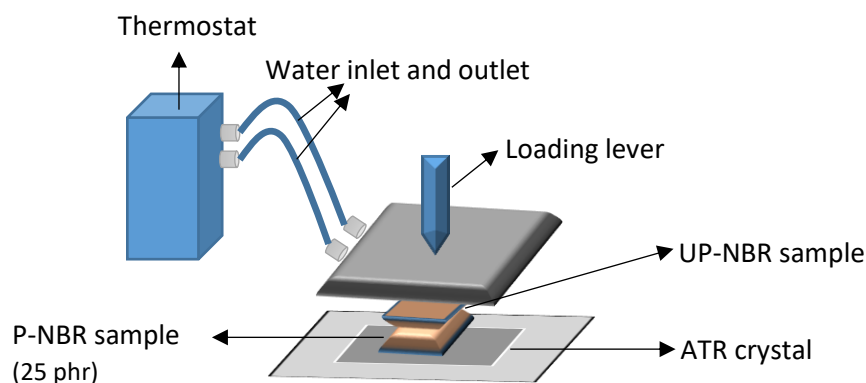
Figure 11. Schematic representation of the experimental setup

Moreover, the quantification study of the plasticizer amount was also performed by following a newly developed method based on the thermogravimetric analysis (TGA). As represented in Figure 13 (a), the mass loss percentage of the samples with gradually increasing plasticizer contents (0, 10, 20, 25 phr) were determined first till 400 °C. This mass loss percentage at 400 °C was plotted against plasticizer contents (phr) to obtain a calibration curve as represent in Figure 13 (b). Similarly, the mass loss of the sample used in the previous in situ migration analysis was determined till 400 °C. Using the calibration curve (Figure 13 (b)), plasticizer migrated contents were estimated.
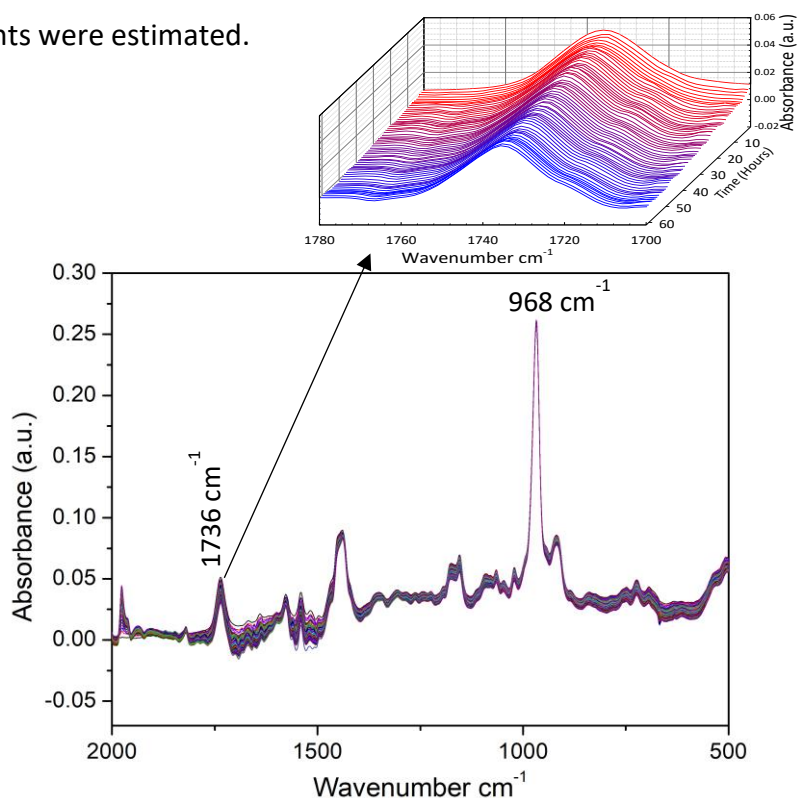
Figure 12. Waterfall plot representation of carbonyl peak area reduction observed via FTIR spectroscopy during heating after every 1 h up to 60 h.

36
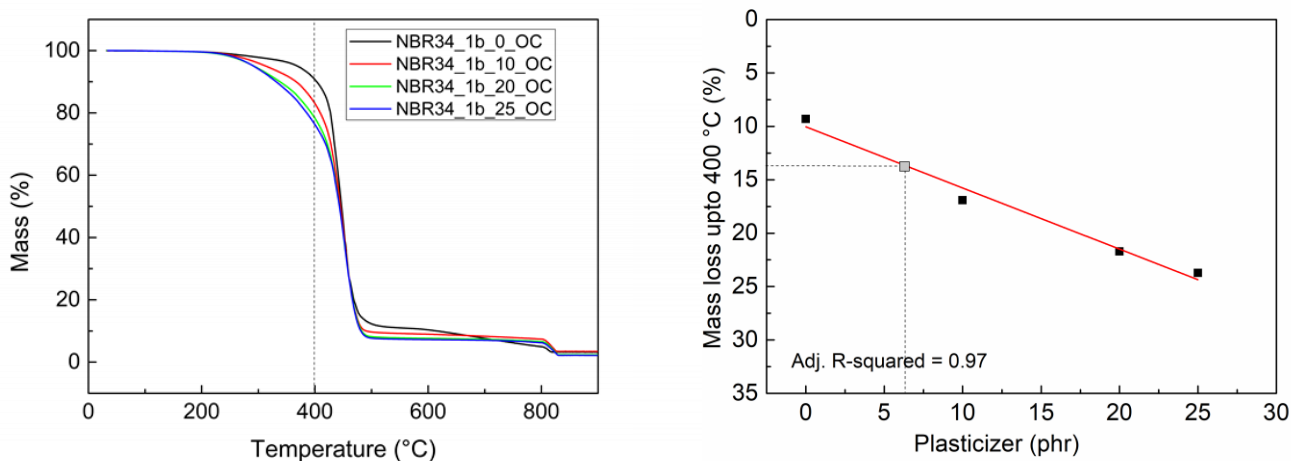
Figure 13(a). TGA analysis of the samples with gradually increasing plasticizer contents. (b) Calibration curve developed by plotting mass loss up to 400 °C vs plasticizer phr and estimation of migrated plasticizer contents.

3.2 Overview of the 2nd publication

As the migration of the epoxidized monoester of glycerol formal based on soybean oil (Bio oil 1) in NBR matrix was observed in the first publication, the aim of this second publication was to reduce this migration by synthetically modifying the plasticizer (Bio-oil 1). The intended objective was achieved by enhancing polarity of the Bio-oil 1 plasticizer by incorporating CO_2 in the epoxy rings of the plasticizer by following a conventional carbonation rection using tetrabutylammonium bromide (TBAB) as phase transfer catalyst and bubbling CO_2 through oil mixture at 110 °C as illustrated by the reaction scheme 3. Periodic Infrared spectroscopic (IR) analysis were performed to examine reaction progress, while the nuclear magnetic resonance spectroscopic (NMR) analysis were performed to confirm the product (Bio-oil 2) purity as demonstrated in Figure 14.
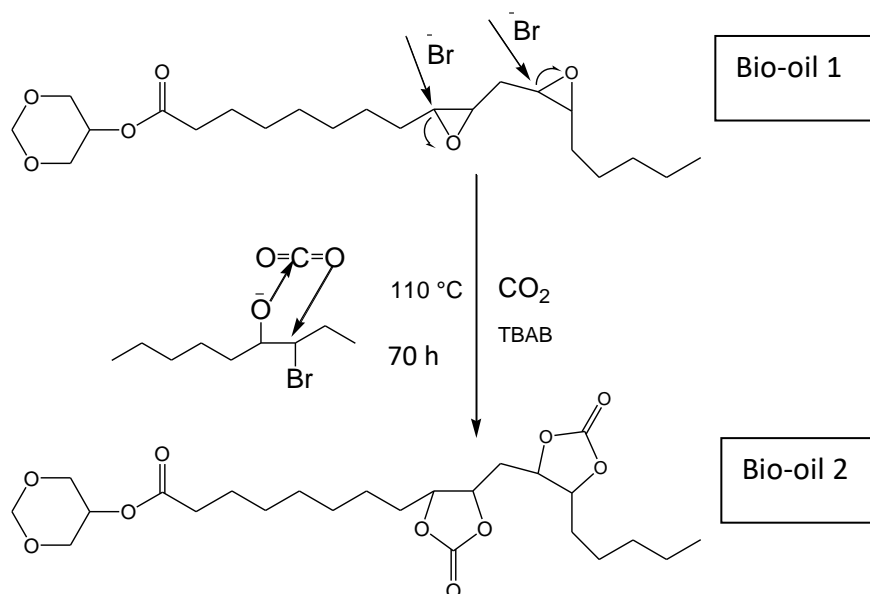
Scheme 3. Exemplary reaction scheme of epoxidized monoester of glycerol formal from soybean oil (Bio-oil 1) with CO_2 to form carbonated oil (Bio-oil 2).

FTIR spectra representing the progress of reaction
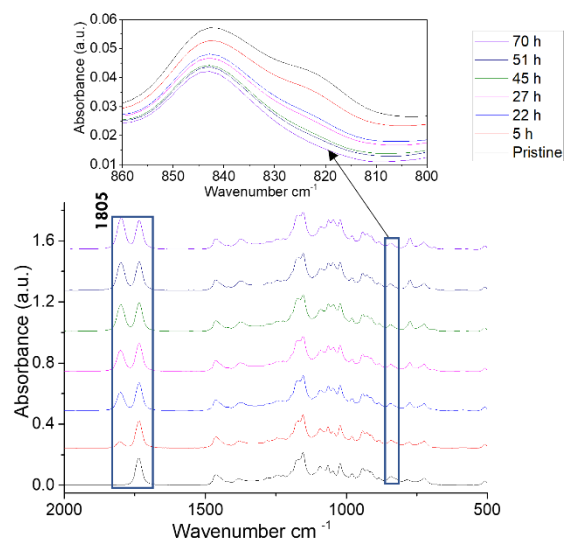
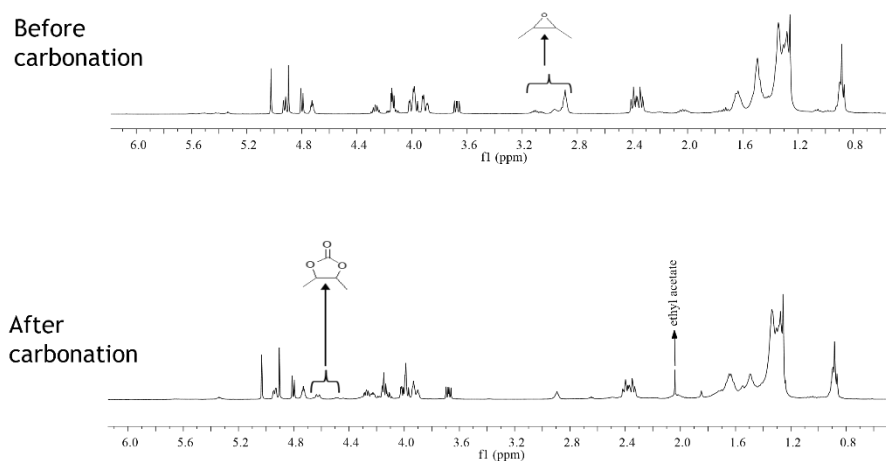**Comparison of ^{1}H-NMR before and after treatment**

Figure 14(a) IR analysis indicating reaction progress. (b) NMR analysis of oil before and after modification

Afterwards, this modified oil (Bio-oil 2) was incorporated to NBR matrix in the same way as described in the first publication and corresponding *in situ* migration and mechanical analysis

were performed to compare the effect of modification. Comparison of migration analysis is demonstrated in Figure 15.
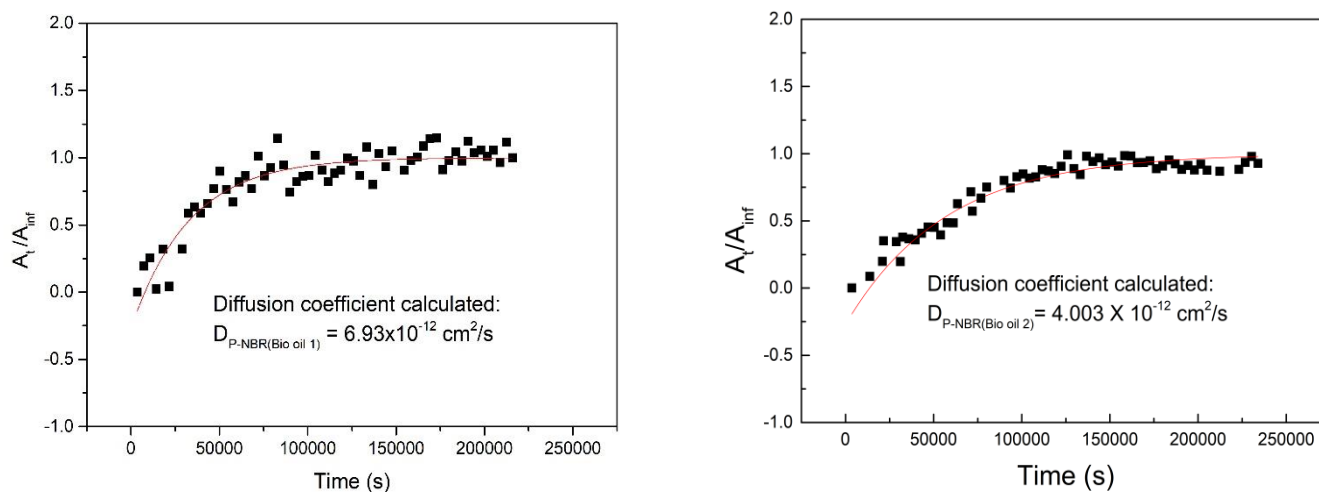
Figure 15. A_t / A_{inf} versus time, for the non-linear exponential fit and the determination of diffusion coefficient (a) with Bio-oil 1 and (b) with Bio-oil 2

3.3 Overview of the 3rd publication

As described in the second publication, the migration of epoxidized monoester plasticizer from plant oil (Bio-oil 1) can be reduced by adopting a green strategy of incorporating CO_2 into the epoxy rings of the plasticizer. But the tedious reaction time of 70 hours is required due to the mass transfer limitations as the two phases (gas-liquid) are involved and the steric hindrance offered by the epoxy rings located in the middle of the molecular structure. The aim of this third publication was to optimize the reaction conditions so that less time is required for reaction completion and at the same time quality is not compromised. This objective was achieved by using deep eutectic solvents and high pressure of 40 bars in a pressure reactor as represented in reaction Scheme 4. Whereas the catalyst system comprising potassium iodide (KI) and 18-crown-6 ether as phase transfer catalyst (PTC) provided satisfactory results.
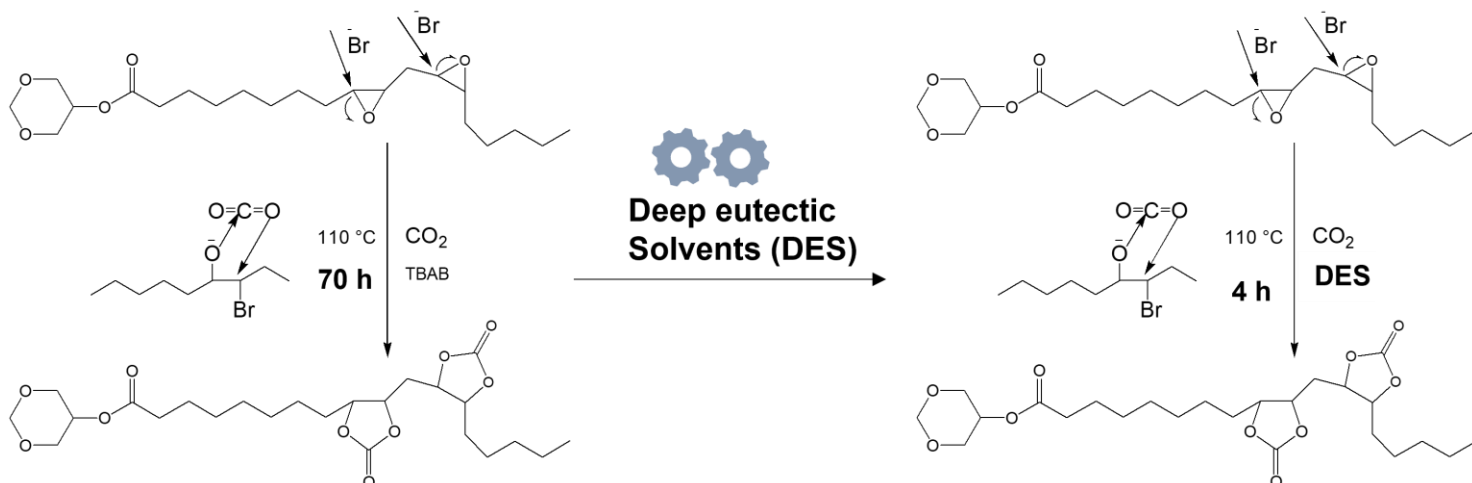
Scheme 4. Exemplary reaction scheme of epoxidized monoester of glycerol formal from soybean oil (Bio-oil 1) with CO2 to form carbonated oil (Bio-oil 2) with deep eutectic solvents.

Reaction conversions were assessed by observing the characteristic carbonate carbonyl peak at 1805 cm^{-1} wavenumber as compared to the reference which was obtained from the conventional method (using TBAB catalyst for 70 hours) as described in the second publication (see Figure 16). Whereas the purity of the product was determined using ^{1}H and ^{13}C NMR.
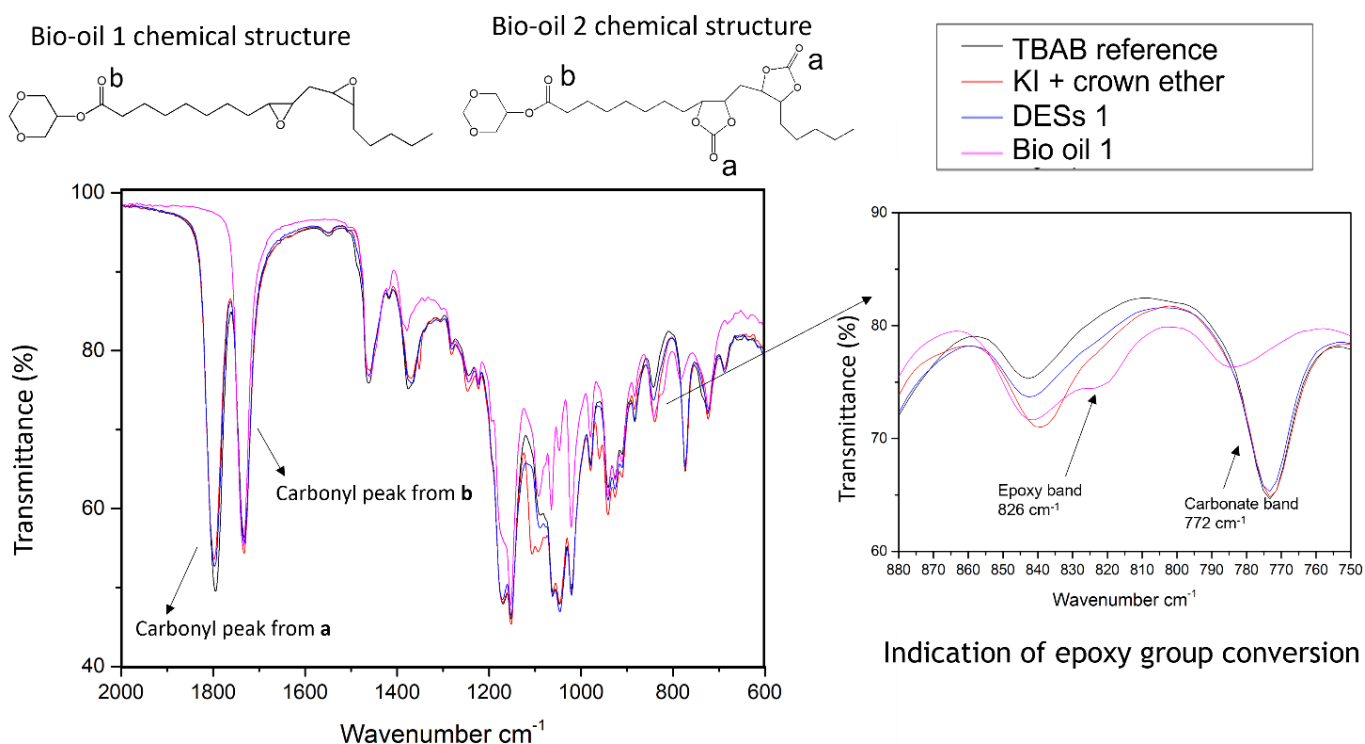
Figure 16. Comparison of characteristic carbonyl peak with the reference obtained by using conventional TBAB catalyst (black curve)

4. Publications

In this chapter, the three main publications contributing to this thesis are presented. The 4th publication will not be the part of this thesis work, as the work was not related to this project work.

"***In situ* migration analysis and diffusion coefficient determination of bio-based plasticizer from NBR using FTIR-ATR and estimation of migrated plasticizer contents by TGA analysis**"

Irfan Shahzad, Sergei Wittchen, Valentin Cepus,

In Situ Migration Analysis and Diffusion Coefficient Determination of Bio-Based Plasticizer From NBR Using FTIR-ATR and Estimation of Migrated Plasticizer Contents by TGA Analysis

Irfan Shahzad, Sergei Wittchen, and Valentin Cepus*

The migration of plasticizer from a product can restrict the usability of the product as this process affects material properties and shorten their service life. The objective of the present study is to investigate this migration process and observe its dynamics under short-term thermal aging. For this purpose, in situ FTIR-ATR spectra are recorded after every hour for continuous 60 h, while the plasticized and unplasticized NBR system is mounted and heated on ATR crystal with a heating plate at 70 °C. The band ratio of the corresponding characteristic peak areas from plasticizer carbonyl (1736 cm^{-1}) and reference C-H stretching from butadiene (968 cm^{-1}) is determined after every hour. TGA analysis carried out on similar NBR samples with gradually increasing plasticizer amounts helped to obtain the calibration curve which is used to determine the migrated plasticizer amount. With the obtained data, it is possible to determine the diffusion coefficient and to quantify the migrated plasticizer amount during short-term thermal aging and thus present a universal tool for the comparison of different plasticizers with respect to their migration behavior.

1. Introduction

Concerning versatility and flexibility, it will not be wrong to say that polymers owe to plasticizers. Plasticizer is added as a processing aid and to promote plasticity by the action of physically incorporating themselves into the polymer chains structure and ultimately reducing the brittleness of final product.[1] The most advanced approach concerning plasticizer action holds that the purpose of plasticizer is to increase the "free volume" in the system.[2,3] However, under different (environmental and loading) conditions, the plasticizer molecules tend to migrate out of the product due to their low-molecular weight.[4,5] The loss of plasticizer is one of the major factors contributing to the aging of flexible PVC, making it useless for many applications.[6,7] Some of the major mechanisms by which

plasticizer molecules can release include, loss by volatility or evaporation, migration into liquids, migration into solids and last but not the least it can also exudate under pressure.[8]

Several studies have been performed to observe the permeation and diffusion of plasticizer through polymers.[9] As there is an increasing interest in efficient measuring methods for characterizing the diffusion behavior of low molecular weight additives in polymer matrices. However, various problems are associated with most of the methods, for example, high expense in terms of time and preparation and the application limitation imposed by the measuring principles.

Lundsgaard et al.[10] observed the migration process of plasticizers into liquids via gas chromatography/mass spectroscopy (GC/MS) technique and studied their dynamics. Rosca et al.[11] investigated the diffusion of phthalates in nitrile rubber using FTIR spectroscopy by following the macroscopical (time-lag) method and microscopical (concentration-distance) method. Plasticizer structure, contents of nitrile group and cross-linking density of the rubber were highlighted as important factors affecting diffusion of plasticizer. In another literature work,[12] the ability of plasticizer to migrate from polyvinyl chloride (PVC) to another polymer was investigated. Few of the important factors which influence plasticizer migration from the polymer matrix include[8]:

1) Polymer type, its compatibility with the plasticizer and its molecular weight,
2) Plasticizer type and its concentration, its molecular weight, branching, and polarity greatly influence its interaction with polymer matrix,
3) the plasticization process and the homogeneity of the product.

Thorough investigations are prerequisite to determine the optimal end use and life span of the product. Primarily, the investigations of plasticizers are being done in polyvinyl chloride while their behavior in elastomers still need more research. The

I. Shahzad, S. Wittchen, V. Cepus
Department of Engineering and Natural Science
Hochschule Merseburg — University of Applied Sciences Merseburg
Eberhard-Leibnitz-Str. 2, Merseburg 06217, Germany
E-mail: valentin.cepus@hs-merseburg.de

present work is an effort in this regard, where the FTIR spectroscopic and TGA thermal investigations are performed to characterize the migration of bio-based plasticizers in acrylonitrile—butadiene rubber (NBR). Infrared spectroscopy is an efficient technology for the identification of polymer, evaluation of raw materials, polymer blend ratio calculation, microstructure determination, and last but not the least for the in-situ analysis of migration processes.[13,14] In one of the reported literature work,[15] ratio of characteristic absorbance peaks obtained by FTIR were correlated with acrylonitrile contents determined by Kjeldhal method. In another literature work,[6,12] TGA analysis was performed to establish the mass-loss relation with the plasticizer contents. FTIR-based monitoring of plasticizer loss from PVC to polystyrene sheet was also reported elsewhere.[13]

NBR, the copolymer of acrylonitrile and butadiene, is an important material in many applications due to its good oil resistance and low gas permeability, it is often used in seals and gaskets. NBR is, however, relatively sensitive to thermo-oxidative aging due to the unsaturated backbone of the butadiene part.[16] Several studies have been conducted to study the thermal degradation behavior of nitrile rubber.[17] The increasing environmental and toxic health concerns due to phthalate-based plasticizer have pushed the researchers to eliminate these market leader plasticizers and find nature friendly bio-based plasticizers.[18] In recent years, considerable efforts have been devoted to the replacement of phthalates in NBR. Besides synthetic plasticizers, bio oil derived plasticizers are also recommended. Products obtained from cashew nut shell oil,[19] or hazelnut oil[20] are described in the literature. In the present study, investigations were performed on NBR samples with the known formulations to study the migration behavior of bio-based plasticizer under short term thermal aging at moderate temperature (70 °C). The focus was to examine the in situ diffusion behavior of bio-based plasticizer from plasticized NBR sample to unplasticized NBR sample. Furthermore, quantitation of migrated plasticizer was performed using the calibration curve obtained by the TGA analysis of similar NBR samples with gradually increasing plasticizer amount. This migration of plasticizer from the material has a large influence on material properties and shortens the service life of the product.

2. Experimental Section

2.1. Materials and Sample Preperation

NBR (34% acrylonitrile content) with the commercial name Perbunan 3445F was purchased from Arlanxeo Deutschland

Table 1. Product specifications of Perbunan 3445F.

Property	Test method	Unit	Results
ACN content	ISO 24698-1	wt %	34
Mooney viscosity (1+4) 100 °C	ISO 289/ASTM D 1646	MU	45 ± 5
Specific gravity	–	–	0.97
t$_{90}$	ISO 6502	min	6.9 ± 1.5

GmbH. Product specifications are mentioned in **Table 1** no carbon black was added during compounding to overcome the absorbance issues during spectroscopic analysis. The Bio oil is the laboratory grade synthesized epoxidized soybean oil (ESBO) provided by Glaconchemie GmbH Merseburg.

To analyze and quantify the migration of the bio oil plasticizer from vulcanized NBR, the samples were prepared according to the recipe given in **Table 2**.

2.2. Compounding

To prepare the homogeneous mixture of rubber, the Brabender N 50 roller mill kneading chamber was used with the following mixing parameters:

Chamber volume: 75 cm^3; Mixing volume: 52.5 cm^3; Degree of filling: 0.7; Mixing time: 10 min; Mixing temperature: 50 °C; Rotation: 50 min^{-1}.

2.3. Sample Preparation

From the vulcanized plates of the plasticized NBR (P-NBR) with 25 phr plasticizer, a square (1 × 1 × 0.2 cm^3) was cut using a special cutting knife. Similarly, a sample of the unplasticized NBR (UP-NBR) without plasticizer was precisely cut with the same dimensions (1 × 1 × 0.2 cm^3). So, the samples can have good contact with each other during experimental analysis.

2.4. Test Methods

#### 2.4.1. Fourier-Transform Infrared Spectroscopy (FTIR) and Migration Test

The experiments were performed on FTIR spectrometer Vertex 70 with platinum ATR by Bruker, Germany and the OPUS (version 8) software was used for the spectral analysis along with ORIGIN 9. The conditions employed were resolution: 4 cm^{-1}, number of scans: 32, background scans:

Table 2. NBR sample preparation recipe.

Name	Comments	Contents (phr)
NBR	34% ACN	100
Carbon black	–	–
Bio oil	–	0, 10, 20, 25
Stearic acid	Processing aids	1
ZnO	Activator	3
6PPD[a]	Antioxidant	1.5
Sulfur	Crosslinking agent	1.5–1.75
CBS[b]	Accelerator	1.05–1.2

[a] 6PPD —N-(1,3-dimethylbutyl)-N'-phenyl-p-phenylenediamine.
[b] CBS—N cyclohexylbenzothiazole-2-sulfenamide.
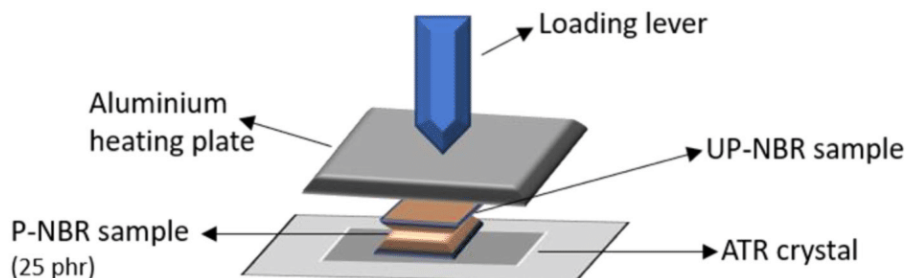
Figure 1. Schematic representation of the experimental setup.
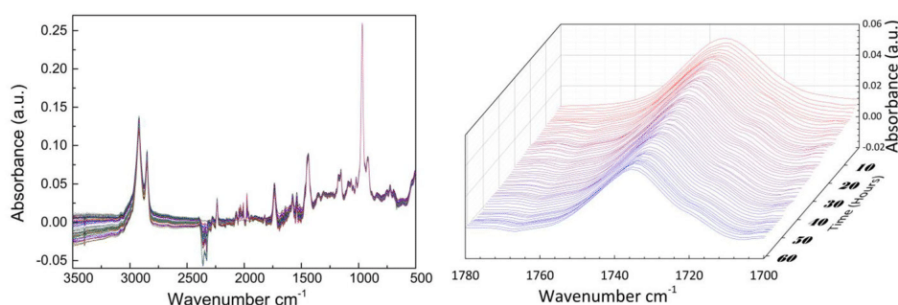

Figure 2. a) In situ FTIR-ATR spectra recorded after every 1 h up to 60 h. b) Waterfall infrared spectra of characteristic carbonyl-peak region of plasticizer obtained after every 1 h up to 60 h.

32 and the data were collected in the range of $400\,cm^{-1}$ to $4000\,cm^{-1}$.

For the in situ analysis of the migration process on FTIR, coupling of the controlled heating system with the device was required. A custom-made heating system was developed using Lauda thermostat along with an aluminum plate having inlet and outlet valves for the circulation of heated water (**Figure 1**).

### 2.4.2. In situ Continuous Plasticizer Migration Resistance Test

Plasticized and unplasticized NBR samples with the similar dimensions as described earlier were obtained. A background spectrum was recorded first before placing the sample on the ATR crystal. Afterwards, the plasticized NBR sample was placed with lower end facing toward ATR crystal while on the upper end unplasticized NBR sample was placed and the system was heated with aluminum heating plate (Figure 1). Optimal
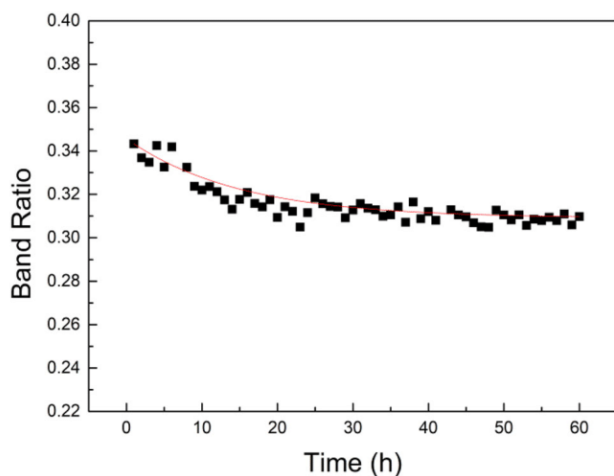
Figure 3. In situ band ratio profile for P-NBR sample during 60 h thermal aging.
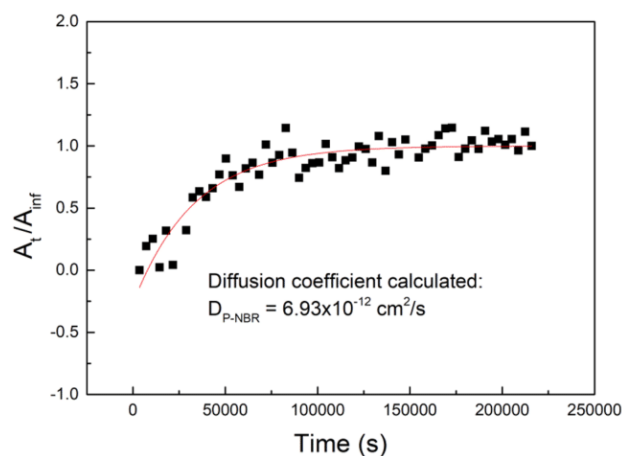
Figure 4. At /Ainf versus time, for the non-linear exponential fit and the determination of diffusion coefficient.
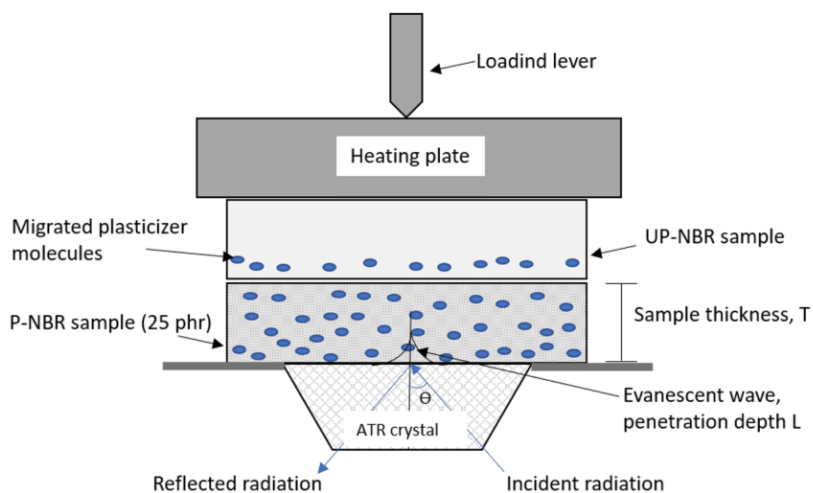
Figure 5. Schematic representation of the ATR equipment for diffusion experiment. The following nonlinear exponential fit Equation (4) was used in the ORIGIN software to calculate the above-mentioned parameters in Equation (2).

The in situ hourly update of the sample at the same exact position presented a precise insight of the migrating plasticizer into the unplasticized NBR sample, reflecting that this process markedly depends on the time and temperature. However, it must be taken into account that precision to determine the diffusion coefficient is restricted to the sample volume which is being penetrated by the evanescent waves of the infrared beam. Moreover, it is considered as a simplifying hypothesis that the plasticizer is uniformly distributed in the matrix.

3.2. Data Analysis and Evaluation

All the spectra obtained were exported to the ORIGIN software. For the precise measurement of the plasticizer carbonyl peak area ($1736 \, cm^{-1}$), a routine was developed first in the ORIGIN software for the base line correction and precise peak area determination. Using the batch processing technique in the software, carbonyl-peak areas for all the 60 spectra were determined applying the developed routine. The batch processing technique not only saved a lot of time needed to analyze each spectrum but also reduced the human error factor to great extent. As slight differences might arise from manual valley to valley base line setting during the measurement. Similarly, area of the reference peak due to C—H stretch from butadiene ($968 \, cm^{-1}$) was also determined.

sample contact with ATR crystal was ensured by applying appropriate load with the lever. To automatically obtain the spectra after every hour for 60 h, corresponding parameters were set in the OPUS software (version 8) using the MACRO module.

2.4.3. Thermogravimetric Analysis (TGA)

TGA tests were carried out using NETZSCH TG 209F1 Iris. Compounded NBR samples with varying plasticizer contents (0, 10, 20, 25 phr) were analyzed. Approximately 16 mg of the samples were weighed in the aluminum pan (164 mg) and were heated from 30 °C to 900 °C at the heating rate of $10 \, °C \, min^{-1}$ under the nitrogen atmosphere (flow rate $20 \, ml \, min^{-1}$). Mass loss percentage up to 400 °C was monitored for all the samples to obtain the calibration curve.

3. Results and Discussion

3.1. Study of Migration Process

For the system under observation, diffusion coefficient was calculated by observing the area reduction of characteristic carbonyl peak of plasticizer at $1736 \, cm^{-1}$. On hourly basis, in situ FTIR spectra were recorded while continuously heating the plasticized NBR sample on ATR crystal as represented in **Figure 2**a. Whereas in Figure 2b the waterfall plot in the carbonyl-peak region ($1736 \, cm^{-1}$) is plotted, illustrating the reduction in peak area with respect to time due to the decrease in concentration (Lambert—Beer law) of migrating plasticizer. Lambert—Beer law explains the relationship between the absorption of electromagnetic waves and the quantity of the absorbing material. It can be observed that area of carbonyl peak reduced gradually with time during aging because of continuous decrease of plasticizer concentration in the NBR sample at the face of diamond crystal.

3.3. Band Ratio Profile

For diffusion coefficient calculation, it was considered that during the diffusion process the concentration of NBR on the surface of diamond crystal is increasing while the concentration of plasticizer is decreasing. Therefore, the absorbance of carbonyl group was normalized to the absorbance of the butadiene group stretching.

$$\text{Band Ratio} = \frac{\text{Peak area}_{1736}}{\text{Peak area}_{968}} \tag{1}$$

The band ratio was obtained to overcome concentration related issues on the surface of the sample. As the plasticizer concentration tends to decrease on surface during thermal aging due to migration while the butadiene concentration seems to increase (Lambert–Beer law), although butadiene concentration remains constant.

The characteristic carbonyl-peak areas ($1736 \, cm^{-1}$) determined with respect to time for all the 60 spectra were divided with the reference-peak area ($968 \, cm^{-1}$) to obtain the relative abundance or band ratio profile using Equation (1). This relative abundance was plotted against time (**Figure 3**), which as a matter of fact represented the fit curve of measured data.

3.4. Diffusion Coefficient Calculation

Band ratios profile obtained was further utilized to determine the diffusion coefficient following the Equation (2) originated from Fick's second law which was further elucidated by Crank and Park[21] and the final version which is applied in the present work is inspired from the literature work of Barbari et al.[22] Band ratio values were normalized first according to reported literature and then plotted against time. Using the custom-defined non-linear exponential fitting Equation (4), the obtained data points were fitted as shown in the **Figure 4**.

The following Equation (2) from the literature[22] was used to determine the diffusion coefficient.

$$\frac{A_t}{A_\infty} = 1 - \frac{4}{\pi} \exp^{\left(\frac{-Dt\pi^2}{4L^2}\right)} \tag{2}$$

where A_t is the carbonyl-peak area at time t, A_∞ is the carbonyl-peak area at equilibrium (Figure 4). L is the pathlength of the evanescent infrared beam into the sample and D is the diffusion coefficient.

According to the principle of ATR technique, when a sample is brought in contact with ATR crystal surface, the evanescent wave will be attenuated in regions of the infrared spectrum where the sample absorbs energy. The evanescent wave decays exponentially with distance from the interface (**Figure 5**) thus making ATR insensitive to sample thickness. The penetration depth (L) of IR beam in sample was calculated using Equation (3).

$$L = \frac{\lambda}{2\pi \left(n_1^2 \sin^2 \theta - n_2^2\right)^{1/2}} \tag{3}$$

where L is the penetration depth of evanescent wave, λ is the wavelength of IR radiation, n_1 and n_2 are the refractive indices of flat diamond crystal and polymer sample respectively and θ is the angle of incidence.

The following nonlinear exponential fit Equation (4) was used in the ORIGIN software to calculate the above-mentioned parameters in Equation (2).

$$y = a - b * \exp^{(-c*d*x)} \tag{4}$$

where $y = \frac{A_t}{A_\infty}$, $a = 1$, $b = \frac{4}{\pi}$, $c = \frac{\pi^2}{4L^2}$, $x = t$, $d = D$ (diffusion coefficient)

The adjusted R-squared value (0.90) depicts the fair fitting of the model used. The data points are satisfactorily fitted, although some of the points presented certain deviation from the theoretical behavior, probably due to the complex nature of the migration process via back migration of the plasticizer to the sample and possible instrumental errors.

The diffusion coefficient value of comparable molecular weight of plasticizers through similar elastomeric matrix (with 34% ACN) was reported to be in the range of 10^{-10} to 10^{-11} cm^2 s^{-1}.[11] Owing to different experimental conditions as in their case solid-liquid contact system was applied which means infinity volume of plasticizer was exposed to polymer matrix during experiment resulting in higher concentration gradient between surface of polymer matrix and polymer
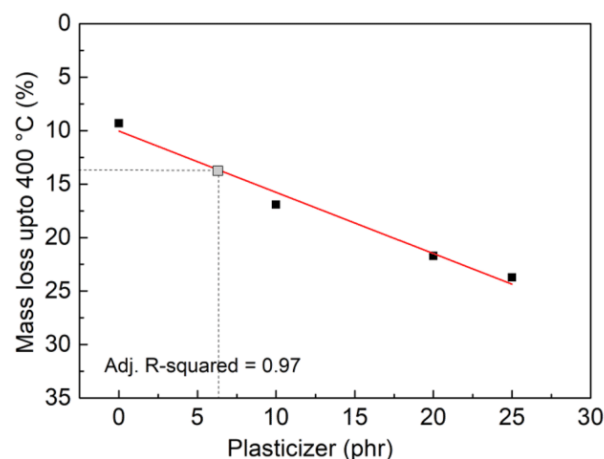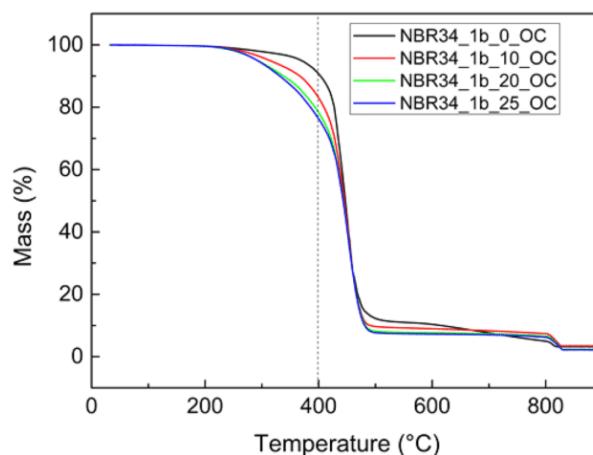
Figure 6. a) shows the behavior of a unplasticized NBR sample (black line) and others (colorful lines) with gradually increasing plasticizers contents (0, 10, 20, 25 phr). While the unplasticized NBR sample shows one unique step in mass loss percentage curve, attributed to the degradation of NBR elastomer, plasticized samples show at least one additional step. An earlier mass loss process can be observed at temperature close to the boiling point of the plasticizer (for example, 227 °C for epoxidized soybean oil), which clearly corresponds to plasticizer release from the NBR sample. Almost linear behavior was observed when mass loss up to 400 °C was plotted against plasticizer contents thus providing a calibration curve (**Figure 6**b). The adjusted R-squared value of 0.97 presented a fair fit with slight fluctuation of the data points due to the different interaction behavior of the sample at higher plasticizer contents.

bulk leading to higher diffusion coefficient value. While in our case solid-solid contact system was utilized with limited amount of plasticizer exposed to polymer matrix resulting in lower concentration gradient which caused lower diffusion rate.

3.5. Calibration Curve Obtained by TGA

TGA analysis method was used for the determination of plasticizer amount migrated to unplasticized NBR sample during short term thermal aging experiment.

3.6. Quantitation of Migrated Plasticizer After Migration Test

For the quantitation of migrated plasticizer amount, likewise, mass loss % up to 400 °C for unplasticized NBR sample placed on top of the plasticized sample during in situ thermal aging was determined. Using the calibration curve (**Figure 6**b) plasticizer contents migrated to this unplasticized NBR sample were estimated. From the calibration curve, the estimated migrated plasticizer content (gray dot) determined was 6.25 phr indicating 1/4 of the total plasticizer contents were migrated during the short term (60 h) thermal aging of the plasticized sample.

4. Conclusions

The described in situ FTIR analysis method can be effectively applied to study precise migration of specific migrants, in particular, for the migration analysis of ESBO (Epoxidized soybean oil) from NBR matrix and finally the data obtained with respect to time can be utilized to determine the diffusion coefficient using fitting Equation (4). Thus, present a universal tool for the comparison of different plasticizers with respect to their migration behavior. The diffusion coefficient values obtained can be very significant in predicting the life span of a product under different environmental conditions. The diffusion coefficient value of $(6.93 \times 10^{-12}\,\text{cm}^2\,\text{s}^{-1})$ calculated by following this new method is comparable to the other reported diffusion coefficient values, calculated following different experimental methods but similar experimental conditions. Correlations observed among the plasticizer contents and mass loss percentage, obtained by TGA served as a handy tool for the fair determination of the migrated plasticizer amount. So, it is a useful additional method to FTIR-migration test for quantitative analysis of migrating substances.

[1] R. H. Schuster, H. Geisler, G. Scholz, *Kautsch. Gummi Kunstst.* **2002**, *55*, 653.

[2] P. C. Hiemenz, *Polym. Chem.* **1984**.

[3] T. G. Fox, P. J. Flory, *J. Appl. Phys.* **1950**, *21*, 10.1063/1.1699711.

[4] T. D. Stark, H. Choi, P. W. Diebel, *57th Can. Geotech. Conf., Montreal* **2004**, p. 1.

[5] V. Ambrogi, W. Brostow, C. Carfagna, M. Pannico, P. Persico, *Polym. Eng. Sci.* **2012**, 10.1002/pen.22070.

[6] K. Z. Gumargalieva, V. B. Ivanov, G. E. Zaikov, J. V. Moiseev, T. V. Pokholok, *Polym. Degrad. Stab.* **1996**, *52*, 73. 10.1016/0141-3910 (95)00209-X.

[7] M. L. Marín, J. López, A. Sánchez, J. Vilaplana, A. Jiménez, *Environ. Contam. Toxicol.* **1998**, *60*, 68.

[8] D. Messadi, J. L. Taverdet, J. M. Vergnaud, *Ind. Eng. Chem. Prod. Res. Dev.* **1983**, *22*, 142. 10.1021/i300009a032.

[9] G. S. Smith, C. B. Skidmore, P. M. Howe, J. Majewski, *J. Polym. Sci., Part B Polymer Phys.* **2004**, *42*, 3258. 10.1002/polb.20171.

[10] R. Lundsgaard, G. M. Kontogeorgis, J. K. Kristiansen, T. F. Jensen, *J Vinyl Addit. Technol.* **2009**, 129.

[11] R. S. C. Rosca, *Prüfen Und Mess.* **2006**, *49*, 86.

[12] A. Marcilla, S. García, J. C. García-Quesada, *J. Anal. Appl. Pyrolysis.* **2004**, *71*, 457. 10.1016/S0165-2370(03)00131-1.

[13] A. Marcilla, S. Garcia, J. C. Garcia-Quesada, *Polym. Test.* **2008**, *27*, 221. 10.1016/j.polymertesting.2007.10.007.

[14] N. González, M. J. Fernández-Berridi *Polym. Polym. Compos.* **2013**, *21*, 449. 10.1002/app.

[15] S. Chakraborty, S. Bandyopadhyay, R. Ameta, R. Mukhopadhyay, A. S. Deuri, *Polym. Test.* **2007**, *26*, 38. 10.1016/j.polymertesting. 2006.08.004.

[16] S. Rajesh Kumar, P. M. Asseref, J. Dhanasekaran, S. Krishna Mohan, *RSC Adv.* **2014**, 12526. 10.1039/c3ra45684f.

[17] M. Hakkarainen, A. C. Albertsson, S. Karlsson, *Int. J. Polym. Anal. Charact.* **2003**, *8*, 279. 10.1080/10236660304883.

[18] C. Bergmann, *Rubber World.* **2018**.

[19] P. S. B. R. Singh, *Rubber World* **2011**, 3.

[20] N. E. K. Karadeniz, *Gummi Kunstst.* **2011**, *7*, 49.

[21] J. Crank, *The Mathematics of Diffusion*, Second ed., Clarendon Press, Oxford **1975**.

[22] G. T. Fieldson, T. A. Barbari, *Polymer (Guildf).* **1993**, *34*, 1146. 10.1016/0032-3861(93) 90765-3.

"**Synthetical modification of plant oil-based plasticizer with CO$_2$ leads to reduced migration from NBR rubber**"

Irfan Shahzad, Mahbubur Rahman, Sergei Wittchen, Katrin Reincke, Beate Langer, Valentin Cepus

Journal of **Applied Polymer** SCIENCE WILEY

Synthetical modification of plant oil-based plasticizer with CO_2 leads to reduced migration from NBR rubber

Irfan Shahzad[1] | Md Mahbubur Rahman[1] | Sergei Wittchen[1] |
Katrin Reincke[2] | Beate Langer[1,2] | Valentin Cepus[1,2]

[1]Department of Engineering and Natural Science, Ingenieur und Naturwissenschaften (INW)-Hochschule Merseburg, Saxony Anhalt, Germany

[2]Polymer Service GmbH Merseburg, Merseburg, Germany

Correspondence
Valentin Cepus, Hochschule Merseburg–University of Applied Sciences Merseburg, Department of Engineering and Natural Science, Eberhard-Leibnitz-Str. 2, 06217 Merseburg, Germany.
Email: valentin.cepus@hs-merseburg.de

Abstract

The increasing environmental and toxic health concerns due to phthalate-based plasticizers are pushing researchers to eliminate these market leader plasticizers and to find nature-friendly bio-based plasticizers with reduced migration. The present study is also an effort in this regard. Herein, the epoxidized monoester of glycerol formal based on soybean oil is synthetically modified by carbonation in the presence of a catalyst to increase the polarity of the plasticizer. These modified and pristine plasticizers were incorporated in acrylonitrile—butadiene rubber and their migration analysis during heating the sample for 60 h were performed using fourier transform infrared spectroscopy with attenuated total reflectance (FTIR-ATR) by observing the absorbance of the characteristic carbonyl stretching vibration peak (1736 cm^{-1}) of plasticizer relative to the C—H stretching vibration of butadiene (968 cm^{-1}). The results of migration kinetics and mechanical testing demonstrated reduction of diffusion coefficients by modification while hardness and tensile strength are hardly affected. In addition to the fact that soybean oil as a natural resource is more sustainable, the additional synthesis step of binding CO_2 is advantageous for a green chemistry approach.

KEYWORDS
mechanical properties, plasticizer, rubber, spectroscopy, structure-property relationships

1 | INTRODUCTION

Acrylonitrile—butadiene rubber (NBR), the copolymer of acrylonitrile and butadiene, is an important polymer for many applications due to its good oil resistance and low-gas permeability.[1] The polar (CN) groups on polymer backbone are responsible for these characteristics. Many properties of NBR, including tensile strength, abrasion resistance, hardness, and heat resistance are dependent on the acrylonitrile (ACN) content. Certainly, the most prominent feature of nitrile rubber that increases with the ACN content is its remarkable resistance to oil.[2] Filler is usually incorporated into NBR matrix to enhance its mechanical properties, although its viscosity is increased making it difficult to process. So, plasticizer is added as an extender, which not only helps to reduce the mixing time and fulfills modern industrial demand by reducing the production cost but also improve the flexibility of the finished product. Due to the polar nature, several plasticizers like phthalates, adipates, and epoxidized soybean oil are compatible with NBR.[3]

Keeping in view the rising health concerns due to the migration of toxic plasticizers from the product, Singh

et al.[4] studied the effect of cashew nut shell oil to replace di-butyl phthalate (DBP) in NBR vulcanizates. Effect of hazelnut oil (HaO) and epoxidized hazelnut oil (EHaO) as plasticizer in NBR and polychloroprene rubber (CR) was investigated by Karadeniz et al.[5] Although, fatty acids impart good flexibility due to their long chain lengths (C_{12}–C_{22}) they have poor solubility in polymer matrix due to less polarity.[6] However, by epoxidizing the double bonds of hydrocarbon chains in fatty acids, their solubility can be enhanced. The higher the number of double bonds present in chain the better will be its suitability to be used as a plasticizer. Among the most commonly used vegetable oils, soybean has a high percentage of double bonds (48.0–52.0) making it more suitable for plasticization purpose.[7] Epoxidized soyabean oil (ESBO) is known for a long time as an important secondary plasticizer in many PVC formulations due to its dual role as plasticizer and stabilizer.[8] ESBO usage as primary plasticizer in PVC demonstrated acceptable plasticizing properties but their prolonged UV-exposure resulted in sticky surface indicating exudation phenomena.[9] Due to this reason it is mostly used as secondary plasticizer.

Epoxy biodiesels (epoxidized fatty acid methyl esters [EFAME]) were developed recently as bio-based plasticizers, as they have better lubricity, compatibility and dispersibility in polymer matrix than epoxidized vegetable oils (EVO) and gives better flexibility to the plastic even at low temperature and, therefore, can be used as primary plasticizers.[10,11] Epoxidized methyl ester of soybean oil, which is a monoglyceride (three time less molecular weight as compared to triglyceride), is more compatible with poly (vinyl chloride) as it can penetrate easily through the polymer chains. However, an adverse effect of migration is associated with this plasticizer due to lower molar mass.[12] Chiaradia et al.[6] tried to overcome this problem in their patent work by esterifying fatty acid (vegetable oil) with cyclic hydroxy acetal or hydroxy ketal and then epoxidizing the double bonds in hydrocarbon chain. The obtained plasticizer was claimed to have less migration and can be utilized up to 50 phr. In a previous reported work,[13] epoxidized ester of glycerol formal from soybean oil was investigated as plasticizer in NBR. Here, the migration of the plasticizer from the plasticized NBR sample to unplasticized NBR sample during short-term thermal aging was investigated using infrared spectroscopy (FTIR).

Various techniques were adopted by different research groups to investigate the migration behavior of a plasticizer from polymer matrix. Rosca et al.[14] investigated a solid–liquid system where the diffusion of phthalates in NBR was observed using FTIR spectroscopy by following the macroscopical (time-lag) method and by a microscopical (concentration-distance) method. Plasticizer structure, contents of nitrile group and cross–linking density of the rubber were highlighted as important factors affecting diffusion of plasticizer. Papakonstantinou et al.[15] investigated a solid–solid system

where the plasticizer migration from plasticized into unplasticized PVC was observed by monitoring the weight change in the sample sandwiched between two unplasticized PVC sheets at regular intervals. Diffusion in a plasticized PVC sheet was recognized as a controlling step in this study. While another research group[16] utilized gas chromatography–mass spectroscopic device to examine the migration of plasticizers.

Different strategies were adopted by various research groups to diminish this migration process. Yuan et al.[17] covalently attached chlorinated paraffin (CP-52) to di (2-ethyl hexyl) phthalate (DEHP) plasticizer to curtail plasticizer migration. The obtained plasticizer was claimed to be highly compatible and nonleaching. Jayakrishnan et al.[18] modified the surface structure of flexible PVC samples by carrying out nucleophilic substitution of chlorine by sodium azide in aqueous media with tetrabutyl ammonium bromide as phase transfer catalyst. It was found that the leaching was considerably reduced, although, color change was observed probably due to dehydrochlorination occurred during grafting process and the elongation at break was reduced considerably. Effect of plasma-induced surface crosslinking of flexible PVC packaging films on limiting leaching of plasticizer molecules was investigated by Audic et al.[19] Argon plasma was found to give best results and the reduction in leaching tendency was observed with increasing plasma treatment time. While others tried treatment or coating to reduce plasticizer migration.[20]

In the present work, epoxidized monoester of glycerol formal based on soybean oil was synthetically modified to carbonated monoester of glycerol formal in the presence of tetrabutylammonium bromide (TBAB) catalyst and constant supply of CO_2 gas, so that the polarity of the plasticizer is enhanced, and its migration is curtailed. Reaction progress was monitored using FTIR spectroscopy and the completion of reaction was analyzed using NMR (nuclear magnetic resonance spectroscopy). To investigate the mechanical properties and migration behavior, NBR samples comprising epoxidized monoester of glycerol formal based on soybean oil and modified oil (carbonated monoester of glycerol formal) were prepared.

2 | EXPERIMENTAL

2.1 | Chemicals, physical properties, and synthesis of the modified plasticizer

Laboratory-grade synthesized epoxidized monoester of glycerol formal from soybean oil (Bio-oil 1) was provided by the industrial partner Glaconchemie GmbH Merseburg, Germany. TBAB and Ethyl acetate were purchased from Sigma Aldrich and used without any further purification.

Bio-oil 1 (50 g) and TBAB (3.38 g; 5 mol% with respect to epoxy groups) were placed in a 200 ml gas washing

bottle as a first step of the modification. The catalyst was dissolved afterwards by heating and stirring the mixture for 10 min up to 110°C. A constant (2 ml/s) flow of CO_2 was introduced then and the reaction progress was monitored using FTIR spectroscopy by taking out the samples at different time intervals. The reaction was completed in about 70 h. Afterwards, the catalyst was removed by dissolving the reaction mixture in ethyl acetate and washing five times with distilled water. Finally, the organic layer was dried on a rotary evaporator under reduced pressure and a clear dark-yellowish viscous liquid of carbonated oil (Bio-oil 2) was obtained. Few of the physical properties of both the oils are also listed in Table 1. While an exemplary synthetic route of this carbonation reaction is presented in Figure 1.

2.2 | Materials, sample preparation, and test methods

NBR (34% acrylonitrile content) with the commercial name Perbunan 3445F from Arlanxeo Deutschland GmbH was used. No carbon black was added during compounding, this means a nonreinforced material was investigated to exclude the influence of filler and to better understand the interaction between polymer and plasticizer. Moreover, carbon black filled rubbers are difficult to be analyzed by IR due to the high-refractive index of the sample. Consequently, near strong absorption bands, the sample refractive index may approach or exceed the refractive index of the ATR crystal, leading to badly distorted spectra.[21]

To analyze and quantify the migration of the Bio-oil 2 plasticizer from vulcanized NBR, the samples were prepared according to the recipe given in Table 2.

2.2.1 | Compounding

To prepare a homogeneous mixture of rubber, the HAAKE Rheochord 300p lab kneader with a chamber volume of 75 cm^3 was used with the following mixing parameters:

- Mixing volume: 54.6 cm^3
- Degree of filling: 0.7
- Mixing time: 10 min

TABLE 1 Physical properties of bio-oil 1 and bio-oil 2

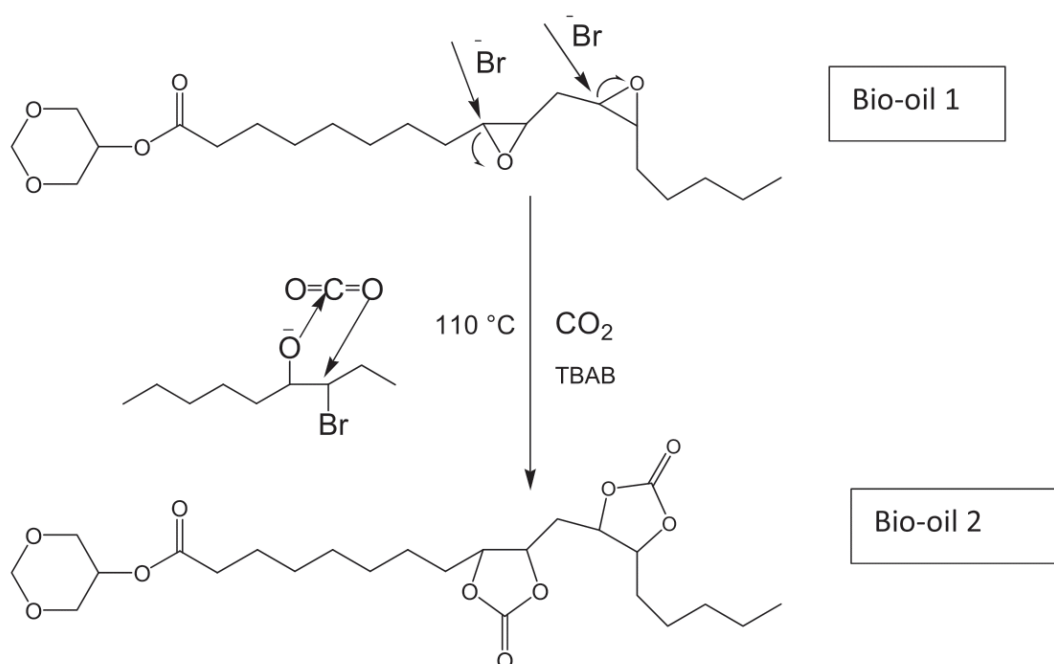| Bio-oil	Density (g/cm^3) at 20°C	Refractive index	Color	Glass transition temperature (T_g) (°C)
Bio-oil 1	1.0057	1.465	Light yellow	−74.4
Bio-oil 2	1.0460	1.468	Dark yellow	−59.7

FIGURE 1 Exemplary reaction scheme of epoxidized monoester of glycerol formal from soybean oil (bio-oil 1) with CO_2 to form carbonated oil (bio-oil 2)

TABLE 2 NBR sample preparation recipe

Name	Comments	Contents (phr)
NBR	34% ACN	100
Carbon black	–	–
Bio-oil 1, bio-oil 2	–	0, 10, 20, 25
Stearic acid	Processing aids	1
ZnO	Activator	3
6PPD[a]	Antioxidant	1.5
Sulfur	Crosslinking agent	1.75
CBS[b]	Accelerator	1.05

[a]6PPD—N-(1,3-dimethylbutyl)-N′-phenyl-p-phenylenediamine.
[b]CBS—N cyclohexylbenzothiazole-2-sulfenamide.

- Mixing starting temperature: 50°C
- Mixing final temperature: 88°C
- Rotation: 50 min^{-1}

During mixing due to friction resistance, the temperature increased up to 88°C maximum (see the torque-temperature plot provided in the supporting information [Figure S2]). But the addition of plasticizer provided the lubrication and hindered the further increase in temperature due to friction.

2.2.2 | Vulcanization kinetics

The oscillating disc rheometer (ODR) was used for investing the vulcanization kinetics. This machine "GÖTTFERT ELASTOGRAPH" was manufactured by The Göttfert–Werkstoff–Prüfmaschinen GmbH. Temperature, time, strain, and strain rate was set in the machine. The clamp rotation degree was 0.5°, and the rotation speed was 50 times per minute. Around 5 g of uncured rubber was set in the sample holder of the machine. The changes of torque with time were investigated during vulcanization. During vulcanization scorch time (t_2) and cure time (t_{90}) was identified from the graph. Scorch time is defined as the beginning of the reaction (cure induction period); the torque measured after 2 min before the start of the reaction. t_{90} is defined as the time required to complete a 90% reaction of the total curing and t_{90} is called optimum curing time. The following equation is used to measure the t_{90}.

$$x = \frac{F_t - F_a}{F_m - F_a},$$

Where F_m is the maximum torque; F_a is the minimum torque; F_t is the torque at 90% of the maximum torque and t_{90} (minutes) time corresponding to F_t. (Figure 2)
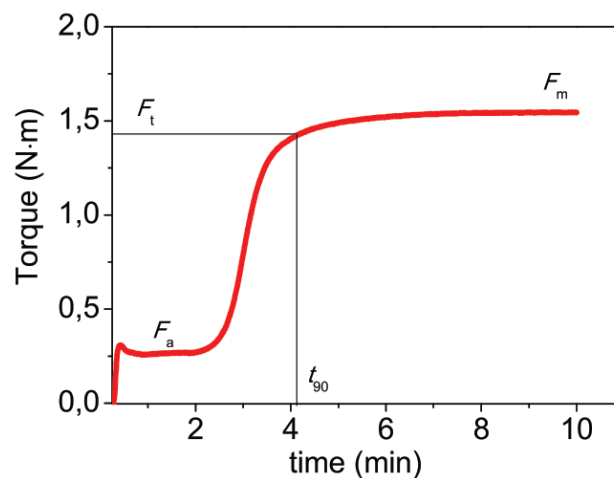

FIGURE 2 A typical vulcanization curve [Color figure can be viewed at wileyonlinelibrary.com]

Afterwards, vulcanization of the compounded mixture was performed up to t_{90} in a press machine at 160°C under the applied pressure of 150—170 bars.

From the vulcanized plates of the plasticized NBR (P-NBR) with 25 phr plasticizer (Bio-oil 2), a square ($1 \times 1 \times 0.2$ cm^3) was cut using a cutter. Similarly, a sample of the unplasticized NBR (U-NBR) without plasticizer was precisely cut with the same dimensions.

2.2.3 | FTIR spectrometry

The experiments were performed by using the FTIR spectrometer Vertex 70 with Platinum-ATR by Bruker, Germany. OPUS and ORIGIN software were used for the spectral analysis. The conditions employed were resolution: 4 cm^{-1}, number of scans was 32, number of background scans was 32 and the data were collected in the range of 400–4000 cm^{-1}.

For the in situ analysis of the migration process by using FTIR spectroscopy during short-term thermal aging, a custom-made heating system was developed. Where an assembly of plasticized and unplasticized NBR sample was heated continuously for 60 h as represented in schematic Figure 3.

2.2.4 | Nuclear magnetic resonance spectroscopy

In a nuclear magnetic resonance spectroscopy (NMR) analysis, ^{1}H-NMR and ^{13}C-NMR spectra were recorded on AVANCE IIITM, Bruker BioSpin GmbH spectrometer at 400 and 100 MHz respectively, while CDCl$_3$ was used as a solvent. Concentration of the test substance was

FIGURE 3 Schematic representation of the experimental setup [Color figure can be viewed at wileyonlinelibrary.com]
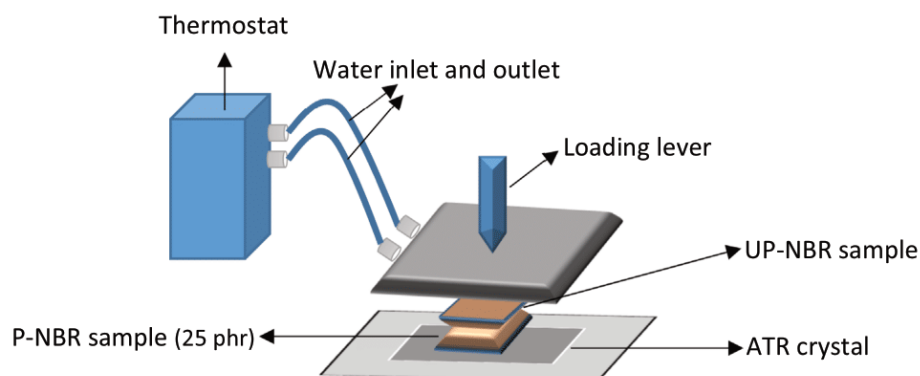
0.15 ml sample with 0.60 ml $CDCl_3$ (20 vol% sample, 80 vol% $CDCl_3$).

2.2.5 | Tensile tests

Tensile tests were performed on a Zwick ZO20 testing machine according to ISO 37 international standard.[22] Preload was 0.5 N, clamp distance was 50 mm, the clamping length from starting position was 50 mm, test speed was 200 mm/min and initial measuring length was 20 mm. An extensometer was also utilized and at least three S2 specimens were used for each material.

From the test, stress–strain diagrams were obtained. Basing on these diagrams, tensile strength (σ_{max}), and tensile strain at break (ε_R) were determined.

2.2.6 | Tear tests

Similarly, tear tests were performed to determine the tearing strength (T_s) on the same device (Zwick ZO20) following the DIN ISO 34-1 standard.[23] The trouser type specimen ($100 \times 15 \times 2$ mm^3) was used for the tests. While the test parameters were as follow: preload 0.5 N, clamp distance 50 mm, test speed 100 mm/min.

2.2.7 | IRHD-m tests

In order to compare the effect of the oils on hardness, IRHD-m tests were carried out by a Zwick-Roell device, following the DIN ISO 48 standard.[24] Specimen thickness was 2 ± 0.5 mm and testing time was 15 s. For each sample, six measurements at different positions were carried out.

SEM and EDX analysis

A morphological and elemental analysis was carried out using a TESCAN VEGA3 scanning electron microscopy

(SEM) along with energy dispersive X-ray spectroscopy EDAX by AMETEK.

3 | RESULTS AND DISCUSSIONS

3.1 | Characterization of carbonated bio-oil 2

To monitor the progress of carbonation reaction via FTIR spectroscopy, samples were taken at different time intervals. As indicated in Figure 4, a new absorbance peak at 1805 cm^{-1} appeared, which is in accordance with the reported literature[25–27] is attributed to C=O stretching associated with five-membered cyclic carbonates formation and its intensity increased with reaction progress which indicates the conversion of Bio-oil 1 to Bio-oil 2. While the carbonyl group stretching peak of the ester bond at 1736 cm^{-1} which is present in both, the pristine material (Bio-oil 1) and the final product (Bio-oil 2), showed no change. Moreover, the twin band at 823 and 841 cm^{-1} assigned to C—O—C stretching from the oxirane vibration vanishes after the carbonation reaction as can be seen in the inset of the Figure 4.

For further confirmation, ^{1}H-NMR spectra of Bio-oil 1 and Bio-oil 2 were recorded (see Figure 5). The ^{1}H-NMR (400 MHz, $CDCl_3$) spectra of starting material Bio-oil 1 (Figure 5a) and final product Bio-oil 2 (Figure 5b) clearly indicate the occurrence of the cycloaddition reaction. The signals intensity from the protons of epoxy ring appeared at $\delta = 2.80–3.20$ ppm were diminished after the synthesis of Bio-oil 2 and new peaks due to the protons of cyclic carbonated group emerged in the range of $\delta = 4.4–4.7$ ppm which is in accordance with the reported literature.[28,29,30] Ethyl acetate peak came from the cleaning step which was performed to remove the catalyst. ^{13}C-NMR (100 MHz, $CDCl_3$) of Bio-oil 2 also confirmed the occurrence of carbonated five-membered cyclic group due to the appearance of new peak at 155 ppm as represented in the supporting information (Figure S1).
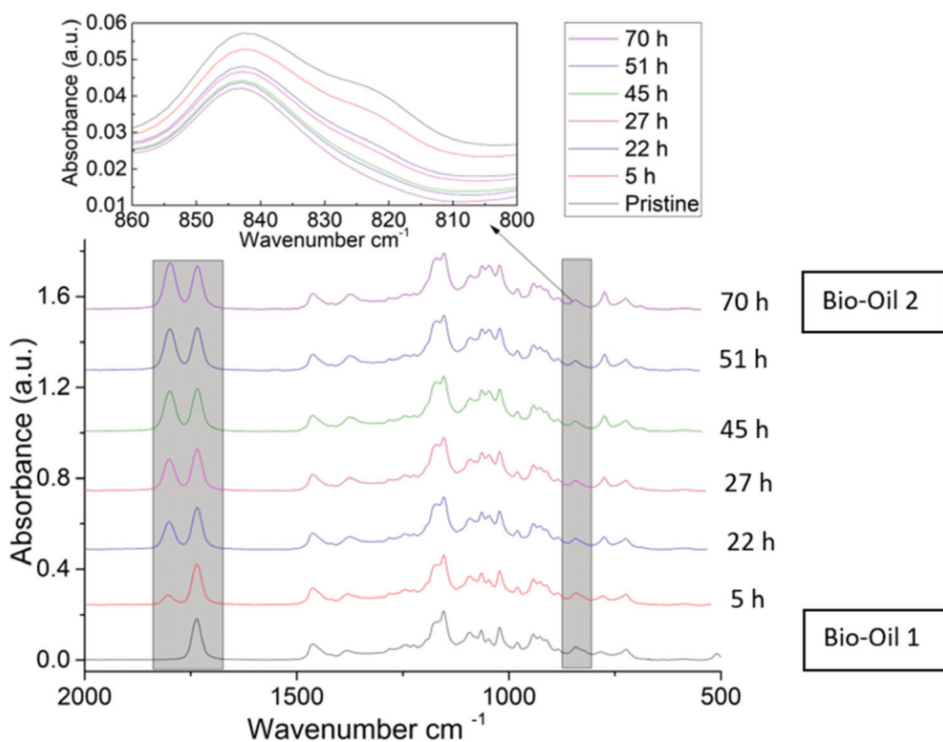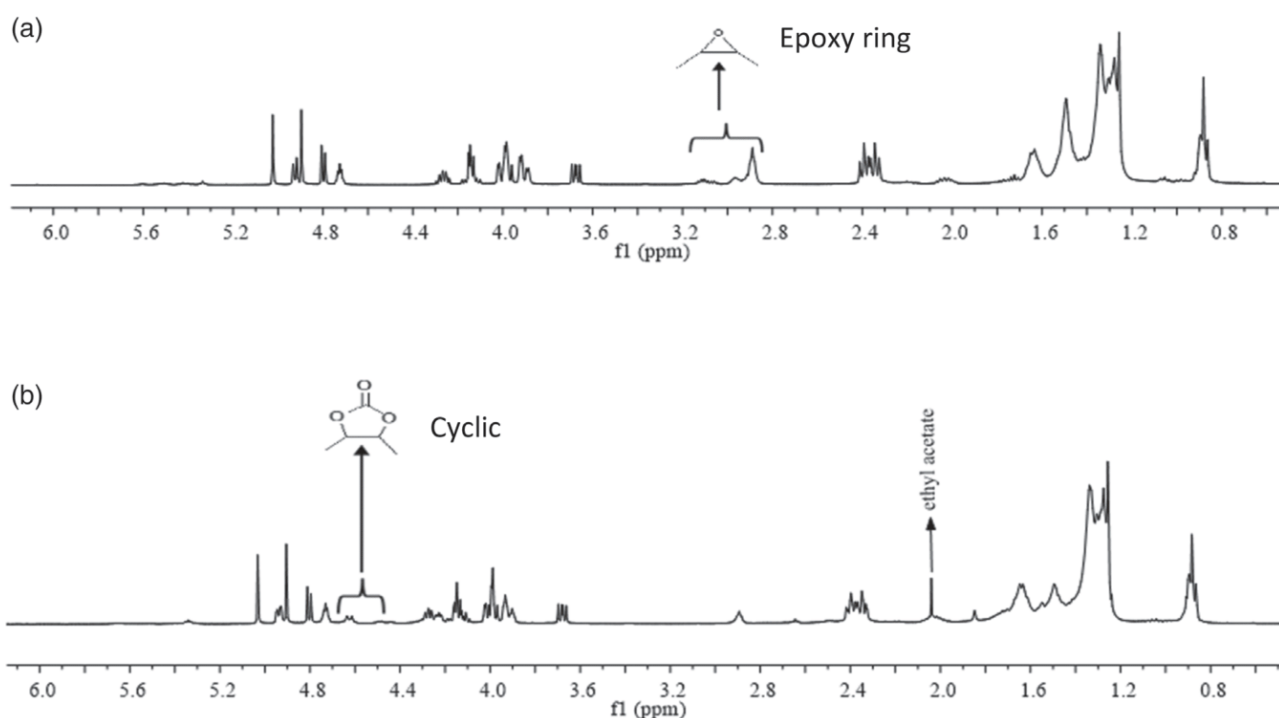
FIGURE 5 ^{1}H-NMR spectra (a) bio-oil 1 and (b) bio-oil 2

3.1.1 | In situ plasticizer migration analysis by FTIR

To observe and compare the migration of Bio-oil 2 plasticizer from NBR sample, similar test as described in our previous work[13] was carried out and corresponding spectra were recorded after every hour as represented in the Figure 6.

The characteristic band ratio profile was obtained first by dividing the peak area at 1736 cm^{-1} (carbonyl peak) and at 968 cm^{-1} (butadiene peak from NBR) to obtain the relative abundance of the carbonyl peak area. Then

Insitu FTIR spectra recorded after every hour upto 60 hours
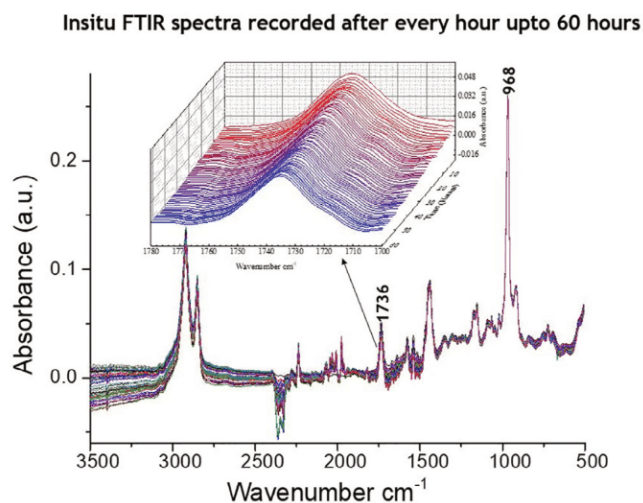
FIGURE 6 In situ FTIR spectra recorded after every hour up to 60 h with the waterfall plot in the inset representing the carbonyl peak area reduction with time [Color figure can be viewed at wileyonlinelibrary.com]

the normalized absorbance data were plotted as a function of time, and the slope of linear least squares regression yielded a value for the diffusion coefficient (D). The following exponential fitting Equation (1) from the literature[31] was applied to the data obtained in Origin software to determine the diffusion coefficient.

$$\frac{A_t}{A_\infty} = 1 - \frac{4}{\pi} exp^{\left(\frac{-D t \pi^2}{4 L^2}\right)}. \quad (1)$$

Here A_t is the carbonyl peak area at time t, A_∞ is the carbonyl peak area at equilibrium (Figure 7). L is the pathlength of the evanescent infrared beam into the sample and D is the derived parameter from Equation (1) which represents diffusion coefficient value.[13,31] In Figure 7a,b it is obvious that the diffusion coefficient value was reduced as compared to previously investigated specimen prepared using Bio-oil 1 plasticizer.

The diffusion coefficient value of comparable molecular weight of plasticizers through similar elastomeric matrix (with 34% ACN) was reported to be in the range of 10^{-10} to 10^{-11} cm^2 s^{-1},[14] which can be associated to different experimental conditions. They utilized a solid–liquid system, where infinity volume of plasticizer was confronted to polymer matrix during experiment. This resulted in a higher concentration gradient between surface of polymer matrix and polymer bulk and thus yielded higher diffusion coefficient values. In contrast, in our case solid–solid contact system was utilized with limited amount of plasticizer exposed to the polymer matrix resulting in a lower concentration gradient and causing lower diffusion rate.

Some possible physical interactions of polymer chains and Bio-oil 2 are demonstrated below in Figure 8. It is obvious in the figure that a greater number of oxygen atoms are available in Bio-oil 2 which are susceptible for physical interactions as compared to Bio-oil 1. Thus, Bio-oil 2 must encounter more hindrance for migration as compared to Bio-oil 1, leading to the reduction in diffusion coefficient value.

More possible physical interactions of polymer chains with the Bio-oil 2 molecules are provided in the supporting information (Figure S3). It can be inferred from these results that the interaction with polymer chains was increased due to the enhanced polarity of Bio-oil 2.

3.2 | Mechanical properties of NBR materials with different oils

The influence of oil modification on the mechanical properties of NBR materials was evaluated by carrying out IRHD−m measurements to analyze and compare the effect of both (Bio-oil 1 and Bio-oil 2) plasticizers on hardness of NBR specimen. According to the widely accepted free volume theory for the mechanism of plasticizer action, the introduction of plasticizer molecules into the polymer involves the addition of more free volume, which leads to the diminution of glass transition temperature and so, more flexibility and ease of movement for macromolecules.[32] Expectedly, by increasing the plasticizer amount, the hardness of the specimen was reduced which can be seen in Figure 9.

The introduction of carbonated cyclic group in the plasticizer helped to increase the polarity due to the addition of two more oxygen atoms in the ring. Thus, the interaction with the polar part of the elastomer chains was increased. As expected for Bio-oil 2, a higher hardness was observed due to higher interaction as compared to Bio-oil 1 with similar plasticizer contents (phr) which can be seen in Figure 9.

As the incorporation of plasticizer increases the flexibility of polymer, it is expected that plasticized material possesses lower tensile strength. However, these properties depend primarily on the concentration and types of plasticizers. As concentration increases, material becomes more flexible and ultimately its tensile strength is reduced. For the evaluation of plasticizer structure modification on mechanical properties of the NBR specimen, tensile tests were carried out.

Figure 10–12 show the tensile-test results of unfilled NBR/bio-oil vulcanizates. The stress−strain behavior of the NBR/bio-oil vulcanizates is depicted in Figure 10. For the graphical representation, only those curves were
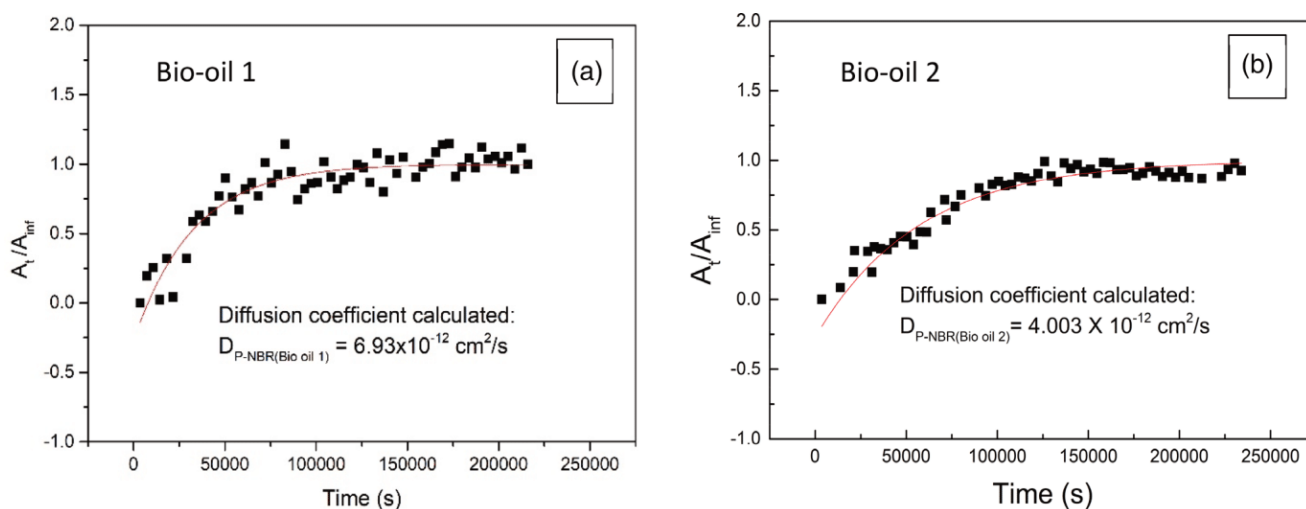
FIGURE 7 A_t/A_{inf} versus time, for the nonlinear exponential fit and the determination of diffusion coefficient (a) with bio-oil 1 and (b) with bio-oil 2 [Color figure can be viewed at wileyonlinelibrary.com]
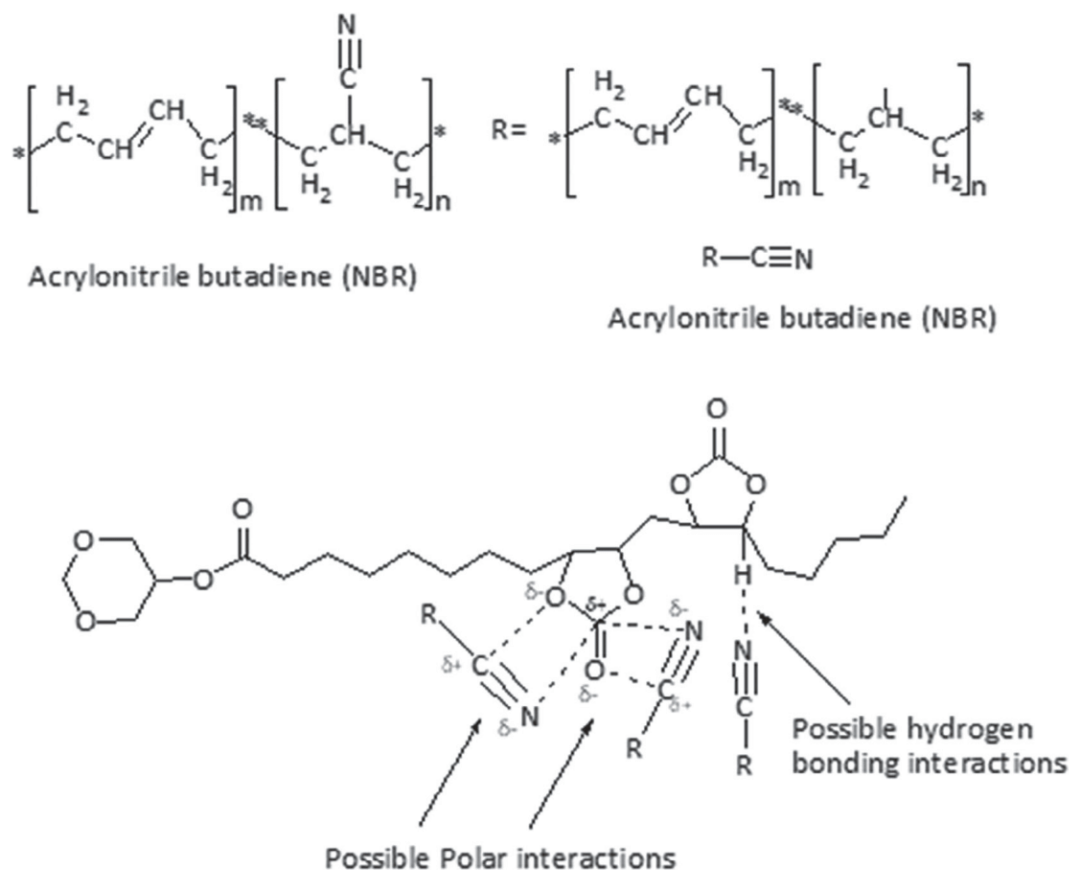

FIGURE 8 Representation of some possible physical interactions of bio-oil 2 with polymer chains

selected which had the values close to the average values calculated. The pure NBR vulcanizate without oil demonstrated highest stress value, which is in accordance with the previously reported result.[33,34] All the oil-extended NBR vulcanizates exhibited lower stress values but higher deformability, expressed by the strain at break, compared to unfilled pure NBR vulcanizate. Initially, with lower oil loading (10 phr), the oil dispersion was nonuniform and hence the strength was not fully developed,[35,36] which can be seen in Figure 10. The
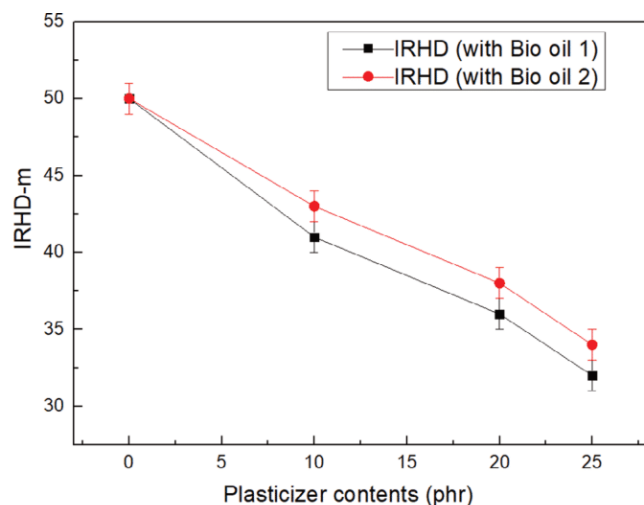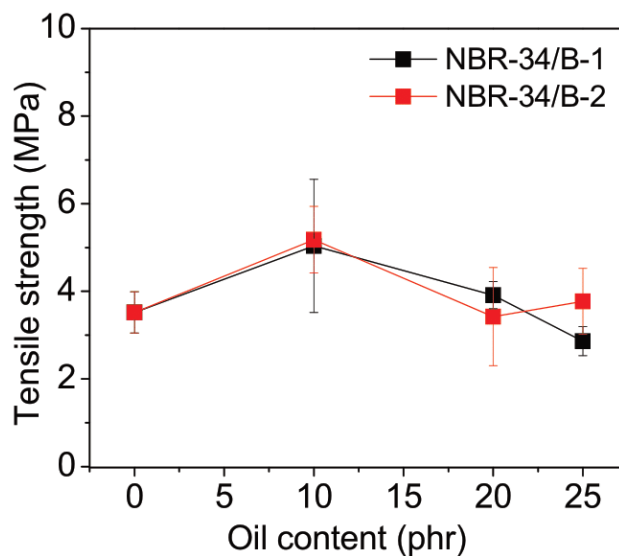
FIGURE 9 IRHD—m comparison of NBR specimen with bio-oil 1 and bio-oil 2 [Color figure can be viewed at wileyonlinelibrary.com]
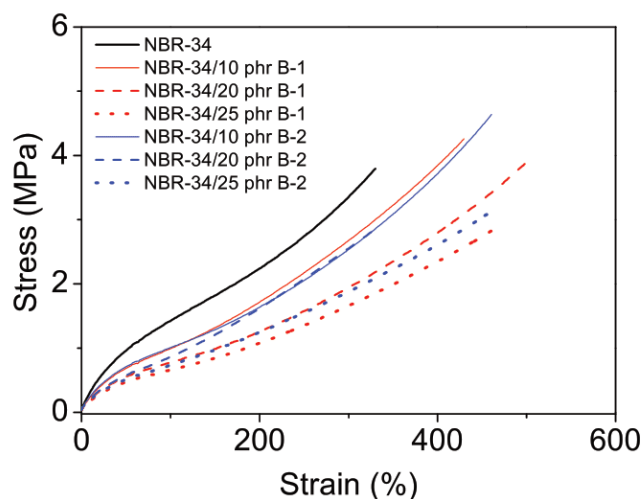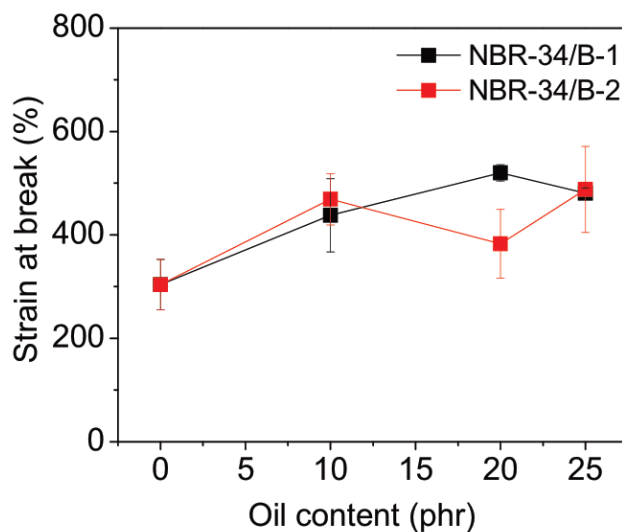

FIGURE 10 Examples of stress—strain diagrams of unfilled oil-extended-NBR vulcanizates [Color figure can be viewed at wileyonlinelibrary.com]

FIGURE 11 Variation of tensile strength with oil content for unfilled NBR vulcanizates [Color figure can be viewed at wileyonlinelibrary.com]

FIGURE 12 Variation of strain-at-break with oil content for unfilled NBR vulcanizates [Color figure can be viewed at wileyonlinelibrary.com]

stress—strain curves represented almost similar trend for NBR/10 phr bio-oils vulcanizates. Similar behavior was observed in tensile strength test with lower oil-content loading (10 phr) as can be seen in Figure 11.

With increasing oil-contents in NBR matrix, a decreasing trend of the stress in stress—strain curves was observed as depicted in Figure 10. This is attributed to the increasing capability of the NBR chains to move pass each other due to the larger free volume between entangled chains provided by plasticizer molecules.[37] Moreover, a continuous decrease in tensile strength but an increase in strain at the break (see Figure 12) with increasing oil loading is attributed to the macro-

plasticization effect, which dominates over micro-plasticization and coupling action.[38]

Figure 13 shows the tear strength values of oil extended unfilled NBR vulcanizates. The tear strength of unfilled NBR vulcanizate without oil yielded almost the same value as reported previously.[39] However, a decreasing trend in tear strength values was observed especially in case of higher oil loading of the bio-oils which can be associated to the formation of viscous layer of oil around

rubber, which causes a decrease in tear strength, as it cannot withstand the tearing force.[40]

In the case of NBR/Bio-oil 1, the tear strength remained almost constant at around 3.7 N/mm till 20 phr loading. In contrast, NBR/bio-oil 2 compounds showed a decrease up to 2.7 N/mm at 20 phr loading range which can be due to nonuniform oil dispersion in the matrix, which is also depicted in Figure 16a. While in case of 25 phr loading, both bio-oils demonstrated almost very close tear strength
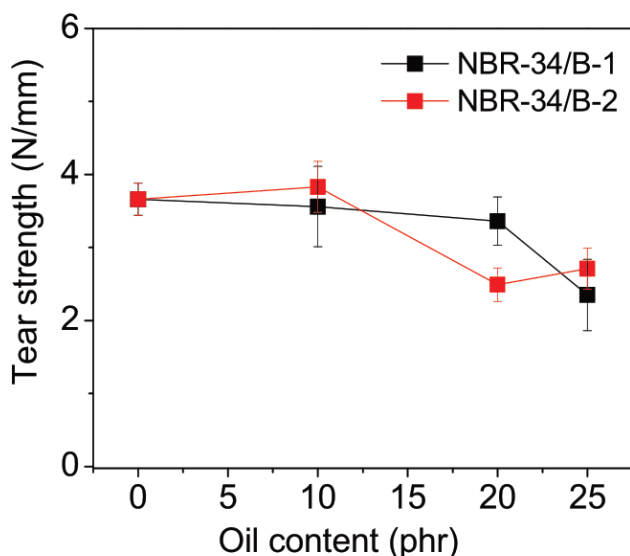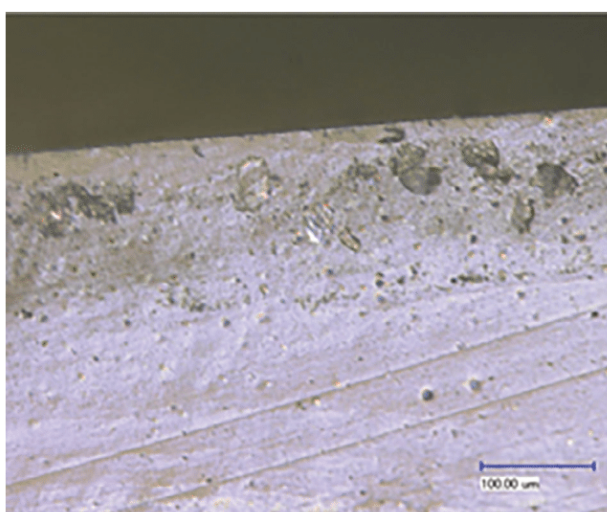

FIGURE 13 Dependence of tear strength on bio-oil content for unfilled NBR vulcanizates [Color figure can be viewed at wileyonlinelibrary.com]

FIGURE 14 Cross-sectional view on the light microscope of unfilled NBR vulcanizates without plasticizers [Color figure can be viewed at wileyonlinelibrary.com]

values. However, keeping in view the standard deviation values the results are comparable for both the oils.

Moreover, light microscopic images at the cross-sectional view were obtained to understand the dispersion of the plasticizer and additives in the nonreinforced NBR vulcanizate. Figure 14 depicts the unplasticized NBR vulcanizate, where minimal number of additive particles is visible because of high friction and internal stress during mixing. In this study only the unfilled NBR vulcanizates were analyzed so the filler influence was avoided. However, elastomers contain plasticizers inside, which help to reduce viscosity and disperse the additives through elastomer matrices.[37] These plasticizers are called primary plasticizers, despite; these properties got affected when fillers are added. Although adding additives (e.g., crosslinking agents and antioxidants) perhaps reduced the efficiency of primary plasticizers, reducing the good dispersion of additives, and due to high internal stress and high viscosity, at a certain point, the additive particles diminished utterly. These effects reduced the homogeneity of materials and gathered additive particles at the edge as reflected in Figure 14.

Nevertheless, Figure 15 shows that the additives were well dispersed when Bio-oil 1 was added up to the concentration range of 20 phr as shown in Figure 15a. The number of dispersed additives particles increased when bio-oil concentration increased to 25 phr (see Figure 15b). Bio-oil 1 helped the additives dispersion, enhancing the elastomer flexibility, and this is perhaps the reason to enhance the mechanical properties as discussed in Section 3.2. The 20 phr Bio-oil 2 content NBR vulcanizates have a small number of additive particles agglomerated as indicated in the Figure 16a which is also reflected by the increased standard deviation values for this sample. However, Figure 16b shows the dispersed additive particles were increased when Bio-oil 2 concentrations was increased to 25 phr. This behavior can be associated with the decreased viscosity and internal stress during mixing at higher concentration.[36] Nevertheless, these properties highly impact mechanical behavior.[35]

Last but not the least, SEM along with Energy dispersive X-ray spectroscopy (EDX) was also performed to further confirm the dispersion and elemental analysis of the additive particles in the matrix. Figure 17 shows the SEM micrograph of the unfilled NBR sample with 20 phr Bio-oil 2 from the cross-sectional view (x2000 and x200 magnified) along with the quantitative analysis performed by EDX. As we have investigated unfilled NBR samples, so the effect of fillers (e.g., carbon black) was avoided and even after magnifying x2000 our images look smooth without the agglomerates. Sulfur and Zinc oxide are the part of curing system used to crosslink NBR, therefore, the corresponding EDX spectra shows peaks of elemental S and Zn. The quantitative analysis revealed the presence
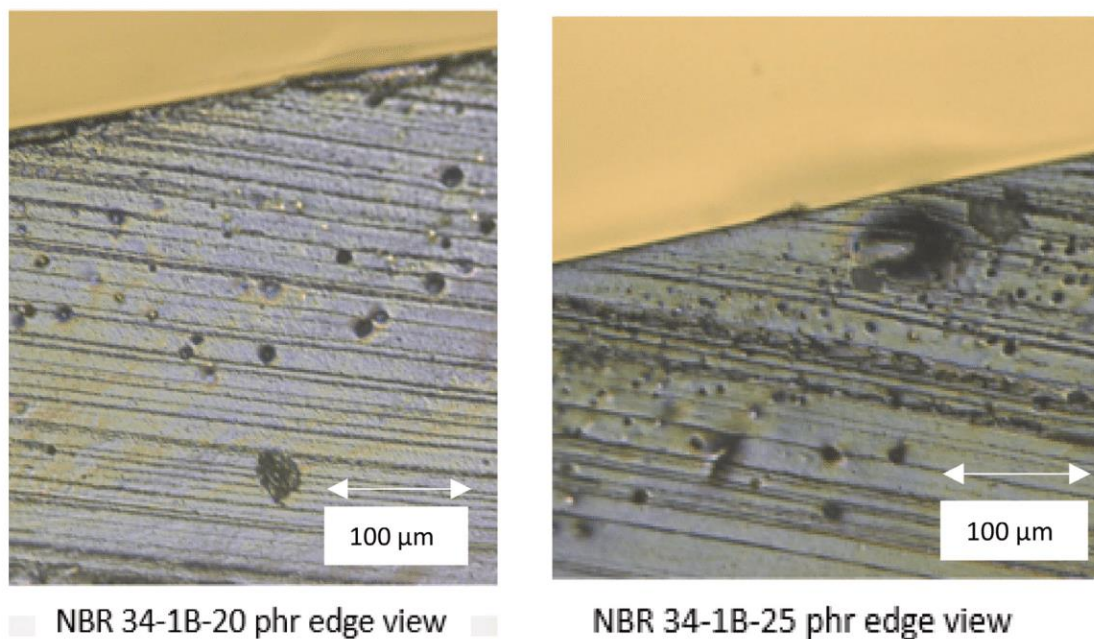
FIGURE 15 Cross-sectional view on the light microscope of unfilled NBR vulcanizates with (a) 20 phr and (b) 25 phr bio-oil 1 [Color figure can be viewed at wileyonlinelibrary.com]
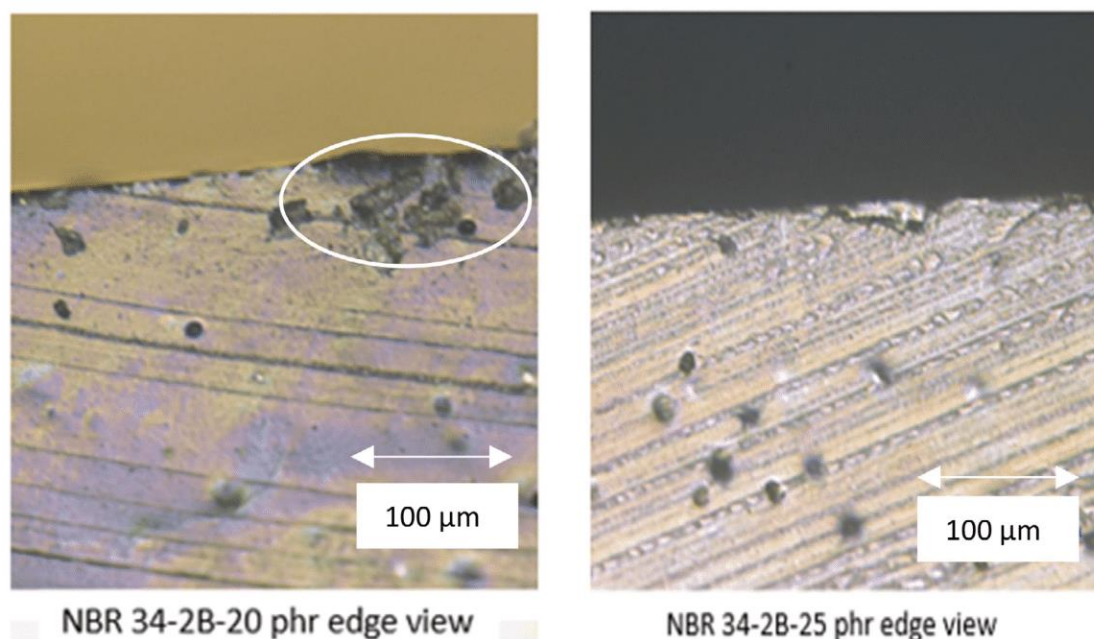

FIGURE 16 Cross-sectional view on the light microscope of unfilled NBR vulcanizates with (a) 20 phr and (b) 25 phr bio-oil 2 [Color figure can be viewed at wileyonlinelibrary.com]

of additive particles while the corresponding areas of the peaks indicate their relative abundance.

Whereas Figure 18 represents the dispersion of different elements in the matrix. To display the dispersion of additives and plasticizer, oxygen, zinc, and sulfur elements were selected. As obvious in the figures all these elements presented a uniform distribution in the matrix area observed, which support our claim of uniform distribution

of additives. The quantitative results obtained using EDX also revealed that the abundance of oxygen atoms in the samples containing Bio-oil 2 is higher than with the similar samples containing Bio-oil 1, which also supports our claim of polarity enhancement by the addition of oxygen in the molecular structure. For more information SEM images of the remaining samples are included in the supporting information (Figures S4–S6).
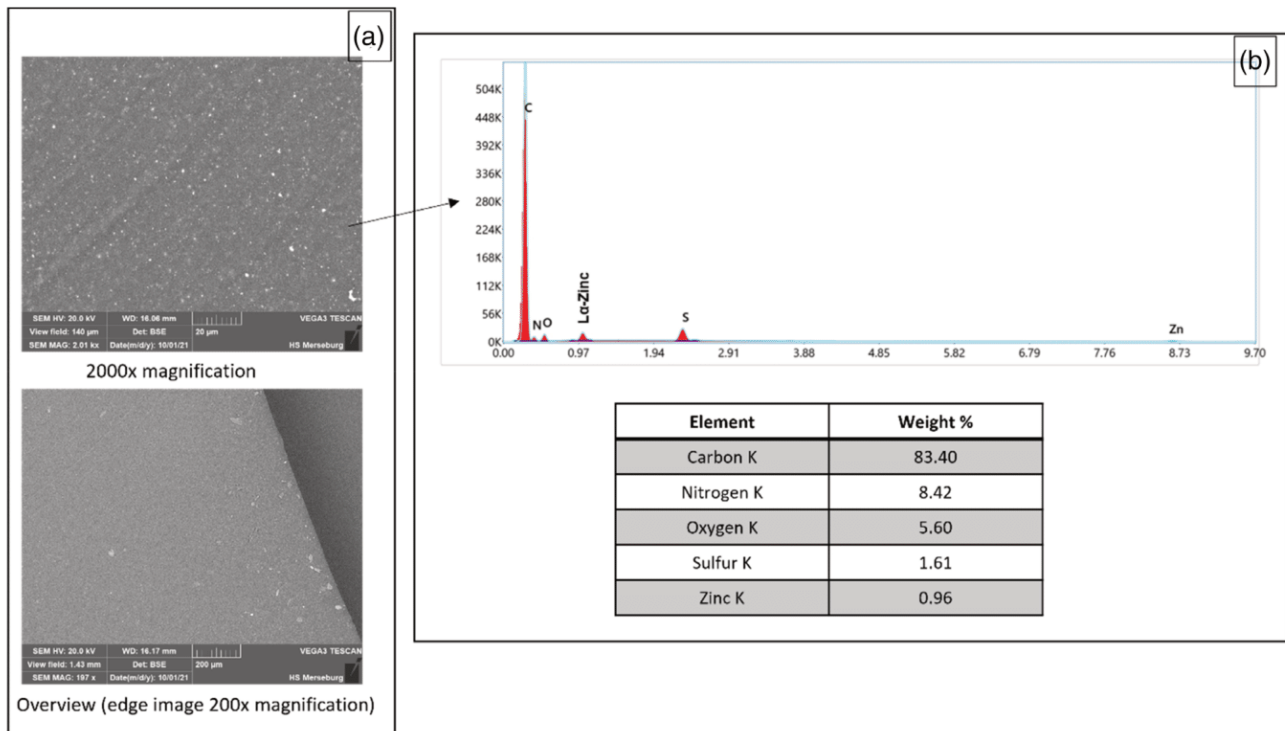
FIGURE 17 (a) SEM micrograph of unfilled NBR vulcanizates with 20 phr bio-oil 2 from cross-sectional view. (b) Quantitative energy dispersive spectroscopic (EDX) analysis [Color figure can be viewed at wileyonlinelibrary.com]
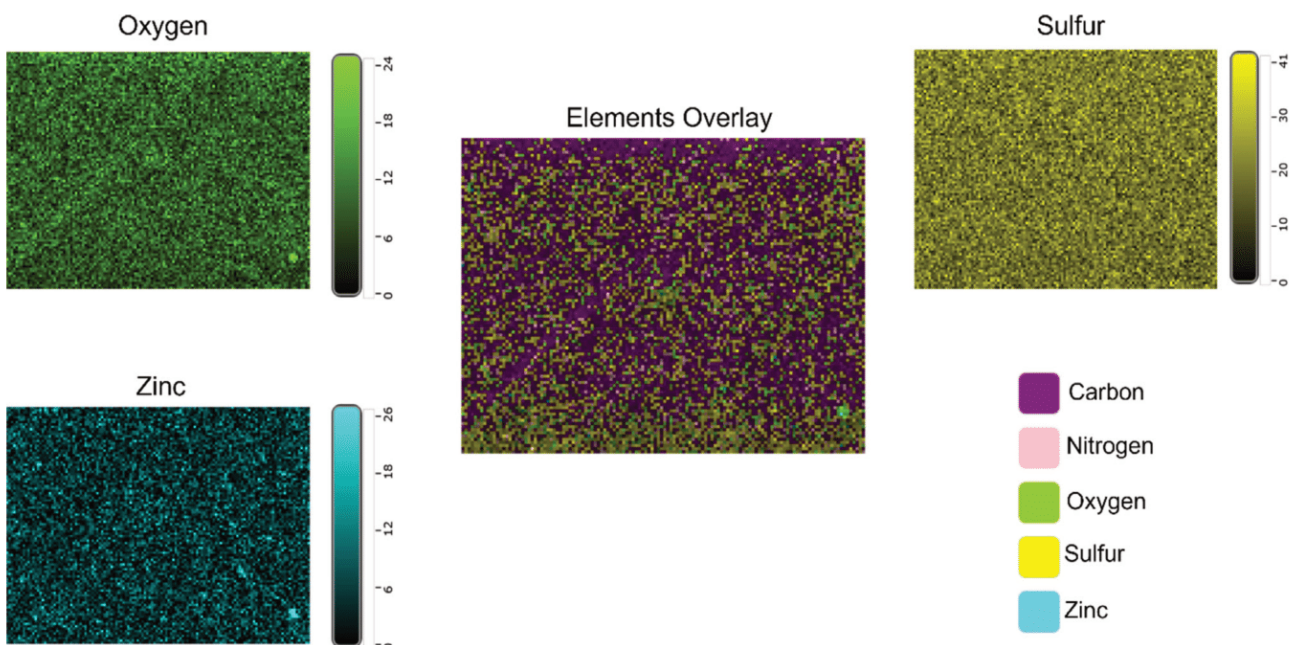
FIGURE 18 Elemental analysis performed by EDX [Color figure can be viewed at wileyonlinelibrary.com]

4 | CONCLUSIONS

In the present study, carbonated bio-oil (Bio-oil 2) was synthesized from epoxidized monoester of glycerol formal with soybean oil (Bio-oil 1) and both were incorporated into an NBR material to evaluate and compare their effects on mechanical properties and migration behavior. The plasticizing performance of Bio-oil 2 in NBR vulcanizate was mainly evaluated by the analysis of tensile properties and hardness (IRHD-m) test, while its migration behavior was compared using in situ FTIR analysis. Minor differences were observed in the mechanical properties of the

specimen as compared to Bio-oil 1 plasticized specimen, as hardness was increased up to 6%, which can be inferred to the introduction of carbonated five-membered cyclic group in the plasticizer, which helped to increase the polarity due to the addition of two more oxygen atoms in the ring. However, in tensile strength up to 20 and 15% reduction was observed with 25 phr of Bio-oil 1 and Bio-oil 2 respectively. The migration behavior revealed a decrease in oil migration, which is expressed by the diffusion coefficient value D of the Bio-oil 2. This is due to enhanced polarity and better compatibility of Bio-oil 2 with the elastomeric matrix. Thus, it can be concluded that cycloaddition reaction of CO_2 with epoxidized ester-based bio plasticizer can be an effective way to increase polarity and reduce migration of plasticizer. Therefore, this value-added product can serve as an appropriate substitute to epoxy based bio-diesel plasticizers in the industry especially where the reduced migration is of utmost importance. Moreover, this synthesis step also provides a green strategy of utilizing CO_2 by incorporating it into the epoxy rings of the plasticizer.

DATA AVAILABILITY STATEMENT
Data available on request due to privacy/ethical restrictions.

ORCID
Irfan Shahzad https://orcid.org/0000-0001-5893-4357

REFERENCES
[1] M. Hakkarainen, A. Albertsson, S. Karlsson, *Int. J. Polym. Anal. Charact.* **2003**, *279–293*, 279. https://doi.org/10.1080/10236660304883
[2] M. Morton, *Rubber Technology*, 2nd ed., Van Nostrand Reinhold Company, New York **1973**.
[3] C. Bergmann, Z. Saleem, *Rubber World* **2014**, *250*, 42.
[4] R. Singh, Bhattacharya., *Rubber World* **2011**, *243*, 20.
[5] K. Karadeniz, N. Ergüler, *Gummi Kunstst* **2011**, *7*, 49.
[6] Chiaradia, G. Plasticizers for polymers, WO 2015/067814 A2. (**2015**).
[7] S. Medows, S. Jeelani, *Proceedings of the American Society for Composites - 31st Technical Conference, ASC* 2016.
[8] O. Fenollar, L. Sanchez-Nacher, D. Garcia-Sanoguera, J. López, R. Balart, *J. Mater. Sci.* **2009**, *44*, 3702.
[9] J. T. Lutz, *Handbook of PVC formulating*, John Wiley & Sons, New York **1993**.
[10] Y. Wei, L. Jianbing, *Chem. Ind. Times* **2013**, *3*, 11.
[11] R. Shi, P. Jiang, S. Shi, *China Oils Fats* **2008**, *6*, 36.
[12] F. Galli, S. Nucci, C. Pirola, C. L. Bianchi, *Chem. Eng. Trans.* **2014**, *37*, 601.
[13] I. Shahzad, S. Wittchen, V. Cepus, *Macromol. Symp.* **2019**, *384*, 1800158.
[14] C. Rosca, R. Schuster, *Prüfen und Mess.* **2006**, *49*, 86.
[15] V. Papakonstantinou, D. Papaspyrides, *J. Vinyl Technol.* **1994**, *16*, 192.
[16] A. Earls, I. Axford, J. Braybrook, *J. Chromatogr. A* **2003**, *983*, 237.
[17] J. Yuan, B. Cheng, *Sci. Rep.* **2017**, *2–7*, 9277. https://doi.org/10.1038/s41598-017-10159-7
[18] A. Jayakrishnan, M. Sunny, *Polymer* **1996**, *37*, 5213.
[19] J. Audic, D. Reyx, J. Brosse, *J. Appl. Polym. Sci.* **2001**, *79*, 1384.
[20] N. Reddy, M. Mohan, K. Varaprasad, S. Ravindra, K. Vimala, M. Raju, *J. Appl. Polym. Sci.* **2010**, *115*, 1589.
[21] Bradley, M., Izzia, F. "Carbon black analysis" Thermo Scientific Application Note: 50829. (**2008**).
[22] DIN ISO 37: 2011 Rubber, vulcanized or thermoplastic—Determination of tensile stress-strain properties. Br. Stand. Publ. (2011).
[23] DIN ISO 34-1:2015, I. Rubber, vulcanized or thermoplastic—Determination of tear strength—Part 1: Trouser, angle and crescent test pieces. (**2015**)
[24] DIN ISO 48:2016–09, D. I. Rubber, vulcanized or thermoplastic–Determination of hardness. (**2016**)
[25] R. Holser, *J. Oleo Sci.* **2007**, *56*, 629.
[26] K. Doll, S. Erhan, *J. Agric. Food Chem.* **2005**, *53*, 9608.
[27] B. Tamami, S. Sohn, G. L. Wilkes, *J. Appl. Polym. Sci.* **2004**, *92*, 883.
[28] W. Liu, G. Lu, *J. Oleo Sci.* **2018**, *2017*, 1.
[29] Z. Li, Y. Zhao, S. Yan, X. Wang, M. Kang, J. Wang, H. Xiang, *Catal. Lett.* **2008**, *123*, 246.
[30] W. Liu, G. Lu, B. Xiao, C. Xie, *RSC Adv.* **2018**, *8*, 30860.
[31] G. T. Fieldson, T. A. Barbari, *Polymer* **1993**, *34*, 1146.
[32] G. Wypych, *Handbook of Plasticizers*, Chemtech Publishing, Toronto, New York **2004**.
[33] Z. Cao, D. G. Wang, C. B. Cong, Y. F. Wang, Q. Zhou, *Tribol. Int.* **2014**, *141–149*, 141. https://doi.org/10.1016/j.triboint.2013.09.011
[34] Y. Guo, H. Tan, Z. Cao, D. Wang, S. Zhang, *Polymers* **2018**, *10*, 1. https://doi.org/10.3390/polym10070705
[35] P. Raju, V. Nandanan, K. N. Kutty, *J. Rubber Res.* **2007**, *10*, 1.
[36] M. Rahman, K. Oßwald, K. Reincke, B. Langer, *Materials* **2020**, *13*, 1.
[37] G. Wypych, *Handbook of Plasticizers*, 2nd ed., William Andrew Publication, Toronto **2012**.
[38] P. Kundu, T. Kukreja, *J. Appl. Polym. Sci.* **2001**, *84*, 256. https://doi.org/10.1002/app.10320
[39] S. Kaang, W. Jin, M. A. Kader, C. Nah, *Polym. Technol.* **2004**, *43*, 1517. https://doi.org/10.1081/PPT-200030263
[40] S. Fernandez, S. Kunchandy, S. Ghosh, *J. Polym. Environ.* **2015**, *23*, 526.

SUPPORTING INFORMATION
Additional supporting information may be found in the online version of the article at the publisher's website.

"**CO2 cycloaddition to plant oil based epoxidized monoester: Optimization and catalyst screening**"

Irfan Shahzad, Valentin Cepus,

CO$_2$ Cycloaddition to Plant Oil Based Epoxidized Monoester: Optimization and Catalyst Screening

Irfan Shahzad* and Valentin Cepus*

Migration of epoxidized monoester plasticizers based on bio-oil can be reduced by adopting a green strategy of incorporating CO$_2$ into the epoxy rings of the plasticizer. In the present work, three different approaches are evaluated to optimize reaction output and the time required to complete the cycloaddition of CO$_2$ in epoxidized monoester of soybean oil with glycerol formal. In the first approach, deep eutectic solvent (DES) is utilized along with conventionally used tetrabutylammonium bromide (TBAB) catalyst to analyze the effect of DES on reaction, while in the second approach a co-catalyst system along with onium halide is employed. In the third strategy, a simple catalyst system comprising potassium iodide (KI) and polyethylene glycol with a molecular weight of 400 (PEG 400) or 18-crown ether as phase transfer catalysts is investigated. In all three approaches, experimental parameters such as temperature, pressure, stirring rate, time, catalyst type, and catalyst concentration are systematically evaluated. TBAB catalyst along with equimolar (DES) under 40 bars pressure demonstrated the best conversion of epoxy groups to five-membered cyclic carbonated rings within 4 h. Fourier transform Infrared spectroscopic (FTIR) analyses are regularly performed to monitor reaction progress while nuclear magnetic resonance spectroscopic (NMR) analysis is performed to confirm purity of the final product.

1. Introduction

Global warming is a burning issue now a days and one of the major contributors to this is carbon dioxide.[2] Few legislations were imposed by European union in this regard to reduce carbon dioxide emission and a strategy was devised in Germany based on the following three points: 1) reduction of CO$_2$ emissions by higher efficiency and alternative energy sources, 2) utilization of CO$_2$, and 3) Storage of CO$_2$.[3,4] However, utilization of CO$_2$ in chemical reactions is not an easy task due to its low chemical

I. Shahzad, V. Cepus
Department of Engineering and Natural Science
Hochschule Merseburg University of Applied Sciences Merseburg
Eberhard-Leibnitz-Str. 2, Merseburg 06217, Germany
E-mail: irfan.shahzad@hs-merseburg.de; valentin.cepus@hs-merseburg.de

activity. Lately, it has been mostly consumed in methanol, urea, and carbonates manufacturing.[5,6]

Cycloaddition reaction of CO$_2$ with epoxides to form carbonates is one of the simple ways to consume CO$_2$ in a chemical reaction.[3,7] Recently due to the restrictions imposed on phthalate-based plasticizers much attention is oriented to develop renewable bio-based plasticizers.[8] However, an epoxidation step is required to make these plasticizers compatible with polymers.[9] Although, migration of these monoester-based plasticizers is still a challenge.[10] In our previously reported work,[1] a strategy to curtail this migration was developed where CO$_2$ was incorporated in the epoxy rings of the plasticizer using phase transfer catalyst (TBAB) and its migration behavior was investigated in comparison to the epoxidized plasticizer. A significant reduction in the migration behavior was observed as the polarity of the plasticizer is enhanced due to a greater number of oxygen atoms in the final plasticizer, which consequently increases the polar and hydrogen bonding interactions with the polymer matrix. However, this cycloaddition reaction needs to be optimized and the various parameters which can significantly influence the output of this reaction includes catalyst type, catalyst concentration, temperature, stirring rate, CO$_2$ flow rate, pressure, and time.

Traditionally, TBAB (tetrabutylammonium bromide) is used as a phase transfer catalyst (PTC) for the cycloaddition of CO$_2$ in the epoxy rings.[7,11] Although, much longer reaction time is needed with this catalyst alone due to the steric hindrance offered by the internal epoxy groups and mass-transfer limitations. Several researchers utilized organic solvents or additives for better mass transfer so that the reaction output is improved. However, this step not only increases production cost but also using organic solvents is not environmentally benign.[12,13]

Wei Liu et al.[14] utilized deep eutectic solvents (DES) along with TBAB to optimize reaction output. DES are the ionic liquids (IL) generally composed of two or three components (Lewis or Brønsted acids and bases) that are capable of self-association, often through hydrogen bond interactions to form a eutectic mixture with a melting point lower than that of each individual component.[15] In most cases, a DES is obtained by mixing a quaternary ammonium salt with metal salts or a hydrogen bond

donor (HBD) that can form a complex with the halide anion of the quaternary ammonium salt. Delocalization of the charge occurring due to this hydrogen bonding for instance between a halide ion and the hydrogen-donor moiety is responsible for the decrease in melting point of the mixture as compared to the individual components.[16] Like ILs, DES predominantly consist of ionic species, and thus also have interesting solvent properties for high CO_2 dissolution.[15] In one of the research work, significant increase in the conversion percentage within 10 h was observed when TBAB based DES were utilized for cycloaddition reaction of CO_2 with epoxides. Although, high pressure of 1 MPa was needed.[14]

Kossev et al.[17] utilized tetraalkylammonium or phosphonium halide (onium halide) along with the co-catalyst $CaCl_2$ for the synthesis of 4-substituted 1,3-dioxolan-2-ones derivatives. $CaCl_2$ was claimed to enhance the catalytic activity of the onium halide. While the opening of the oxirane ring activated by the catalytic system was assumed as rate-determining step.

Benjamin Schäffner et al.[3] performed screening of simple catalyst systems based on halide salts in combination with a PTC (e.g., polyethylene glycols and crown ethers) for this cycloaddition reaction. Implementation of simple halide as catalyst for the carbonation step is reported for the low molecular weight carbonates.[18] However, a PTC is required along with these simple salts for efficient performance. In few of the research works it is indicated that the ether linkages of these PTCs, for example, PEGs (polyethylene glycols) can weekly interact with CO_2, which leads to the improvement of CO_2 adsorption rates.[19] Moreover, the hydroxyl groups of PEGs assist in forming cyclic carbonates by activating substrate through hydrogen bonding.[20]

In this present work, the above-mentioned strategies were evaluated for the optimization of cycloaddition reaction of CO_2 with epoxidized monoester of soybean oil. TBAB based DES (Catalyst system 1) with different catalyst concentrations and reaction parameters were assessed first, then the effect of co-catalyst (calcium chloride) along with onium halide (Catalyst system 2) on this carbonation reaction was evaluated. Last but not the least simple catalyst system based on potassium iodide (halide salt) along with polyethylene glycol 400 or 600 as PTC (Catalyst system 3) were tested by varying reaction parameters and concentrations. Within the same system, the effect of 18-crown-ether as PTC was also assessed.

2. Experimental Section

2.1. Materials

CO_2 was supplied by Air Liquide Deutschland GmbH with 99.7 % purity. Laboratory grade synthesized epoxidized monoester from soybean oil with glycerol formal (Bio-oil 1) was provided by the industrial partner Glaconchemie GmbH, Merseburg. Tetrabutylammonium bromide (TBAB, 99.0%), polyethylene glycol 400 (PEG 400), polyethylene glycol 600 (PEG 600), 18-crown-6 ether (99.0%), TEBACl (99.0%), and calcium chloride ($CaCl_2$), were purchased from Sigma Aldrich Germany, while triethylene glycol (99.0%), ethylene glycol (99.0%), potassium iodide (KI) and ethyl acetate was purchased from Carl Roth Germany. All the

chemicals were utilized as they were received without any further purification or modification.

2.2. Synthesis of DES

DES were easily prepared by following a simple step of heating and mixing the components (TBAB and HBD, e.g., triethylene glycol) at 80 °C in a small vial until a homogeneous and clear mixture was formed. As indicated in **Table 1**, two types of TBAB based DES were tested in this work. DES1 was composed of TBAB and equimolar ratio of triethylene glycol while the DES2 was based on TBAB and double molar amount of ethylene glycol as opaque and milky appearance was observed at room temperature with equimolar amount indicating the inadequacy of this amount for DES2 formation.

2.3. Synthesis of Carbonated Oil (Bio-oil 2) with Catalyst System 1

One hundred grams of Bio-oil 1 (epoxidized monoester from soybean oil with glycerol formal) was placed in a 200 ml gas washing bottle along with a magnetic stirrer. DES1 was added to the Bio-oil 1 and the mixture was stirred for 10 min at 120 °C in an oil bath until the catalyst was dissolved completely. Afterwards, a constant (5 ml s^{-1}, 0.223 mmoles s^{-1}) flow of CO_2 which was monitored using a gas flow meter was introduced. Meanwhile, samples were withdrawn at different time intervals with a pipet for FTIR analysis to monitor the reaction progress. Finally, the catalyst was removed by dissolving reaction mixture in ethyl acetate and washing five times with distilled water. The organic layer was dried on a rotary evaporator under reduced pressure and a clear dark-yellowish viscous liquid of carbonated oil (Bio-oil 2) was obtained.

2.4. Synthesis of Carbonated Oil (Bio-oil 2) with Catalyst System 2

Following the similar method, 100 g of Bio-oil 1 was placed in the washing bottle. Total 10 mol % of the catalyst based on 2:1 molar ratio of triethylbenzylammonium chloride (TEBACl) and calcium chloride ($CaCl_2$) with respect to the epoxy rings of the plasticizer was added to Bio-oil 1 and the mixture was stirred for 10 min at 120 °C until the catalyst was dissolved and then CO_2 was introduced. Similar purification step was performed to remove TEBACl catalyst while $CaCl_2$ was decanted to obtain brownish liquid of carbonated oil (Bio-oil 2). Finally, FTIR analysis were performed to check reaction progress.

2.5. Synthesis of Carbonated Oil (Bio-oil 2) with Catalyst System 3

Likewise, 100 g of Bio-oil 1 along with a magnetic stirrer was placed in a 200 ml gas washing bottle. 8 mol% of the catalyst (equimolar amount of KI and PEG 400 or 18-crown-6 ether, 5 mol %: 5 mol %) with respect to the epoxy rings of the plasticizer was added to Bio-oil 1 and the mixture was stirred for 10 min at 120 °C until the catalyst was dissolved. Afterwards, a constant and monitored (5 ml s^{-1}, 0.223 mmoles s^{-1}) flow of CO_2 was introduced and maintained for 70 h. Finally, to obtain the product, the oily liquid (Bio-oil 2) was decanted.

Table 1. Reaction optimization using traditional TBAB catalyst and catalyst system 1.

	Temperature (°C)	Pressure (bar)	Gas flow rate (ml s⁻¹)	Stirring speed (rpm)	Catalyst type	Catalyst concentration (w.r.t epoxy groups of plasticizers)	[a] Ratio of carbonyl peak area of carbonate vs carbonyl peak area of fatty acid chain	Time (hours)
1	120	1	5	500	—	—	**0**	24
2	120	1	5	500	TBAB	5 mol %	1.49	70
3	120	1	5	500	TBAB	12 mol %	1.28	48
4	120	1	5	500	[b] DES1	5 mol %	1.20	45
5	120	1	5	500	[b] DES1	12 mol %	1.31	30
6	120	1	5	500	[c] DES2	12 mol %	1.24	30
7	120	40	50	500	[b] DES1	5 mol %	1.28	4

[a] Conversion was estimated from the ratio of carbonyl peak area of carbonate at 1804 cm⁻¹ versus the carbonyl peak area of the fatty acid chain at 1736 cm⁻¹ obtained by FTIR (as more than one carbonyl groups of the carbonate are also there in the oil structure compared to the reference carbonyl group from fatty acid chain, the ratio is higher than 1 with the maximum value obtained with our oil is 1.49); [b] DES1: TBAB+ triethylene glycol (1:1) — Deep eutectic solvent based on quaternary ammonium salt of bromide (tetrabutylammonium bromide) which is a hydrogen bond acceptor and equimolar amount of triethylene glycol which is a hydrogen bond donor. The dynamic viscosity at room temperature for DES1 was 212.2 mPa.s; [c] DES2: TBAB+ ethylene glycol (1:2) — Deep eutectic solvent based on quaternary ammonium salt of bromide (tetrabutylammonium bromide) which is a hydrogen bond acceptor and double molar amount of ethylene glycol which is a hydrogen bond donor. The dynamic viscosity at room temperature for DES2 was 144.6 mPa.s.
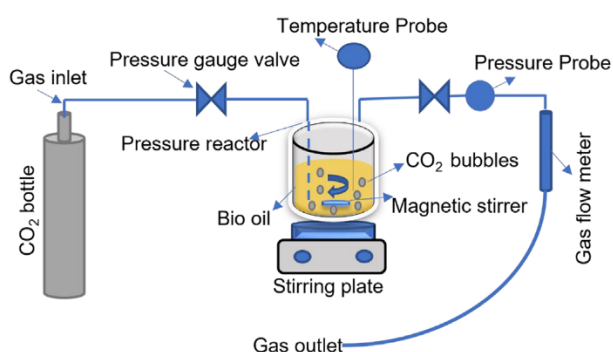
Figure 1. Schematic diagram of pressure reactor.

2.6. Synthesis of Carbonated Oil (Bio-oil 2) with Catalyst System 1, 2, and 3 in a Pressure Reactor

Similarly, 100 g of Bio-oil 1 along with a magnetic stirrer was placed in a stainless-steel pressure reactor (300 ml maximum capacity) equipped with gas inlet and outlet valves see **Figure 1**. A stirring plate was placed below this pressure reactor to stir the oil mixture as there was no inbuilt stirring facility in the reactor. DES1 as described above was added to the Bio-oil 1 and the mixture was stirred first for 10 min at 120 °C before sealing the reactor. Afterwards, a constant (50 ml s⁻¹, 2.23 mmoles s⁻¹) flow of CO_2 was introduced and slowly the pressure was increased to 40 bars which was maintained for 4 h at 120 °C. An adequate sample was withdrawn for FTIR analysis. Thereafter, the catalyst was removed as described above by dissolution in ethyl acetate and washing with water and the final organic layer (Bio-oil 2) was obtained by drying on rotary evaporator under reduced pressure. In the same way with catalyst system 2 and 3 the same amount of Bio-oil 1 was placed in pressure reactor and the same amount of catalyst as described under headings 2.4 and 2.5 were added and the mixture were heated and stirred for 10 min at 120 °C to dissolve the catalyst before sealing the reactor and introducing CO_2. Likewise, 40 bars of pressure were maintained for 4 h, and the

initial results were analyzed using FTIR. Finally, the oil layer was decanted to obtain carbonated oil (Bio-oil 2).

2.7. Methods Used

2.7.1. Fourier Transform Infrared Spectroscopy (FTIR)

The experiments were performed by using the FTIR spectrometer Vertex 70 with Platinum-ATR cell by Bruker, Germany. OPUS and ORIGIN software were used for the spectral analysis. The conditions employed were resolution: 4 cm⁻¹, number of scans was 32, number of background scans was 32 and the data were collected in the range from 400 to 4000 cm⁻¹.

2.7.2. Nuclear Magnetic Resonance Spectroscopy (NMR)

¹H-NMR and ¹³C-NMR analysis were performed for conversion confirmation. NMR spectra were recorded on an Advance III 400 NMR spectrometer by Bruker, Germany, at 400 MHz at 27 °C and $CDCl_3$ was used as solvent.

3. Results and Discussions

To the best of our knowledge, the reaction does not proceed without a catalyst as indicated in Table 1 entry 1 and TBAB is mostly used as a catalyst for the cycloaddition of CO_2 in epoxides as also explained in previously reported literatures.[7,8] Although, tedious reaction time (70 h) under atmospheric pressure conditions is required due to the steric hindrance offered by the internal epoxy groups and mass transfer limitations due to the two-phases (gas-liquid) involved. The said three strategies were systematically evaluated and their results are listed below in Tables 1–3.

3.1. Using Deep Eutectic Solvents Along with TBAB Catalyst

In this optimization approach, first only TBAB based catalyst was evaluated by varying its concentration to obtain reference.

Table 2. Reaction optimization using catalyst system 2.

	Temperature [°C]	Pressure [bar]	Stirring speed [rpm]	Gas flow rate [ml s⁻¹]	Catalyst type	Catalyst concentration (w.r.t epoxy groups of plasticizers)	*Ratio of carbonyl peak area of carbonate vs carbonyl peak area of fatty acid chain	Time [h]
1	150	1	500	5	TEBACl + CaCl₂ (2:1)	10 mol %	0.010	24
2	150	40	500	50	TEBACl + CaCl₂ (2:1)	10 mol %	0.017	4

Table 3. Reaction optimization using catalyst system 3.

|	Temperature [°C]	Pressure [bar]	Gas flow rate [ml s⁻¹]	Stirring speed [rpm]	Catalyst type	Catalyst concentration (w.r.t epoxy groups of plasticizers)	*Ratio of carbonyl peak area of carbonate vs carbonyl peak area of fatty acid chain	Time [h]
1	120	1	5	500	KI + PEG 400 (1:1)	5 mol %	0.5	70
2	120	1	5	500	KI + PEG 400 (1:1)	8 mol %	0.6	70
3	120	1	5	500	KI + PEG 600 (1:1)	8 mol %	0.55	70
4	120	40	50	500	KI + PEG 400 (1:1)	5 mol %	0.66	4
5	120	1	5	500	KI + 18-crown-6 ether (1:1)	5 mol %	0.92	70
6	120	40	50	500	KI + 18-crown-6 ether (1:1)	5 mol %	1.16	4

Thereafter, TBAB based DES (DES1, DES2) were assessed under normal atmospheric pressure conditions. Since this cycloaddition reaction involves two phases (gas-liquid), the contact area among these phases plays a vital role. As indicated by many studies DES possesses the ability to capture and separate acidic gases.[21,22] Thus when dissolved with CO_2 helps to increase the contact area with epoxides of Bio-oil 1. Accordingly, concentration of TBAB based DES would affect absorption amount of CO_2 as can be seen in Table 1 entry 4. Where much longer reaction time (45 h) was needed to obtain the conversion of 80 %. However, a significant reduction in the reaction time (30 h) was observed with 12 mol % of TBAB based DES. Last but not the least following Henry's law, effect of pressure on the solubility of gases was also assessed by varying pressure in a pressure reactor. As indicated in entry 7, similar conversion percentage, indicated by the carbonyl peak ratio, was obtained within 4 h when a pressure of 40 bars was applied.

3.2. Using Co-Catalyst with Onium Halides

As obvious from **Table 2**, almost no conversion was observed when this combination of catalyst system was utilized for our long chain monoesters with the oxirane groups laying in the middle. However, in the research work of Kossev et al. they observed high yields when propylene or 1,2 butylene carbonates were synthesized, as in their case oxirane ring were located at the edge of the molecule and did not have to encounter steric hindrance offered by the lengthy fatty acid chains. Moreover, the applied high reaction temperature of 150 °C can also cause the decomposition of the catalyst as observed by Zheng et al for TBAB catalyst. They observed higher mass loss of catalyst in a TGA (Thermal gravimetric analysis) experiment above 130 °C.[23]

3.3. Using Simple Catalyst System Comprising KI and PEG 400/600 or 18-crown-6 Ether

To avoid the subsequent tedious cleaning step the research work of Benjamin Schäffner et al.[3] was followed where they performed screening of halide-salts based catalyst along with increasing molecular weight PEGs (as PTC) to find the best catalyst system for the cycloaddition reaction of CO_2 in epoxides. In this work a catalyst system composed of KI and polyethylene glycol 400 (PEG 400) was evaluated first by varying their molar ratios under normal atmospheric conditions and then under high pressure conditions in a pressure reactor. As indicated in **Table 3**, the conversion ratio was increased to 0.6 by increasing the catalyst concentration (8 mol % with respect to the epoxy rings of the plasticizer) under atmospheric conditions. However, the conversion ratio was still lower as compared to when TBAB based DES were utilized as catalyst for cycloaddition reaction. Afterwards, higher molecular weight PEG (e.g., PEG 600) was also assessed, but no prominent effect on the reaction output was observed as can be seen in Table 3, entry 3. Last but not the least, effect of high pressure (40 bars) on this catalyst system was also examined but in comparison with the earlier reported literature[3] our conversion percentage was lower as our reaction conditions were not similar. Especially the applied pressure conditions (100 bars) significantly affected our results, indicating that high pressure is required for sufficient conversion when this simple catalyst system is employed. Although when 18-crown-6 ether was used as PTC in place of polyethylene glycol, a prominent difference in the reaction output was observed as can be seen in Table 3, entries 5 and 6. Entry 5 indicates atmospheric pressure as reaction condition with a ratio of the carbonyl peaks of 0.92, whereas entry 6 demonstrates the effect of the reaction in a pressure reactor leading to a peak ratio of 1.16. As obvious from the
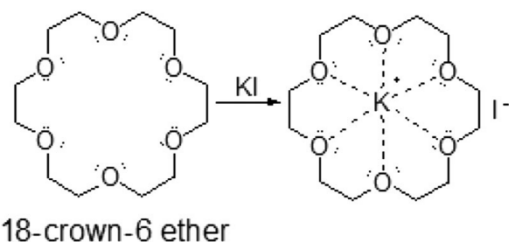
Scheme 1. Proposed formation of [K+ {crown ether} I−] complex.

results presented, the catalytic activity of the alkali metal salts increases with an increase in the anion nucleophilicity. 18-Crown-6 ether forms a complex with potassium ion by using all six oxygen atoms as donor atoms, while the anion becomes naked nucleophile as represented in **Scheme 1**, which facilitates the strong nucleophilic attack of the anion on the oxirane ring and causes the opening of the ring, which is the rate determining step.[24,25]

Various other parameters, for example, temperature, stirring rate, CO_2 flow rate, pressure, and time, which can significantly impact the result were also systematically evaluated. These parameters cannot be overlooked during optimization. Even if the stirring is not proper than the gas is not homogenously dispersed in bulk and consequently less conversion is observed. Similarly, if the temperature is not regulated during the reaction even than conversion percentage is affected. In the same way, if the gas flow is not uniform and homogeneous than less conversion is observed.

4. Characterization of Carbonated BIO-OIL 2

For the characterization of synthesized carbonated Bio-oil 2, FTIR, proton and carbon nuclear magnetic resonance spectroscopy (^{1}H and ^{13}C NMR) were exploited. The results obtained are discussed below in detail.

4.1. FTIR Analysis

To examine the conversion of Bio-oil 2 with different catalyst systems, FTIR analysis were performed as represented in the **Figure 2** and the characteristic peaks were assessed. For the pristine Bio-oil 1, only one characteristic carbonyl peak was observed in the region of 1736 cm^{-1}. While the emergence of new peak at 1805 cm^{-1} is associated to the carbonyl stretching of five-membered cyclic carbonate (carbonyl peak from a) which is in accordance to reported literature [26–28] indicates the formation of carbonate groups in the newly synthesized Bio-oil 2. The corresponding area of the peak at 1805 cm^{-1} indicates the relative conversion with respect to the peak area at 1736 cm^{-1}. Moreover, the characteristic shoulder at 826 cm^{-1} from the epoxy group of Bio-oil 1 diminishes after the reaction and a new characteristic peak appears at 772 cm^{-1} which is associated to the generation of carbonate group in the oil.[29] As can be derived from Figure 2 with the reference catalyst TBAB (Table 1, entry 2) maximum conversion was achieved after 70 h of reaction time, whereas in case of DES 1 catalyst (Table 1, entry 7) and crown ether catalyst (Table 3, entry 6), with high pressure of 40 bars almost similar conversion was observed within 4 h.

As independent second confirmation, ^{1}H and ^{13}C NMR spectra of Bio-oil 1 and Bio-oil 2 were recorded. **Figure 3** represents
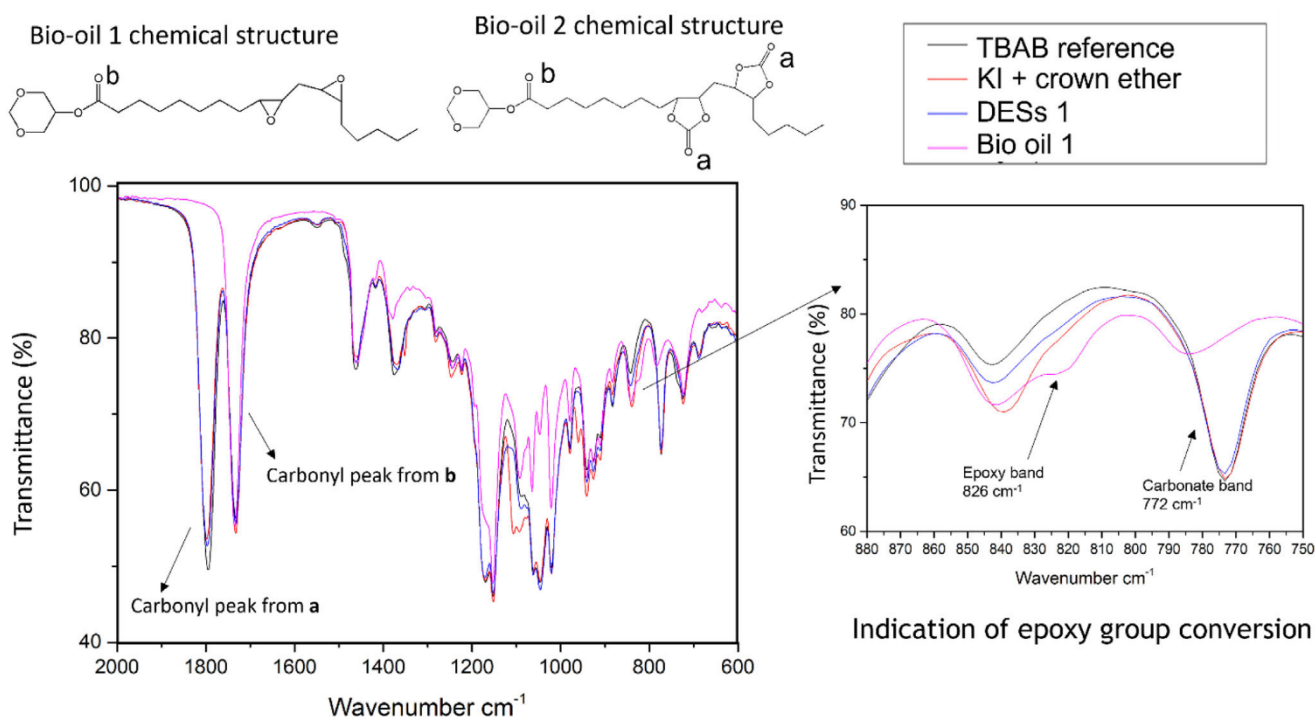

Figure 2. FTIR spectra of pristine Bio-oil 1 and Bio-oil 2 synthesized with different catalyst systems: TBAB (black), KI + crown ether (red), DES1 (blue), Bio-oil 1 (pink).
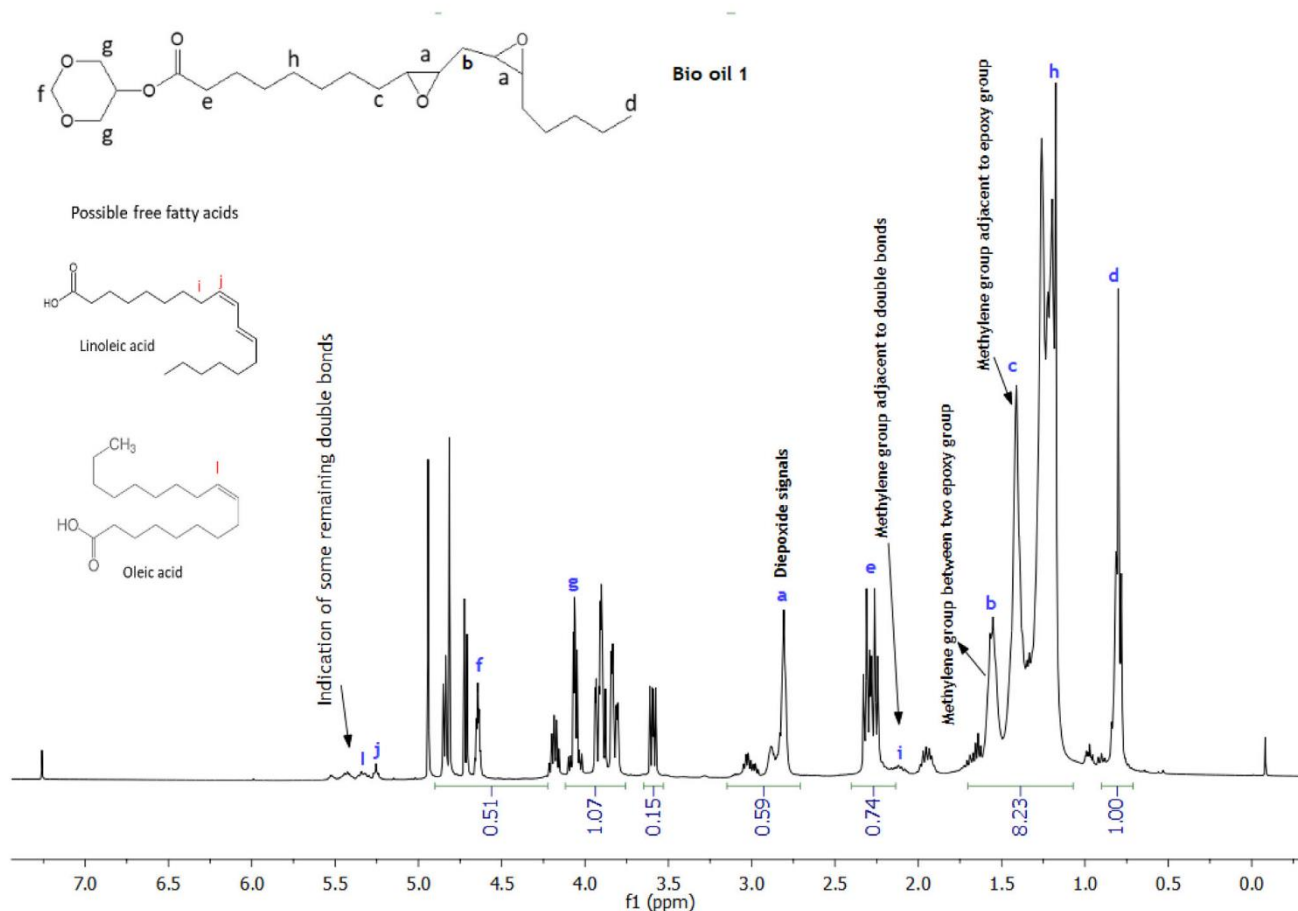
Figure 3. ^{1}H NMR spectra of Bio-oil 1.

the ^{1}H NMR spectra of Bio-oil 1, where all the protons from the chemical structure of the oil were assigned to their corresponding peaks. The characteristic multiplet signals from the protons of epoxy group (*a*) appeared at $\delta = 2.80–3.20$ ppm and the methylene group protons (*c*) adjacent to the epoxy group gave a multiplet signal at $\delta = 1.45–1.60$ ppm. The appearance of some proton signals in the region $\delta = 3.5–4.0$ ppm can be associated to —OH groups, which appear due to the possible ring opening of the epoxide groups in the oil due to the side reactions of hydrolysis and acylation taking place owing to reaction environment (epoxidation reaction with peroxides) which contains water, mineral (catalyst) and organic acids.[30,31] Moreover, since the starting material Bio-oil 1 is based on the natural product, so the variation in the fatty acid composition and possibility of other residues cannot be denied which depends on various factors for example, origin, climate, harvesting period. Few of the proton signals from these residues (e.g., *i*, *j*, and *l*) are also indicated in the NMR spectra obtained.

Figure 4 represents the ^{1}H NMR spectra for Bio-oil 2, where new multiplet characteristic signals from the protons of the carbonate group (*m*) emerged at $\delta = 4.2–4.9$ ppm, while the signals from the epoxy group (*a*) diminished. Moreover, the characteristic signals from the protons of adjacent methylene group (*c*) also diminished after the reaction which indicates the conversion of epoxy groups. For more information ^{13}C NMR spectra of the Bio-

oil 1 and Bio-oil 2 is added in Supporting Information which also confirmed the generation of carbonated ring by giving a characteristic signal at 155 ppm for Bio-oil 2 which is associated to the carbonated ring.

Based on the integration values obtained from the corresponding characteristic peaks, quantification of the reaction was performed following the Equation (1).

$$S\% = 100\% \cdot \frac{A - B}{A} \tag{1}$$

Where *A* indicates the integration of the peak area from Bio-oil 1 in the region from 2.8 to 3.2 ppm (proton signals from the epoxide ring [initial amount]), *B* is the integration of the same area (2.8–3.2 ppm) in Bio-oil 2 (final remaining epoxide groups after reaction). The final value obtained indicated the conversion of 79.6 %.

5. Conclusions

In this work three different optimization strategies were evaluated for the cycloaddition reaction of CO_2 with epoxidized fatty acid methyl esters. Effect of DES were assessed first, then the effect of co-catalyst (Calcium chloride) along with Onium halide on this carbonation reaction was evaluated. Lastly, the catalyst
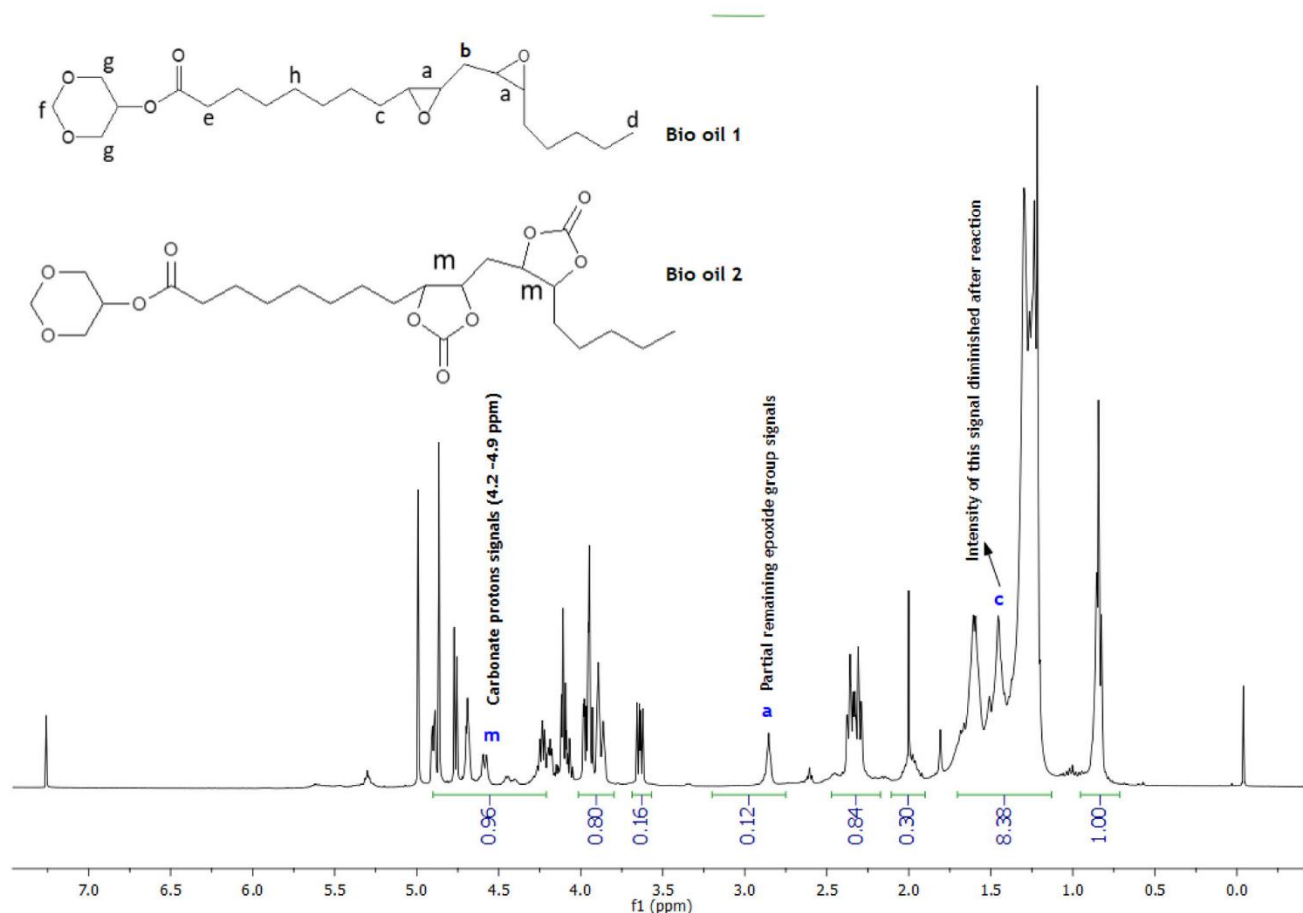
2100508 (6 of 8)

Figure 4. ^{1}H NMR spectra of Bio-oil.

system based on KIand phase transfer catalysts (polyethylene glycol 400/600 or crown ether) were tested by varying reaction parameters and concentrations systematically.

During the optimization process, the conversion increased up to 86 % with respect to reference within 4 h when DES1 (TBAB+ triethylene glycol [1:1]) based catalyst system was utilized under the high-pressure conditions of 40 bars. The dominant ionic species in deep eutectic solvent-based catalyst assisted in capturing CO_2 molecules and accelerated the reaction output. In case of co-catalyst system along with onium halide almost no conversion was observed which can be associated to steric hindrance due to lengthy fatty acid chain structure and high temperature which led to the possible decomposition of catalyst system. However, the phase transfer catalysts (PEG 400) along with potassium halide catalyst yielded moderate results with our epoxidized fatty acid methyl esters (Bio-oil 1). Although, with crown ether as PTC a comparatively good conversion of up to 78 % was observed with respect to reference within 4 h in a pressure reactor.

Supporting Information

Supporting Information is available from the Wiley Online Library or from the author.

Conflict of Interest

The authors declare no conflict of interest.

Data Availability Statement

The data that support the findings of this study are available on request from the corresponding author. The data are not publicly available due to privacy or ethical restrictions.

[1] I. Shahzad, V. Cepus, *J. Appl. Polym. Sci.* 51854, **2021**, doi:10.1002/app.51854.

[2] T. R. Anderson, P. D. Jones, *Endeavour* **2016**, *40*, 178.

[3] B. Schäffner, S. Buchholz, *Chem. Sus. Chem.* **2014**, 1133, doi:10.1002/cssc.201301115.

[4] CO$_2$-emission trading system in Europe and Germany: www.dehst.de

[5] G. A. Olah, *Alain Goeppert "Beyond oil and gas: the methanol economy"*, John Wiley & Sons, Weinheim **2018**.

[6] B. Schäffner, F. Schäffner, *Chem. Rev.* **2010**, 4554.

[7] M. Doll, Z. Erhan, *J. Agric. Food Chem.* **2005**, 9608. doi:10.1021/jf0516179.

[8] B. Tamami, S. Sohn, G. L. Wilkes, *J. Appl. Polym. Sci.* **2003**.

[9] F. Galli, S. Nucci, C. Pirola, C. L. Bianchi, *Chem. Eng. Trans.* **2014**, *37*, 601.

[10] G. Chiaradia, "Plasticizers for polymers" WO 2015/067814 A2, **2015**.

[11] S. Yan, *Catal. Lett.* **2015**, 246. doi:10.1007/s10562-008-9414-8.

[12] Z. Li, H. Xiang, *Catal. Lett.* **2008**, *123*, 246.

[13] L. Xiao, F. Li, C. Xia, *App. Catal.* **2005**, *279*, 125.

[14] W. Liu, G. Lu, *J. Oleo Sci.* **2017**, 1.

[15] Q. Zhang, F. Jerome, *Chem. Soc. Rev.* **2012**, 7108. doi:10.1039/c2cs35178a.

[16] E. L. Smith, A. P. Abbott, K. S. Ryder, *Chem. Rev.* **2014**, 11060. doi:10.1021/cr300162p.

[17] K. Kossev, N. Koseva, K. Troev, *J. Mol. Catal. A. Chem.* **2003**, *194*, 29.

[18] T. Sakakura, J. Choi, H. Yasuda, *Chem. Rev.* **2007**, 2365. doi:10.1021/cr068357u.

[19] J. Steinbauer, T. Werner, *Chem. Sus. Chem.* **2017**, 3025. doi:10.1002/cssc.201700788.

[20] S. Kaneko, S. Shirakawa, *ASC. Sustainable. Chem. Eng.* **2017**, 2836. doi:10.1021/acssuschemeng.7b00324.

[21] M. Carriazo, C. Ania, J. Parra, M. Luisa, *Energy Environ. Sci.* **2011**, 3535. doi:10.1039/c1ee01463c.

[22] M. Wise, A. Chapoy, *Fluid Phase Equilib.* **2016**, *419*, 39.

[23] J. L. Zheng, F. Burel, T. Salmi, B. Taouk, S. Leveneur, *Ind. Eng. Chem. Res.* **2015**, *54*, 10935.

[24] G. Rokicki, W. Kuran, B. Pogorzelska-Marciniak, *Monatshefte Für Chemie /Chem. Mon.* **1984**, *115*, 205.

[25] C. L. Liotta, H. P. Harris, *J. Am. Chem. Soc.* **1974**, *96*, 2250.

[26] R. A. Holser, *J. Oleo Sci.* **2007**, *56*, 629.

[27] K. M. Doll, S. Z. Erhan, *J. Agric. Food Chem.* **2005**, *53*, 9608.

[28] B. Tamami, S. Sohn, G. L. Wilkes, *J. Appl. Polym. Sci.* **2004**, *92*, 883.

[29] A. Boyer, H. Cramail, *Green Chem.* **2010**, *12*, 2205.

[30] E. Milchert, A. Smagowicz, G. Lewandowski, *Org. Process Res. Dev.* **2010**, *14*, 1094.

[31] S. Allauddin, R., *Ind. Crops Prod.* **2016**, *85*, 361.

5. Discussion

The manuscripts published in my doctorate studies includes a green strategy of modifying plasticizer by incorporating CO_2 in the epoxy rings of the plasticizer and thereby enhancing polarity of the plasticizer, moreover the mechanical properties of the samples (based on acrylonitrile butadiene rubber (NBR)) prepared using this plasticizer were observed as compared to the epoxidized plasticizer [P2]. However, optimization of this reaction was required since this cycloaddition reaction needed long reaction time of 72 hours [P3]. Last but not the least a novel technique was developed to study the in-situ migration of the plasticizer using Infrared spectroscopy with the attenuated total reflection (ATR) device [P1].

As described above in the first publication [P1], a new method to observe in situ migration of the plasticizer from plasticized NBR matrix was developed. Where the assembly of plasticized and unplasticized NBR samples was heated continuously for artificial aging with a home-made aluminum plate, while the unplasticized sample served as a concentration gradient to induce migration. On hourly basis, FTIR spectra were recorded from the plasticized sample on the same exact position. As represented in the waterfall plot (Figure 17), the reduction in area of characteristic carbonyl peak of plasticizer was observed which corresponds to the decrease of its concentration as explained by Lamber-Beer law. This law explains the relationship between the absorption of electromagnetic waves and the quantity of the absorbing material. Although, it must be clarified that precision to determine the diffusion coefficient is restricted to the sample volume which is being penetrated by the evanescent waves of the infrared beam. Moreover, it is considered as a simplifying hypothesis that the plasticizer is uniformly distributed in the matrix.
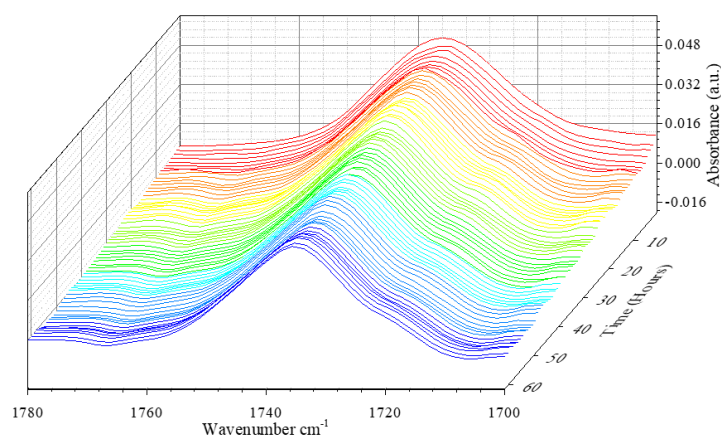

Figure 17. Waterfall plot of characteristic carbonyl peak area after every hour

To avoid the possible human errors, a method was developed in the origin software (batch processing technique) to accurately determine the area of the carbonyl peak in all the corresponding spectra which were recorded after every hour. The normalized absorbance data obtained was plotted as a function of time and the slop of linear least squares regression yielded a value for the diffusion coefficient (D). The exponential fitting equation 19 was utilized to determine diffusion coefficient, this equation is wholly analogous to equation 6 which was used to determine the diffusion coefficient in gravimetric sorption experiment at long times, as explained briefly in the theory part. The diffusion coefficient value of comparable molecular weight of plasticizers through similar elastomeric matrix (with 34 % ACN) was reported to be in the range of 10^{-10} to 10^{-11} cm^2/s [65]. Owing to different experimental conditions as in their case solid-liquid contact system was applied which means infinity volume of plasticizer was exposed to polymer matrix during experiment resulting in higher concentration gradient between surface of polymer matrix and polymer bulk leading to higher diffusion coefficient value. While in our case solid-solid contact system was utilized with limited amount of plasticizer exposed to polymer matrix resulting in lower concentration gradient which caused lower diffusion rate.

The diffusion coefficient data holds a significant value in predicting the life span of the product under different environmental loadings. This novel method can be effectively applied to monitor the precise migration of IR active migrant species in a system under observation. Thus, presenting a universal tool for the migration determination.

Moreover, a new method based on thermogravimetric analysis was developed which helped to quantify the amount of migrated plasticizer during thermal ageing. Where a calibration curve was developed by plotting the mass loss at certain temperature in the samples with step wise increasing plasticizer contents. This calibration curve helped to estimate the amount of plasticizer migrated to unplasticized sample when its mass loss percentage at same temperature was determined. High precision of adjusted R-squared value (0.97) presented a fair fit of the data points.

In the second publication [P2], a green strategy of incorporating CO_2 in the epoxy rings of the plant oil-based monoester plasticizer was adopted as modification step to increase the polarity. Where the conventional reaction path based on tetrabutylammonium bromide (TBAB) as phase transfer catalyst was followed. As represented earlier in the exemplary reaction scheme 2, the role of the TBAB catalyst in cyclic carbonate synthesis is to open the epoxide ring to form bromo-alkoxide, which then reacts with carbon dioxide and cyclizes to give the cyclic carbonate with regeneration of the tetrabutylammonium bromide catalyst.[79]
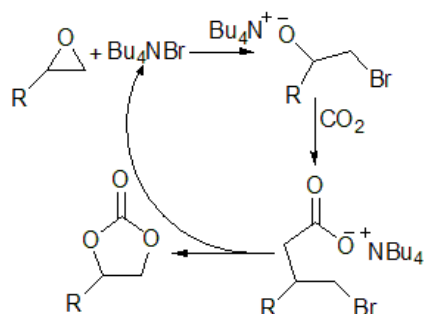
Scheme 2. role of TBAB in cyclic carbonate synthesis

Corresponding infrared (IR) and nuclear magnetic resonance spectroscopic (NMR) analysis indicated reaction progress and generation of cyclic carbonates by giving characteristic signals in the spectra, which were in accordance with the reported literature.[100][77][101][102][103] For instance, in IR analysis the emergence of characteristic carbonyl stretching peak at 1805 cm^{-1} indicates the generation of carbonated species. Whereas the shoulder of the twin band appearing at 823 cm^{-1} diminishes after the reaction, this corresponds to the conversion of the epoxy groups in the Bio-oil 1. Likewise, in ^{1}H-NMR spectra the characteristic proton signals from the epoxy ring appearing at δ = 2.80–3.20 ppm diminishes after the reaction and new signals corresponding to the newly generated carbonate ring emerged at δ = 4.4–4.7 ppm.

To analyse the mechanical performance of the modified oil, samples based on Acrylonitrile butadiene rubber (NBR) were prepared and their properties were compared. The data of mechanical properties analysis demonstrated almost similar trend in the properties with epoxidized (Bio-oil 1) and carbonated (Bio-oil 2) plasticizers. However, the samples with Bio-oil 2 demonstrated increase in hardness, which was expected due to the enhanced polarity, as comparatively a greater number of oxygen atoms were there in the modified oil. The following interaction model also suggests the polarity enhancement in Bio-oil 2.
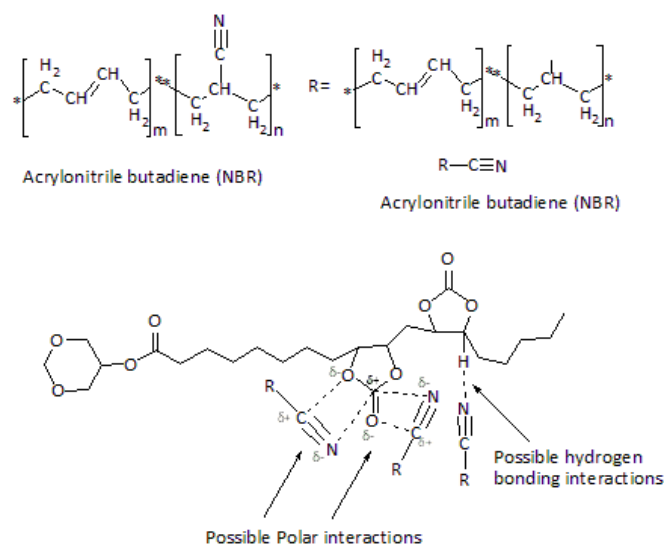
Figure 18. Possible interaction model of Bio-oil 2 with NBR

As indicated in the interaction model number of possible interaction sites are more in Bio-oil 2 as compared to Bio-oil 1, which leads to higher interaction with the polymer matrix. This enhancement in interaction also helped to curtail the diffusion of the plasticizer as demonstrated by the diffusion coefficient value, which was obtained by following the novel in situ migration test with the FTIR-ATR as described earlier in the first publication.

To observe the dispersion of the plasticizer and additives in the nonreinforced NBR vulcanizate, light microscopic and scanning electron microscopic (SEM) images with elemental analysis (EDX) were obtained at the cross-sectional view. Since the unfilled NBR samples were investigated so the effect of fillers (e.g., carbon black) was avoided and the images illustrated the uniform dispersion of the plasticizer and additives even after magnification (x2000). Last but not the least, the quantitative results obtained using EDX also revealed that the abundance of oxygen atoms in the sample containing Bio-oil 2 is higher than with the similar sample containing Bio-oil 1, which also support our claim of polarity enhancement by the addition of carbon dioxide in the molecular structure of the plasticizer.

This value-added product can serve as an appropriate substitute to epoxy based monoester plasticizers in the industry especially where the reduced migration is of utmost importance. Moreover, this synthesis process is a step in the green chemistry direction and an effort to mitigate global warming by consuming CO_2 in a chemical reaction.

In third publication [P3], different approaches were evaluated for the optimization of the cycloaddition reaction of CO_2 in the epoxy rings of the Bio-oil 1 plasticizer, because long reaction time of 70 hours was required due to steric hindrances and mass transfer limitations.

Deep eutectic solvents (DES) have recently emerged as green solvents, which belongs to the class of Ionic liquids (ILs) but has some additional properties which makes them more prominent as compared to the ILs. For example, significant depression in the melting point at the eutectic composition compared to the constituent components, ease of formation, comparatively inexpensive raw material and toxicologically well characterized. Moreover, the usage of DES for the adsorption and sequestering of CO_2 has demonstrated promising results.

Han et al.[89] also reported the high catalytic activity of a DES catalyst system (choline chloride: urea) impregnated on molecular sieves for the chemical fixation of CO_2 to cyclic carbonates, but the substrate used in the investigation had the epoxy group at the edge of the molecular structure for example propylene oxide, so they did not have to encounter the steric hindrance, which is one of the limiting factors in our case where we had long chain fatty acid monoester (Bio-oil 1). Whereas Wie Liu et al. conducted the carbonation of similar epoxidized methyl soyates using TBAB based DES and demonstrated significant reduction in the reaction time.[98]

In the present work, DES system based on TBAB (hydrogen bond acceptor) and triethylene glycol (hydrogen bond donor) (1:1) demonstrated the best conversion results within 4 hours under 40 bars of pressure. Halide anion from the TBAB made a complex with HBD, while the delocalization of the charge occurring due to this hydrogen bonding is postulated as the reason for the depression in melting point of the DES at the eutectic composition. Whereas the interaction between the anion and CO_2 can be considered as one of the contributing factors alongside others to the high solubility of this gas. [91] As highlighted earlier by Rizana et al. the properties e.g., density and viscosity of the DES are greatly affected by the selection of hydrogen bond donor (HBD). The length of alkyl chain and numbers of hydroxyl group in HBD lead to changes in physical properties, where the DES composed of longer HBD, and more hydroxyl groups demonstrated higher viscosity. The same was observed in our case where the dynamic viscosity of DES with triethylene glycol as HBD(DES1) was higher (212.2 mPa.s) as compared to when ethylene glycol (144.6 mPa.s) as HBD(DES2) was utilized. The entanglement of the longer molecular chains was postulated to be the reason behind increase

in viscosity, while the existence of extra hydroxyl group creates more hydrogen bonds thus increasing the attractive forces between the molecules [95]. Additionally high pressure helped to improve the solubility of CO_2 as also reported by Han et al [87].

In another approach simple catalyst system based on potassium iodide (KI) and phase transfer catalysts (PTC) including polyethylene glycols with increasing molar mass (e.g., PEG400 or PEG600) or 18-crown-6 ether were investigated to optimize reaction output. Low conversions were observed in case of PEG400 or PEG 600, however a significant increase in conversion was observed when crown ether as PTC was employed. As demonstrated by the results, the catalytic activity of the alkali metal salts increases with an increase in the anion nucleophilicity. 18-Crown-6 ether forms a complex with potassium ion by using all six oxygen atoms as donor atoms, while the anion becomes naked nucleophile as represented in scheme 5 below, which facilitates the strong nucleophilic attack of the anion on the oxirane ring and causes the opening of the ring, which is the rate determining step.[104][105]

18-crown-6 ether
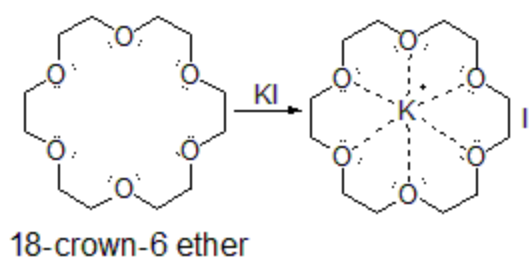
Scheme 5. Proposed formation of [K+ {crown ether} I-] complex

Conversion ratio calculation

Conversion ratio was determined based on the IR spectra obtained from the sample after completion of the reaction following the Equation 22. Where the peak area of the newly generated carbonyl group in the carbonated five membered ring at 1804 cm^{-1} was compared with the peak area of the carbonyl group from the fatty acid chain at 1736 cm^{-1}. Since more than one carbonyl groups of the carbonate are also there in the oil structure compared to the reference carbonyl group from fatty acid chain, the ratio is higher than 1 with the maximum conversion observed with our oil is 1.49.

$$Conversion\ ratio = \frac{peak\ area\ of\ carbonyl\ group\ from\ carbonate\ at\ 1804\ cm^{-1}\ wavenumber}{peak\ area\ of\ carbonyl\ group\ from\ fatty\ acid\ chain\ at\ 1736\ cm^{-1}\ wavenumber} \quad (22)$$

Corresponding NMR spectroscopic analysis were also performed to study the reaction as described earlier in the second publication. However, in depth study of the ^{1}H-NMR spectra revealed the presence of some hydroxyl groups which can be associated to the opening of the epoxy groups in the oil due to the possible side reaction of hydrolysis and acylation taking place due to reaction environment. Moreover, since the starting material Bio-oil 1 is based on the natural product, so the variation in the fatty acid composition and possibility of other residues cannot be denied which depends on various factors including, origin, climate, harvesting period etc. Few of the proton signals from these residues were also identified in the NMR spectra obtained. Last but not the least quantification of this reaction was also performed by taking the integration of the characteristic signals following equation 23.

$$S \% = 100 \% \cdot \frac{A-B}{A} \qquad\qquad (23)$$

Where A indicates the integration of the peak area from Bio-oil 1 in the region from 2.8 – 3.2 ppm (proton signals from the epoxide ring (initial amount)), B is the integration of the same area (2.8 – 3.2 ppm) in Bio-oil 2 (final remaining epoxide groups after reaction).

6. Conclusion and Outlook

The toxic health concerns due to phthalate-based plasticizers and the depleting petroleum resources triggered the debate in scientific community to replace these synthetic plasticizers by nature-friendly and bio-based green plasticizers with reduced migration. The present study is also concluded in this regard, where an effort was made to develop a bio-based green plasticizer with reduced migration keeping at par its purpose of plasticization.

The epoxidized monoester of glycerol formal from soybean oil (Bio oil 1) as presented in Figure (19) was provided by the industrial partner and its performance as primary plasticizer in acrylonitrile–butadiene rubber (NBR) was investigated by mechanical, thermal and migration analysis techniques. Corresponding migration analysis demonstrated higher migration due to less interaction with the matrix material.
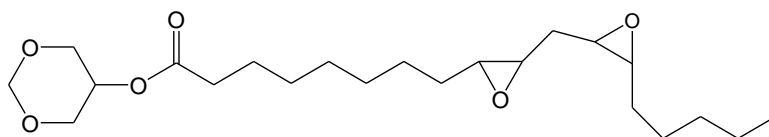

Figure 19. Bio oil 1

Meanwhile in this thesis work, a novel technique to monitor the in-situ migration of the plasticizer from the matrix was developed. Where the assembly of plasticized and unplasticized NBR samples was heated continuously for artificial aging with a custom-made aluminum heating plate, while the unplasticized sample served as a concentration gradient to induce migration as represented in Figure 20 (a). For the system under observation, diffusion coefficient was calculated by observing the area reduction of characteristic carbonyl peak of plasticizer at 1736 cm^{-1} as compared to the reference butadiene peak at 968 cm^{-1}. On hourly basis, *in situ* FTIR spectra were recorded while continuously heating the plasticized NBR sample on ATR crystal. Whereas in Figure 20 (b) the carbonyl-peak region (1736 cm^{-1}) is plotted, illustrating the reduction in peak area with respect to time due to the decrease in concentration (Lambert–Beer law) of migrating plasticizer. Lambert–Beer law explains the relationship between the absorption of electromagnetic waves and the quantity of the absorbing material. It can be observed that area of carbonyl peak reduced gradually with time during ageing because of continuous decrease of plasticizer concentration in the NBR sample at the face of diamond crystal.
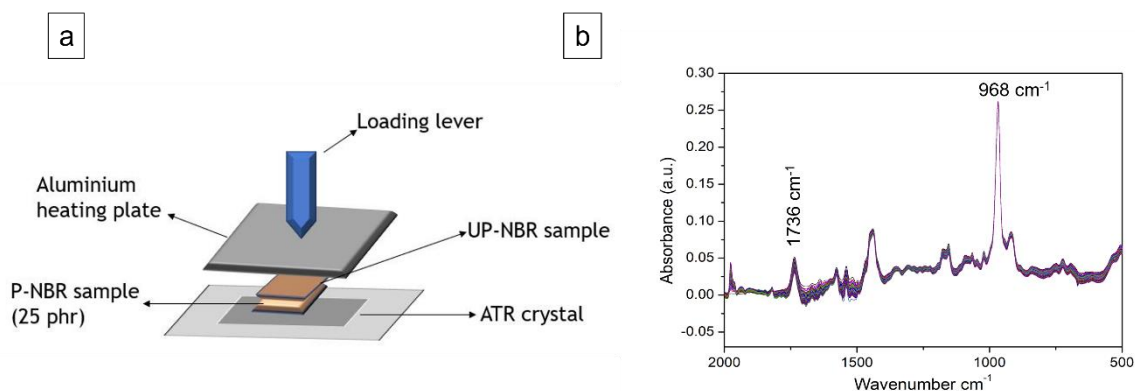
Figure 20(a). Schematic representation of experimental setup (b) representation of carbonyl peak area reduction observed via FTIR spectroscopy during heating after every 1 h up to 60 h

The in situ hourly updates of the sample at the same exact position presented a precise insight of the migrating plasticizer into the unplasticized NBR sample, reflecting that this process markedly depends on the time and temperature. However, the precision to determine the diffusion coefficient is restricted to the sample volume which is being penetrated by the evanescent waves of the infrared beam. The data obtained with respect to time was utilized to determine the diffusion coefficient using fitting Equation (19). Thus, present a universal tool for the comparison of different plasticizers with respect to their migration behavior. The diffusion coefficient values obtained can be very significant in predicting the life span of a product under different environmental conditions. The diffusion coefficient value of (6.93 x 10^{-12} cm^2/s) calculated by following this new method is comparable to the other reported diffusion coefficient values, calculated following different experimental methods but similar experimental conditions.

Modification of the Bio oil 1 was required to overcome this challenge of exudation. In the present work a simple synthetical modification approach was adopted by incorporating CO_2 in the epoxy rings of the plasticizer molecule in the presence of a catalyst (TBAB), thus enhancing polarity of the plasticizer molecule and increasing interaction with the matrix. The proposed polymer plasticizer (Bio oil 2) interaction model is demonstrated in the Figure (21).
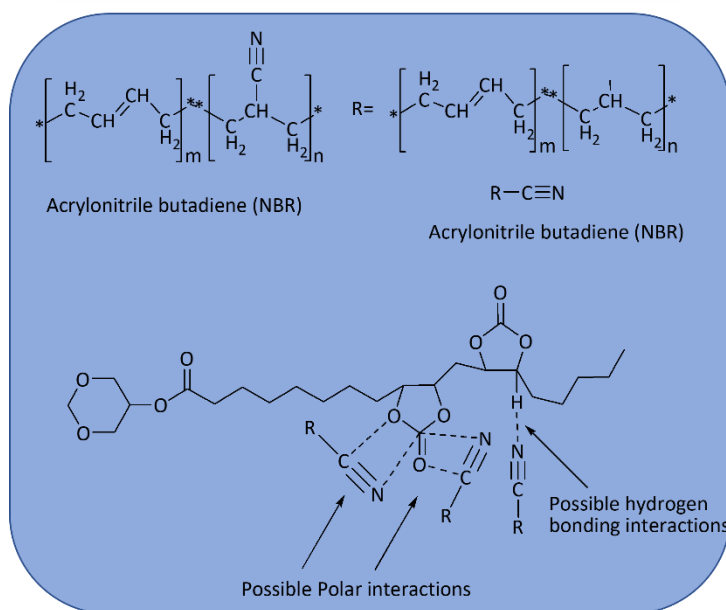
Figure 21. Polymer plasticizer (Bio oil 2) interaction model

The plasticizing performance of Bio-oil 2 in NBR vulcanizate was mainly evaluated by the analysis of tensile properties and hardness (IRHD-m) test, while its migration behavior was compared using in-situ FTIR analysis. Minor differences were observed in the mechanical properties of the specimen as compared to Bio-oil 1 plasticized specimen, as hardness was increased up to 6 % which can be inferred to the introduction of carbonated five-membered cyclic group in the plasticizer, which helped to increase the polarity due to the addition of two more oxygen atoms in the ring. The migration behavior revealed a decrease in oil migration which is expressed by the diffusion coefficient value D of the Bio-oil 2. This is due to enhanced polarity and better compatibility of Bio-oil 2 with the elastomeric matrix. Thus, it can be concluded that cycloaddition reaction of CO_2 with epoxidized monoester-based bio plasticizer can be an effective way to increase polarity and reduce migration of plasticizer. So, this value-added product can serve as an appropriate substitute to epoxy based bio-diesel plasticizers in the industry especially where the reduced migration is of utmost importance.

Although, good conversion of the plasticizer from Bio oil 1 to Bio oil 2 was obtained using TBAB as catalyst, but the cumbersome reaction time of 70 hours was required for the completion of reaction. Therefore, different strategies were evaluated for optimization of this reaction.

Deep eutectic solvents presented a fair solution in this regard. The delocalization of the charge occurring due to the hydrogen bonding among the halide anion from Tetrabutylammonium bromide (TBAB) and triethylene glycol as hydrogen bond donor (HBD) is postulated as the reason for the depression in melting point of the DES at the eutectic composition (see Figure 22). While the interaction between the anion and CO_2 is regarded as the contributing factors alongside others to the high solubility of this gas. Moreover, increase in solubility with increase in pressure as reported by Han et al., contributed to reduce the reaction time.

Corresponding analysis using different techniques for example, NMR and FTIR demonstrated purity and completion of reaction.
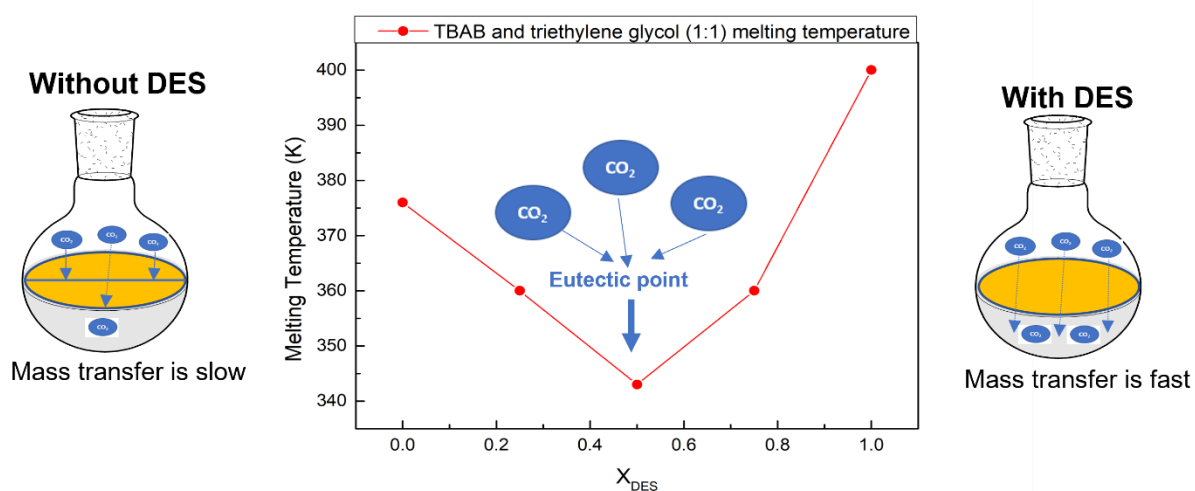
Figure 22. Effect of using DES

Our studies and corresponding investigations which are schematically depicted in Figure 23, suggest carbonation of the epoxidized monoester glycerides presents a fair solution to curtail the exudation phenomena, while keeping at par the purpose of plasticization. This green strategy of utilizing carbon dioxide in a chemical reaction also contribute to mitigate the global challenge of carbon dioxide emission. Moreover, the utilization of deep eutectic solvents also assisted to optimize the reaction output. Last but not the least, in situ FTIR analysis provides a precise tool to investigate the migration of penetrants.

Figure 23. Our proposed model: Carbonation of the epoxidized monoester plasticizer helps to curtail migration.

7. References

[1]   C. Brazel and S. Rosen, *Fundamental principles of polymeric materials*, 3rd ed., vol. 53, Jhon Wiley & Sons, **2012**.

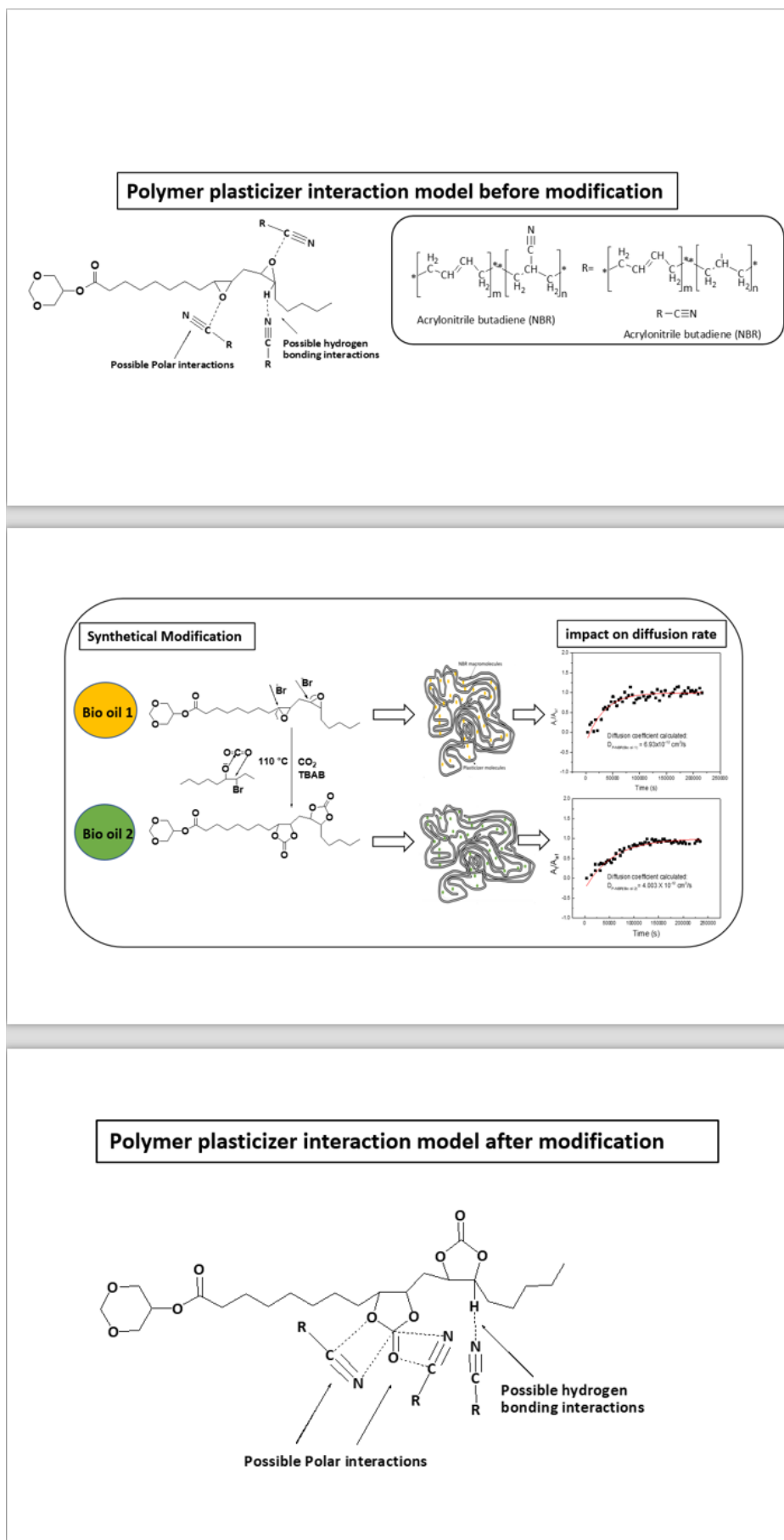[2]   M. Rahman and C. Brazel, "The plasticizer market: An assessment of traditional plasticizers and research trends to meet new challenges," *Prog. Polym. Sci.*, vol. 29, no. 12, pp. 1223–1248, **2004**.

[3]   M. Bocqué, C. Voirin, V. Lapinte, S. Caillol, and J. Robin, "Petro-based and bio-based plasticizers: Chemical structures to plasticizing properties," *J. Polym. Sci. Part A Polym. Chem.*, vol. 54, no. 1, pp. 11–33, **2016**.

[4]   K. Gumargalieva, V. Ivanov, G. Zaikov, J. Moiseev, and T. Pokholok, "Problems of ageing and stabilization of poly(vinyl chloride)," *Polym. Degrad. Stab.*, vol. 52, no. 1, pp. 73–79, **1996**.

[5]   M. Marín, J. López, A. Sánchez, J. Vilaplana, and A. Jiménez, "Analysis of Potentially Toxic Phthalate Plasticizers Used in Toy Manufacturing," *Environ. Contam.Toxicol.*, vol. 60, pp. 68–73, **1998**.

[6]   O. Geiss, S. Tirendi, J. Barrero-Moreno, and D. Kotzias, "Investigation of volatile organic compounds and phthalates present in the cabin air of used private cars," *Environ. Int.*, vol. 35, no. 8, pp. 1188–1195, **2009**.

[7]   Z. Petrović, M. Ionescu, J. Milić, and J. Halladay, "Soybean oil plasticizers as replacement of petroleum oil in rubber," *Rubber Chem. Technol.*, vol. 86, no. 2, pp. 233–249, **2013**.

[8]   P. Raju, V. Nandanan, and K. Kutty, "A Study on the Use of Coconut Oil as Plasticiser in Natural Rubber Compounds," *J. Rubber Res.*, vol. 10, no. 1, pp. 1–16, **2007**.

[9]   S. Srivastava and Y. Mishra, "Nanocarbon reinforced rubber nanocomposites: Detailed insights about mechanical, dynamical mechanical properties, payne, and mullin effects," *Nanomaterials*, vol. 8, no. 11, pp. 1–56, **2018**.

[10]   A. Khalaf, A. Yehia, M. Ismail, and S. El-Sabbagh, "High performance oil resistant rubber," *KGK Kautschuk Gummi Kunststoffe*, vol. 66, no. 9, pp. 28–32, **2013**.

[11]   R. Rajasekar, K. Pal, G. Heinrich, A. Das, and C. Das, "Development of nitrile butadiene rubber-nanoclay composites with epoxidized natural rubber as compatibilizer," *Mater. Des.*, vol. 30, no. 9, pp. 3839–3845, **2009**.

[12]   O. Fenollar, L. Sanchez-Nacher, D. Garcia-Sanoguera, J. López, and R. Balart, "The effect of the curing time and temperature on final properties of flexible PVC with an epoxidized fatty acid ester as natural-based plasticizer," *J. Mater. Sci.*, vol. 44, no. 14, pp. 3702–3711, **2009**.

[13]   J. Lutz, *Handbook of PVC formulating*. John Wiley & Sons: New York, USA, **1993**.

[14]   Y. Itoi, M. Inoue, and S. Enomoto, "Epoxidation of fatty acid esters with aqueous hydrogen peroxide in the presence of molybdenum oxide–tributyltin chloride on charcoal catalyst," *Bull. Chem. Soc. Jpn.*, vol. 59, no. 12, pp. 3941–3943, **1986**.

[15] Y. Wei and L. Jianbing, "Kinetics of epoxidation and oxirane cleavage of fatty acid methyl ester in formic acid auto catalytic system," *Chem. Ind. Times*, p. 3, **2013**.

[16] R. SHI, P. JIANG, and S. SHI, "Epoxidized synthesis of nontoxic and environmental-friendly plasticizer from soy acidic oil methyl esters," *China Oils Fats*, vol. 6, **2008**.

[17] F. Galli, S. Nucci, C. Pirola, and C. Bianchi, "Epoxy methyl soyate as bio-plasticizer : two different preparation strategies," *Chem. Eng. Trans.*, vol. 37, pp. 601–606, **2014**.

[18] G. CHIARADIA, "Plasticizers for polymers, WO 2015/067814 A2," WO 2015/067814 A2, **2015**.

[19] I. Shahzad, S. Wittchen, and V. Cepus, "In situ migration analysis and diffusion coefficient determination of bio-based plasticizer from NBR using FTIR-ATR and estimation of migrated plasticizer contents by TGA analysis," *Macromol. Symp.*, vol. 384, no. 1, **2019**.

[20] R. Gore, "Infrared Spectroscopy," *Anal. Chem.*, vol. 30, no. 4, pp. 570–579, **1958**.

[21] Kirk-othmer, *Encyclopedia of Chemical Technology*, no. 1. John Wiley & Sons, **2000**.

[22] J. Grdadolnik, "ATR-FTIR spectroscopy: Its advantages and limitations," *Acta Chim. Slov.*, vol. 49, no. 3, pp. 631–642, **2002**.

[23] G. Fieldson and T. Barbari, "The use of FTIR-ATR spectroscopy to characterize penetrant diffusion in polymers," *Polymer (Guildf).*, vol. 34, no. 6, pp. 1146–1153, **1993**.

[24] J. Comyn, "Introduction to polymer permeability and the mathematics of diffusion," in *Polymer permeability*, New York: Springer, **1985**.

[25] J. Vergnaud, *Liquid transport processes in polymeric materials: modeling and industrial applications/JM Vergnaud*. Prentice Hall, **1991**.

[26] N. Harrick, "Electric field strengths at totally reflecting interfaces," *JOSA*, vol. 55, no. 7, pp. 851–857, **1965**.

[27] H. Tompkins, "The physical basis for analysis of the depth of absorbing species using internal reflection spectroscopy," *Appl. Spectrosc.*, vol. 28, no. 4, pp. 335–341, **1974**.

[28] M. Brown and P. Gallagher, "Handbook of thermal analysis and calorimetry: recent advances, techniques and applications," **2011**.

[29] P. Haines, *Thermal methods of analysis*, vol. 70. Glasgow, UK: MARCEL DEKKER AG, **1995**.

[30] X. Liu, "Structural Identification of Organic compounds," in *Organic Chemistry I*, Kpu.pressbooks.pub, pp. 204–210, **2021**.

[31] J. Goldstein, D. Newbury, J. Michael, N. Ritchie, J. Scott, and D. Joy, *Scanning electron microscopy and X-ray microanalysis*. Springer, **2017**.

[32] C. Wilkes, C. Daniels, and W. Summers, *PVC Handbook*. Hanser Publications: Munich, Germany, **2005**.

[33] T. Mekonnen, P. Mussone, H. Khalil, and D. Bressler, "Progress in bio-based plastics

and plasticizing modifications," *J. Mater. Chem. A*, vol. 1, no. 43, p. 13379, **2013**.

[34] M. Vieira, M. Da Silva, L. Dos Santos, and M. Beppu, "Natural-based plasticizers and biopolymer films: A review," *Eur. Polym. J.*, vol. 47, no. 3, pp. 254–263, **2011**.

[35] S. Kumar, "Recent Developments of Biobased Plasticizers and Their Effect on Mechanical and Thermal Properties of Poly(vinyl chloride): A Review," *Ind. Eng. Chem. Res.*, vol. 58, no. 27, pp. 11659–11672, **2019**.

[36] J. Murphy, *Additives for plastics handbook*. Elsevier, **2001**.

[37] G. Wypych, *"Handbook of Plasticizers" ChemTech Publishing*. **2004**.

[38] G. Wypych, *PVC degradation and stabilization*. Elsevier, **2020**.

[39] M. Meier, J. Metzger, and U. Schubert, "Plant oil renewable resources as green alternatives in polymer science," *Chem. Soc. Rev.*, vol. 36, no. 11, pp. 1788–1802, **2007**.

[40] M. Benaniba and V. Massardier-Nageotte, "Evaluation effects of biobased plasticizer on the thermal, mechanical, dynamical mechanical properties, and permanence of plasticized PVC," *J. Appl. Polym. Sci.*, vol. 118, no. 6, pp. 3499–3508, **2010**.

[41] B. Bouchareb and M. Benaniba, "Effects of epoxidized sunflower oil on the mechanical and dynamical analysis of the plasticized poly (vinyl chloride)," *J. Appl. Polym. Sci.*, vol. 107, no. 6, pp. 3442–3450, **2008**.

[42] L. Gan, K. Ooi, S. Goh, L. Gan, and Y. Leong, "Epoxidized esters of palm olein as plasticizers for poly (vinyl chloride)," *Eur. Polym. J.*, vol. 31, no. 8, pp. 719–724, **1995**.

[43] P. Jia, M. Zhang, L. Hu, C. Bo, and Y. Zhou, "Synthesis, application, and flame-retardant mechanism of a novel phosphorus-containing plasticizer based on castor oil for polyvinyl chloride," *J. Therm. Anal. Calorim.*, vol. 120, no. 3, pp. 1731–1740, **2015**.

[44] G. Fogassy, C. Pinel, and G. Gelbard, "Solvent-free ring opening reaction of epoxides using quaternary ammonium salts as catalyst," *Catal. Commun.*, vol. 10, no. 5, pp. 557–560, **2009**.

[45] G. Fogassy *et al.*, "Catalyzed ring opening of epoxides: application to bioplasticizers synthesis," *Appl. Catal. A Gen.*, vol. 393, no. 1–2, pp. 1–8, **2011**.

[46] J. Chen, Z. Liu, J. Jiang, X. Nie, Y. Zhou, and R. Murray, "A novel biobased plasticizer of epoxidized cardanol glycidyl ether: synthesis and application in soft poly(vinyl chloride) films," *RSC Adv.*, vol. 5, no. 69, pp. 56171–56180, **2015**.

[47] P. Daniels, "A Brief Overview of Theories of PVC Plasticization and Methods Used to Evaluate PVC-Plasticizer Interaction*," *J Vinyl Addit. Technol*, vol. 21, no. 2, pp. 129–133, **2009**.

[48] A. Kirkpatrick, "Some relations between molecular structure and plasticizing effect," *J. Appl. Phys.*, vol. 11, no. 4, pp. 255–261, **1940**.

[49] "F. Clark," *Chem. Ind.*, vol. 60, p. 225, **1941**.

[50] "R. Houwnik," *Pure Appl Chem London*, pp. 575–583, **1947**.

[51] W. Aiken, T. Alfrey, A. Janssen, and H. Mark, "Creep behavior of plasticized vinylite VYNW," *J. Polym. Sci.*, vol. 2, no. 2, pp. 178–198, **1947**.

[52] D. Cadogan and C. Howick, "Plasticizers in Kirk-Othmer Encyclopedia of Chemical Technology," *John Wiley Sons New York*, vol. 10, **1996**.

[53] T. Fox Jr and P. Flory, "Second-order transition temperatures and related properties of polystyrene. I. Influence of molecular weight," *J. Appl. Phys.*, vol. 21, no. 6, pp. 581–591, **1950**.

[54] K. Sears and J. Darby, "'Mechanism of plasticizer action' John Wiley and Sons, New York," in *The Technology of Plasticizers*, **1982**.

[55] T. Stark, H. Choi, and P. Diebel, "Plasticizer molecular weight and plasticizer retention in PVC geomembranes," in *57th Canadian Geotechnical Conference*, **2004**.

[56] V. Ambrogi, W. Brostow, C. Carfagna, M. Pannico, and P. Persico, "Plasticizer Migration From Cross-Linked Flexible PVC : Effects on Tribology and Hardness," *Polym. Eng. Sci.*, **2012**.

[57] D. Messadi, J. Taverdet, and J. Vergnaud, "Plasticizer Migration from Plasticized Polyvinyl chloride) into Liquids. Effect of Several Parameters on the Transfer," *Ind. Eng. Chem. Prod. Res. Dev.*, vol. 22, no. 1, pp. 142–146, **1983**.

[58] J. Yuan and B. Cheng, "A strategy for nonmigrating highly plasticized PVC," *Sci. Rep.*, no. August, pp. 2–7, **2017**.

[59] A. Jayakrishnan and M. Sunny, "Phase transfer catalysed surface modification of plasticized poly (vinyl chloride) in aqueous media to retard plasticizer migration," *Polymer (Guildf).*, vol. 37, no. 23, pp. 5213–5218, **1996**.

[60] J. Audic, D. Reyx, and J. Brosse, "Cold plasma surface modification of conventionally and nonconventionally plasticized Poly (vinyl chloride) based flexible films : global and specific migration of additives into Isooctane," *J. Appl. Polym. Sci.*, vol. 79, pp. 1384–1393, **2001**.

[61] N. Reddy, M. Mohan, K. Varaprasad, S. Ravindra, K. Vimala, and M. Raju, "Surface treatment of plasticized Poly (vinyl chloride) to prevent plasticizer migration," *J. Appl. Polym. Sci.*, vol. 115, no. February, **2010**.

[62] I. Shahzad, M. Rahman, S. Wittchen, K. Reincke, B. Langer, and V. Cepus, " Synthetical modification of plant oil-based plasticizer with CO 2 leads to reduced migration from NBR rubber ," *J. Appl. Polym. Sci.*, no. October, p. 51854, **2021**.

[63] G. Smith, C. Skidmore, P. Howe, and J. Majewski, "Diffusion , Evaporation , and Surface Enrichment of a Plasticizing Additive in an Annealed Polymer Thin Film," *J. Polym. Sci., Part BPolymer Phys.*, vol. 42, pp. 3258–3266, **2004**.

[64] R. Lundsgaard, G. Kontogeorgis, J. Kristiansen, and T. Jensen, "Modeling of the Migration of Glycerol Monoester Plasticizers in Highly Plasticized Poly(vinyl chloride)," *J Vinyl Addit. Technol*, pp. 129–133, **2009**.

[65] C. Rosca and R. Schuster, "Investigation of diffusion of phthalates in Nitrile rubber by means of FTIR-spectroscopy," *Prüfen und Mess.*, vol. 49, pp. 86–92, **2006**.

[66] A. Marcilla, S. García, and J. García-Quesada, "Study of the migration of PVC plasticizers," *J. Anal. Appl. Pyrolysis*, vol. 71, no. 2, pp. 457–463, **2004**.

[67] A. Marcilla, S. Garcia, and J. Garcia-Quesada, "Migrability of PVC plasticizers," *Polym. Test.*, vol. 27, no. 2, pp. 221–233, **2008**.

[68] M. Fernendez, B. Gonza´lez, "Fourier Transform Infrared Spectroscopy in the Study of the Interaction Between PVC and Plasticizers: PVC/Plasticizer compatibility," *Polym. Polym. Compos.*, vol. 21, no. 7, pp. 449–456, **2013**.

[69] S. Chakraborty, S. Bandyopadhyay, R. Ameta, R. Mukhopadhyay, and A. Deuri, "Application of FTIR in characterization of acrylonitrile-butadiene rubber (nitrile rubber)," *Polym. Test.*, vol. 26, no. 1, pp. 38–41, **2007**.

[70] B. Schäffner *et al.*, "Synthesis and application of carbonated fatty acid esters from carbon dioxide including a life cycle analysis," *ChemSusChem*, vol. 7, no. 4, pp. 1133–1139, **2014**.

[71] M. Aresta, *Carbon dioxide as chemical feedstock*. John Wiley & Sons, **2010**.

[72] J. Comerford, I. Ingram, M. North, and X. Wu, "Sustainable metal-based catalysts for the synthesis of cyclic carbonates containing five-membered rings," *Green Chem.*, vol. 17, no. 4, pp. 1966–1987, **2015**.

[73] A. Decortes, A. Castilla, and A. Kleij, "Salen-complex-mediated formation of cyclic carbonates by cycloaddition of CO2 to epoxides," *Angew. Chemie Int. Ed.*, vol. 49, no. 51, pp. 9822–9837, **2010**.

[74] T. Sakakura and K. Kohno, "The synthesis of organic carbonates from carbon dioxide," *Chem. Commun.*, no. 11, pp. 1312–1330, **2009**.

[75] J. Sun, S. Fujita, and M. Arai, "Development in the green synthesis of cyclic carbonate from carbon dioxide using ionic liquids," *J. Organomet. Chem.*, vol. 690, no. 15, pp. 3490–3497, **2005**.

[76] B. Tamami, S. Sohn, and G. L. Wilkes, "Incorporation of Carbon Dioxide into Soybean Oil and Subsequent Preparation and Studies of Nonisocyanate Polyurethane Networks," **2003**.

[77] K. Doll and S. Erhan, "Synthesis of carbonated fatty methyl esters using supercritical carbon dioxide," *J. Agric. Food Chem.*, vol. 53, no. 24, pp. 9608–9614, **2005**.

[78] W. Peppel, "Preparation and properties of the alkylene carbonates," *Ind. Eng. Chem.*, vol. 50, no. 5, pp. 767–770, **1958**.

[79] M. North and R. Pasquale, "Mechanism of cyclic carbonate synthesis from epoxides and CO2," *Angew. Chemie Int. Ed.*, vol. 48, no. 16, pp. 2946–2948, **2009**.

[80] E. Smith, A. Abbott, and K. Ryder, "Deep Eutectic Solvents (DESs) and Their Applications," *Chem. Rev.*, **2014**.

[81] A. Abbott, G. Capper, and M. Davies, "D.; Rasheed, HR; Tambyrajah, V," *Chem. Commun*, **2010**.

[82] A. Abbott, J. Barron, K. Ryder, and D. Wilson, "Eutectic-based ionic liquids with metal-

containing anions and cations," *Chem. Eur. J.*, vol. 13, no. 22, pp. 6495–6501, **2007**.

[83] S. Sarmad, Y. Xie, J. Mikkola, and X. Ji, "Screening of deep eutectic solvents (DESs) as green CO 2 sorbents: from solubility to viscosity," *New J. Chem.*, vol. 41, no. 1, pp. 290–301, **2017**.

[84] R. Leron and M. Li, "Solubility of carbon dioxide in a choline chloride–ethylene glycol based deep eutectic solvent," *Thermochim. Acta*, vol. 551, pp. 14–19, **2013**.

[85] L. Zubeir, D. Van Osch, M. Rocha, F. Banat, and M. Kroon, "Carbon dioxide solubilities in decanoic acid-based hydrophobic deep eutectic solvents," *J. Chem. Eng. Data*, vol. 63, no. 4, pp. 913–919, **2018**.

[86] C. Dietz *et al.*, "PC-SAFT modeling of CO2 solubilities in hydrophobic deep eutectic solvents," *Fluid Phase Equilib.*, vol. 448, pp. 94–98, **2017**.

[87] X. Li, M. Hou, B. Han, X. Wang, and L. Zou, "Solubility of CO2 in a choline chloride+ urea eutectic mixture," *J. Chem. Eng. Data*, vol. 53, no. 2, pp. 548–550, **2008**.

[88] G. Wang *et al.*, "Novel ionic liquid analogs formed by triethylbutylammonium carboxylate-water mixtures for CO2 absorption," *J. Mol. Liq.*, vol. 168, pp. 17–20, **2012**.

[89] A. Zhu, T. Jiang, B. Han, J. Zhang, Y. Xie, and X. Ma, "Supported choline chloride/urea as a heterogeneous catalyst for chemical fixation of carbon dioxide to cyclic carbonates," *Green Chem.*, vol. 9, no. 2, pp. 169–172, **2007**.

[90] J. Anthony, E. Maginn, and J. Brennecke, "Solubilities and thermodynamic properties of gases in the ionic liquid 1-n-butyl-3-methylimidazolium hexafluorophosphate," *J. Phys. Chem. B*, vol. 106, no. 29, pp. 7315–7320, **2002**.

[91] S. Kazarian, B. Briscoe, and T. Welton, "Combining ionic liquids and supercritical fluids: in situ ATR-IR study of CO2 dissolved in two ionic liquids at high pressures Electronic" *Chem. Commun.*, no. 20, pp. 2047–2048, **2000**.

[92] M. Chary, N. Keerthysri, S. Vupallapati, N. Lingaiah, and S. Kantevari, "Tetrabutylammonium bromide (TBAB) in isopropanol: An efficient, novel, neutral and recyclable catalytic system for the synthesis of 2, 4, 5-trisubstituted imidazoles," *Catal. Commun.*, vol. 9, no. 10, pp. 2013–2017, **2008**.

[93] N. Jain, A. Kumar, S. Chauhan, and S. Chauhan, "Chemical and biochemical transformations in ionic liquids," *Tetrahedron*, vol. 5, no. 61, pp. 1015–1060, **2005**.

[94] E. Duan, B. Guo, M. Zhang, B. Yang, and D. Zhang, "pH measurements of caprolactam tetrabutyl ammonium bromide ionic liquids in solvents," *J. Chem. Eng. Data*, vol. 55, no. 9, pp. 3278–3281, **2010**.

[95] R. Yusof, E. Abdulmalek, K. Sirat, and M. Rahman, "Tetrabutylammonium bromide (TBABr)-based deep eutectic solvents (DESs) and their physical properties," *Molecules*, vol. 19, no. 6, pp. 8011–8026, **2014**.

[96] Z. Li *et al.*, "Catalytic synthesis of carbonated soybean oil," *Catal. Letters*, vol. 123, no. 3, pp. 246–251, **2008**.

[97] V. Calo, A. Nacci, A. Monopoli, and A. Fanizzi, "Cyclic carbonate formation from

carbon dioxide and oxiranes in tetrabutylammonium halides as solvents and catalysts," *Org. Lett.*, vol. 4, no. 15, pp. 2561–2563, **2002**.

[98] W. Liu and G. Lu, "Carbonation of epoxidized methyl soyates in tetrabutylammonium bromide-based deep eutectic solvents," *J. Oleo Sci.*, vol. 2017, pp. 1–8, **2018**.

[99] J. Crank, *THE MATHEMATICS OF DIFFUSION*, Second edi. CLARENDON PRESS. OXFORD, **1975**.

[100] R. Holser, "Carbonation of epoxy methyl soyate at atmospheric pressure.," *J. Oleo Sci.*, vol. 56, no. 12, pp. 629–632, **2007**.

[101] B. Tamami, S. Sohn, and G. Wilkes, "Incorporation of carbon dioxide into soybean oil and subsequent preparation and studies of nonisocyanate polyurethane networks," *J. Appl. Polym. Sci.*, vol. 92, no. 2, pp. 883–891, **2004**.

[102] W. Liu, G. Lu, B. Xiao, and C. Xie, "Potassium iodide-polyethylene glycol catalyzed cycloaddition reaction of epoxidized soybean oil fatty acid methyl esters with CO2," *RSC Adv.*, vol. 8, no. 54, pp. 30860–30867, **2018**.

[103] Z. Li *et al.*, "Catalytic synthesis of carbonated soybean oil," *Catal Lett*, vol. 123, pp. 246–251, **2008**.

[104] G. Rokicki, W. Kuran, and B. Pogorzelska-Marciniak, "Cyclic carbonates from carbon dioxide and oxiranes," *Monatshefte für Chemie / Chem. Mon.*, vol. 115, no. 2, pp. 205–214, **1984**.

[105] C. Liotta and H. Harris, "Chemistry of naked anions. I. Reactions of the 18-crown-6 complex of potassium fluoride with organic substrates in aprotic organic solvents," *J. Am. Chem. Soc.*, vol. 96, no. 7, pp. 2250–2252, **1974**.

8. Acknowledgment

9. Academic Curriculum Vitae

"Has been removed for data protection reasons."